Additive Manufacturing of Advanced Ceramic Materials

Y. Lakhdar[1], C. Tuck[1], J. Binner[3], A. Terry[2], R. Goodridge[1*]

[1] Centre for Additive Manufacturing (CfAM), ~~Advanced Manufacturing Building~~School of Engineering, University of Nottingham, Nottingham NG8 1BB, United Kingdom
[2] AWE, Aldermaston, Reading RG7 4PR, United Kingdom
[3] School of Metallurgy and Materials, University of Birmingham, Birmingham B15 2TT, United Kingdom
*Corresponding author

ABSRACT:

Additive manufacturing (AM) has the potential to disrupt the ceramic industry by offering new opportunities to manufacture advanced ceramic components without the need for expensive tooling, thereby reducing production costs and lead times and increasing design freedom. Whilst the development and implementation of AM technologies in the ceramic industry has been slower than in the polymer and metal industries, there is now considerable interest in developing AM processes capable of producing defect-free, fully dense ceramic components. A large variety of AM technologies can be used to shape ceramics, but variable results have been obtained so far. Selecting the correct AM process for a given application not only depends on the requirements in terms of density, surface finish, size and geometrical complexity of the part, but also on the nature of the particular ceramic to be processed. This paper provides a detailed review of the current state-of-the-art in AM of advanced ceramics through a systematic evaluation of the capabilities of each AM technology, with an emphasis on reported results in terms of final density, surface finish and mechanical properties. An in-depth analysis of the opportunities, issues, advantages and limitations arising when processing advanced ceramics with each AM technology is also provided.

~~Advanced ceramics are key engineering materials for a wide range of technical applications due to their unique combinations of thermal, mechanical, chemical and electromagnetic properties. However, their lack of ductility, very high melting point and extreme hardness make processing and forming advanced ceramics into complex shapes challenging and expensive. Additive manufacturing (AM) has the potential to disrupt the ceramic manufacturing industry by offering new opportunities to produce advanced ceramic components without the need for expensive dies and moulds. By using AM, ceramists hope to reduce production costs and lead times whilst freeing themselves from the design limitations of conventional manufacturing processes. Whether to choose additive or conventional manufacturing to shape ceramics at an industrial scale, however, depends on the number of parts to be made, as AM isn't currently suitable for mass production. Whilst the development and implementation of AM technologies in the ceramic industry has been slower than in the polymer and metal industries, there is now a considerable interest for the development of AM processes capable of producing defect-free, fully dense ceramic components. Nowadays, a large variety of AM technologies can be used to shape ceramics, but variable results have been obtained so far. Selecting the right AM process for a given application not only depends on the requirements in terms of density, surface finish, size and geometrical complexity of the part, but also on the nature of the particular ceramic material to be processed. This paper provides a detailed review of the current state-of-the-art in AM of advanced ceramic materials through a systematic evaluation of the capabilities of each AM technology, with an emphasis on reported results in terms of final density, surface finish and mechanical properties. An in-depth analysis of the opportunities, issues, advantages and limitations arising when processing advanced ceramics with each AM technology is also provided.~~

Contents

List of Abbreviations

2PP	Two-photon polymerisation
3DP	Three-dimensional printing
3PB	Three-point bending
3DGP	Three-dimensional gel printing
4PB	Four-point bending
ABEF	Aqueous-based extrusion fabrication
AM	Additive manufacturing
ASTM	American Society for Testing and Materials
B3B	Ball-on-three-balls
BJ	Binder jetting
CAD	Computer-aided design
CAM-LEM	Computer-aided manufacturing of laminated engineering materials
CIJ	Continuous inkjet printing
CLF	Ceramic laser fusion
CLG	Ceramic laser gelling
CLS	Ceramic laser sintering
CODE	Ceramic on-demand extrusion
DED	Directed energy deposition
DIP	Direct inkjet printing
DIW	Direct ink writing
DLP	Digital light processing
dLS	Direct laser sintering
DoD	Drop-on-demand
EFF	Extrusion freeform fabrication
FDC	Fused deposition of ceramics
FEF	Freeze-form extrusion fabrication
iLS	Indirect Laser Sintering
LAS	Lithium aluminosilicate
LCM	Lithography-based ceramic manufacturing
LENS	Laser engineered net shaping
LOM	Laminated object manufacturing
LPIM	Low pressure injection moulding
LS	Laser sintering
LSD	Layerwise slurry deposition
LSI	Liquid silicon infiltration
μCT	Micro-computed tomography
MJS	Multiphase jet solidification
PBF	Powder bed fusion
PDC	Polymer-derived ceramics
PHASE	Photopolymerisation-assisted syringe-based extrusion
PIP	Polymer infiltration and pyrolysis
RC	Robocasting
Rz	Ten-point mean roughness
SL	Stereolithography
SLC	Selective laser curing
SLM	Selective laser melting
SLS	Selective laser sintering
SPPW	Self-propagating photopolymer waveguide technology
T3DP	Thermoplastic three-dimensional printing
TCP	Tri-calcium phosphate
TD	Theoretical density
TZP	Tetragonal zirconia polycrystal
YSZ / Y-TZP	Yttria-stabilised zirconia

1. Introduction

Manufacturing defect-free near-net-shape three-dimensional (3D) advanced ceramic parts cost-effectively is not a straightforward task due to the extreme properties of this class of materials. Indeed, the very high melting temperature and low ductility of advanced ceramic materials makes processing them from the molten liquid state extremely challenging, whilst their poor thermal shock resistance often results in the formation of cracks and pores when forming parameters and temperature treatments are not perfectly well controlled. Moreover, their high hardness and brittleness often make it difficult to machine sintered components without introducing defects and surface microcracks; machining is also extremely expensive, mostly due to the use of diamond cutting and grinding tools, and it is estimated that it can account for more than 70% of total manufacturing costs [1]. As a result, polycrystalline advanced ceramics are mainly produced from a powder processing route, as shown in **Figure 1**Figure 1, whether directly as dry powders or in the form of powder slurries [1]. Ceramic powders are commonly mixed with a binder and other additives, such as a deflocculant and a plasticiser, to form a dry powder mix for shaping of the green body by die pressing or cold isostatic pressing (dry forming). Alternatively, the powder can be dispersed in a liquid carrier to form a colloidal ceramic slurry of ceramic powder in a solvent for tape casting and slip casting (wet forming), or in a wax[1] for injection moulding (plastic forming) [2]. However, dry forming processes are currently far more commonly used in industry than wet forming techniques since they are the cheapest approaches. Indeed, the liquid removal in wet forming is very energy- and time-intensive, and the same can be said for the removal of the polymer from plastic forming routes such as injection moulding; wet forming techniques are therefore being used only when dry forming does not provide the performance required. After forming, a debinding step is carried out at a controlled heating rate to remove the organic binder, yielding a "brown" body that is then sintered by firing in a furnace at elevated temperature, usually between 50 and 90% of the melting temperature, in order to induce a physicochemical transformation that gives the component its final material properties and microstructure. Additional post-processing steps such as machining, grinding and polishing are often necessary in order to ensure parts have the desired surface finish and comply with required tolerances [3]. Conventional ceramic manufacturing processes such as slip casting [4], injection moulding [5] and gelcasting [6] all work according to this general principle. Although they differ greatly in both the composition of starting material systems and the way parts are shaped, they all have in common the use of moulds or dies to shape green parts.

Additive manufacturing (AM), often also referred to as 3D printing, is a range of processes that build 3D parts by adding material, usually layer-by-layer, directly from computer-based 3D model data [7]. AM offers an alternative approach to conventional formative processes, making it possible to manufacture geometrically complex near-net-shape 3D ceramic parts without using expensive tooling. However, the implementation of AM technologies in the ceramic industry has been much slower than in the polymer and metal industries due to the poor resolution, surface quality, mechanical properties, and scalability of additively manufactured ceramic parts compared to conventional ceramic manufacturing processes. The first obvious advantage of AM for the ceramic industry lies in its ability to enable the economical manufacturing of prototypes, low-volume productions and even individual customised parts, without the use of high-cost dedicated mould tooling. Indeed, because moulds used in injection moulding are extremely expensive, large production volumes are usually required to amortise the high tooling costs, although this does not necessarily apply to all conventional formative technologies as, for instance, plaster of Paris moulds used in slip casting are relatively inexpensive.

---

[1] In the context of this review, the term "wax" describes a polymeric phase used as suspension medium for ceramic powders. In most cases, "wax" refers to a thermoplastic polymer, except for the PHASE process where it refers to a photocurable polymer.
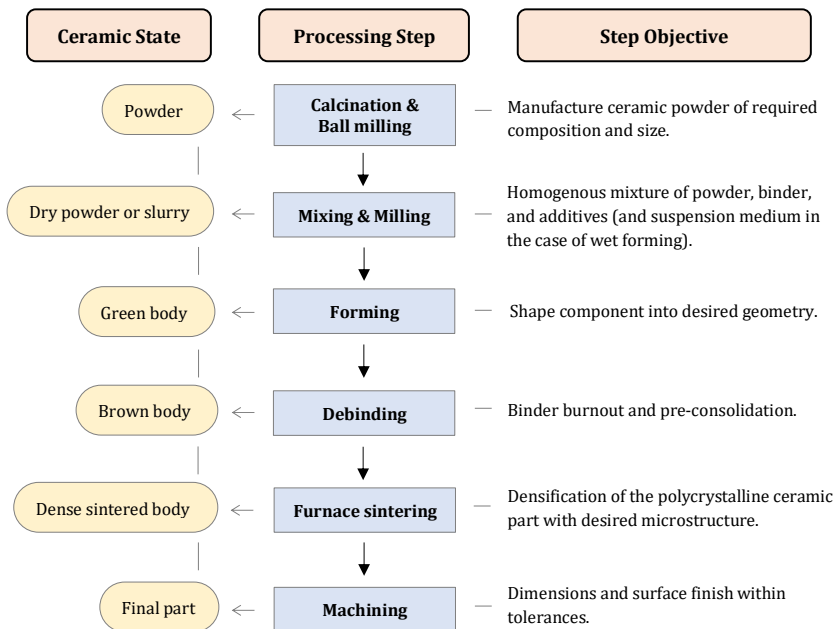
Figure 1: *Flowchart for the ceramic powder processing route from starting powder to final part.*

Moreover, design modifications and functional prototypes must be kept to a minimum since each design iteration requires the fabrication of a new mould, which is both time-consuming and expensive. Modifying the design of a component in the context of AM, however, is as simple as updating the corresponding digital design files, which can involve a change in build orientation and optimisation of processing parameters, but does not involve any physical modifications to the machine itself nor any custom tooling. As a result, the cost-per-part is no longer contingent upon production volume since there is no tooling cost. The overall manufacturing cost of AM technologies is therefore relatively independent from design complexity and is rather only related to material use (i.e. cost of materials and size of the build), machine power consumption, and cost of labour. Therefore, as shown in **Figure 2**, unlike conventional manufacturing processes such as injection moulding, the overall manufacturing cost-per-part with AM technologies is almost completely independent from design complexity; it is rather mostly related to material use and depends on the number of parts to be produced. This consideration is a key part of the overall argument for ceramics AM. Indeed, many applications of ceramic components require significantly smaller production volumes compared to those of metals or polymers, making AM a particularly attractive and economical solution to replace injection moulding for small production volumes, even more so if parts are geometrically complex (**Figure 2**).

Moreover, the lack of custom tooling not only results in cost savings, but also in much shorter prototyping and production lead times. Another significant advantage of AM lies within the inherent design freedom brought about by the layer-wise part formation, which enables the fabrication of objects of high geometrical complexity that would be difficult or even impossible to produce using subtractive or formative manufacturing processes. This increased design freedom offered by AM also tends to facilitate the reduction, or even in some cases the complete elimination, of additional forming, cutting and assembling steps, resulting in shorter lead times and lower manufacturing costs.
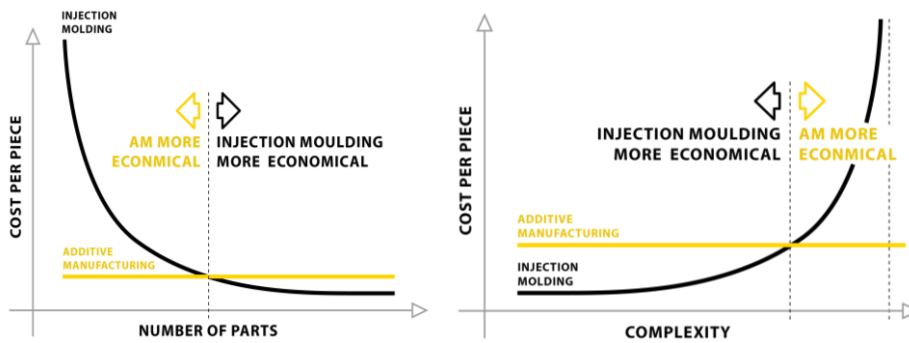
Figure 2: *Graphs showing that AM is more economical than injection moulding when working with small production volumes due to the lack of economies of scale and/or when manufacturing highly complex parts since hardware and tooling modifications are not required when increasing part complexity. (Graphs kindly provided by Dr. Johannes Homa, CEO of Lithoz GmbH)*

Ceramic AM processes can be categorised according to whether they are "single-step" or "multi-step" processes. Multi-step AM processes result in the formation of a green body that requires subsequent debinding and sintering thermal treatments in order to obtain the final advanced ceramic part. Most AM technologies, as they have been implemented up until now, belong to this category: sheet lamination processes [8][9], extrusion-based technologies such as fused deposition of ceramics (FDC) [10], freeze-form extrusion fabrication (FEF) [11] and robocasting (RC) [12], vat photopolymerisation-based technologies [13][14], direct inkjet printing (DIP) [15], binder jetting [16][17], and indirect laser sintering (LS) [18] have all been applied using a multi-step process. On the other hand, there are currently only two AM processes that have been demonstrated to be capable of directly shaping and sintering advanced ceramics in a single-step: direct laser sintering (dLS, commonly known as selective laser melting (SLM)) [19] and directed energy deposition (DED) [20]. The most extensive list to date of AM technologies that have been used to shape advanced ceramics is provided in **Figure 3**.

Direct Additive Manufacturing of Advanced Ceramics							
Single-step processes		Multi-step processes					
Bedless	Bed	Bed			Bedless		
Directed Energy Deposition	Powder Bed	Fusion	Binder Jetting	Sheet Lamination	Material Extrusion	Material Jetting	Vat Photopolymerisation
LENS	Powder- dLS	Powder-iLS	Powder-BJ	LOM	Wax-based / Water-based	Solvent-DIP	SL
	Slurry- dLS	Slurry-iLS	Slurry-BJ	CAM-LEM	FDC / RC / DIW	Wax-DIP	DLP / LCM
					MJS / FEF		SPPW
					T3DP / CODE		2PP
					PHASE* / 3DGP		

LENS: Laser Engineered Net Shaping
dLS/iLS: direct/indirect Laser Sintering
BJ: Binder Jetting
LOM: Laminated Object Manufacturing
CAM-LEM: Computer-Aided Manufacturing of Laminated Engineering Materials
SL: Stereolithography
DLP: Digital Light Projection
LCM: Lithography-based Ceramic Manufacturing
SPPW: Self-Propagating Photopolymer Waveguide
2PP: Two-Photon Photopolymerisation

FDC: Fused Deposition of Ceramics
MJS: Multiphase Jet Solidification
T3DP: Thermoplastic 3D Printing
PHASE: PHotopolymerisation-ASsisted Extrusion - *suggested acronym
RC: Robocasting
DIW: Direct Ink Writing
FEF: Freeze-Form Extrusion Fabrication
CODE: Ceramic On-Demand Extrusion
3DGP: 3D Gel Printing
DIP: Direct Inkjet Printing

Figure 3: Additive manufacturing technologies applied to ceramic materials in the literature.

Commented [YL(aM1)]: Updated figure, formatting was fixed

Alternatively, another ceramic additive manufacturing route, which is usually referred to as *negative ceramic AM*, consists in using AM to first shape sacrificial polymer moulds that are then impregnated with a ceramic slurry by investment casting [21] or gelcasting [22]; the polymer is then removed by dissolution or thermal burn-out. This method has the advantage of using AM to shape polymers, which are both easier and more cost-effective to additively manufacture than ceramics, then use conventional colloidal casting processes to shape ceramic parts. Polymer moulds for negative ceramic AM can be manufactured using most polymer AM technologies, including FDM [23][24], material jetting [25][26], LS [27], and SL [28][29]. For instance, **Figure 4** describes a negative AM process using a commercial desktop 3D printer to make an ABS mould followed by gelcasting to produce dense boron carbide parts [22]. Furthermore, the indirect AM approach should be more readily scalable for high volume production whilst still enabling relatively complex geometries, including functional grading, and keeping the ability to customise each part independently. However, the negative ceramic AM method does not enable spatial control over material composition, such as material grading and multi-material fabrication, although not all direct AM processes provide such capability (see Section 4). In addition, the complexity of design can be reduced, particularly where complex internal geometries are required. Another disadvantage of negative AM compared to both multi-step and single-step direct AM is its increased lead-times due to counting more manufacturing steps, as described in **Figure 5**. The flowchart also shows the potential of single-step ceramic AM to significantly reduce production times by removing the need for post-shaping densification steps. This review will focus on direct ceramic AM methods and negative AM will not be further discussed, although the authors note that it shows significant potential to work alongside direct ceramic AM, especially when producing a high number of semi-geometrically-complex parts.
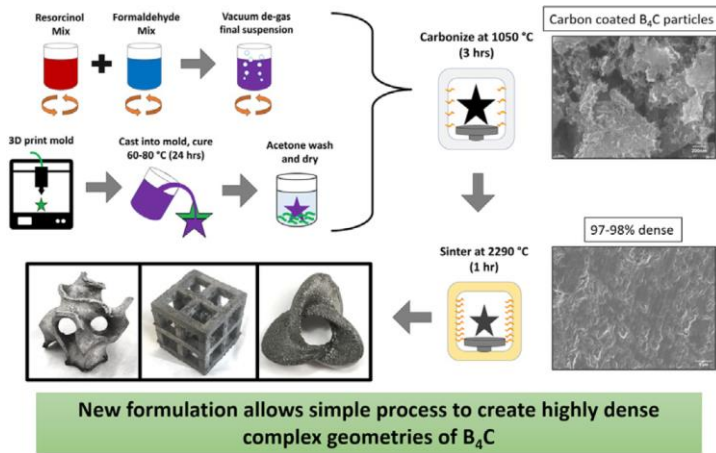
Figure 4: *Negative additive manufacturing processes based on gelcasting to create complex B₄C components.* [22]

For a given ceramic manufacturing process, two distinct types of pore formation must be distinguished: controlled, macro- or meso-porosity, and uncontrolled, random micro-and nano-porosity, which are commonly called *designed porosity* and *residual porosity*, respectively. Residual porosity is one of the most common defects that can hinder the performance of monolithic ceramic materials, and for ceramics to have optimum physical and mechanical properties, unwanted porosity should be minimised. The other main defects that commonly occur in ceramic manufacturing are surface irregularities and cracking. Macro- and micro-cracks are initiated at internal pores and at internal or external irregularities, and are propagated in ceramic materials by mechanical stresses, fast drying kinetics and thermal gradients.

Therefore, when trying to manufacture dense ceramic components it is essential to minimise the formation of residual porosity while preventing the formation of cracks, which remains one of the main challenges in AM of advanced ceramics, as will be detailed throughout this review. Amongst currently available ceramic AM technologies, only a few processes can successfully and reliably produce dense ceramic parts without any unwanted residual micro-porosity, whilst most technologies are only suited to making porous structures. For this reason, research and development efforts in the ceramic AM community have for a number of years primarily focused on applications where designed and residual porosity are beneficial, with a strong emphasis on porous components for biomedical applications, and especially on scaffolds for tissue engineering [30][31][32]. However, researchers are now increasingly focusing their efforts on enabling AM of monolithic ceramics. Indeed, for ceramic AM to reach the same level of technological maturity as metal and plastic AM, AM methods and ceramic feedstocks that are specifically designed to produce monolithic near-net-shape technical ceramic parts with controlled microstructures and without restrictions on part dimensions, geometrical complexity, nor material selection must be developed and perfected. Eventually, ceramic AM will have reached its full potential when single-step direct AM methods are able to produce ceramic components to the level of quality expected by industrial standards for commercialisation.

Negative AM

AM of polymer mould

Ceramic slurry formulation

Retrieval of polymer mould

Ceramic gelcasting or investment casting

Polymer mould removal

Green part

Binder burn-out

Brown part

High-temperature furnace sintering

Sintered ceramic component

Multi-step AM

Ceramic feedstock preparation

AM of ceramic

Retrieval of as-printed ceramic part

Green part

Binder burn-out

Brown part

High-temperature furnace sintering

Sintered ceramic component

Single-step AM

Ceramic feedstock preparation

AM of ceramic

Retrieval of as-printed ceramic part

Sintered ceramic component

Figure 5: Flowchart showing the number of steps of negative ceramic AM, multi-step direct AM, and single-step direct AM, from AM feedstock to sintered ceramic part.

1.1. Aims of this review

A list of reviews on the additive manufacturing of ceramics that have been published in the past 20 years is given in **Table 1**. Most of these reviews, however, were focused on a particular set of AM processes applied to ceramics. Furthermore, significant developments and important technological innovations have arisen in the field in the past few years and, as a result, several AM technologies described in this article were not discussed, or even mentioned, in any of the previous reviews.

This review is specifically aimed at:
  i. **Ceramists** who are considering using their expertise in ceramic materials and conventional ceramics processing to investigate ceramic AM, but who first need to obtain a more in-depth knowledge of the current capabilities and limitations of AM processes as well as understand the differences between the various AM technologies better.
 ii. **AM specialists** who may consider applying their extensive knowledge of AM to explore ceramic materials, but first need to understand the specific opportunities and challenges associated with processing and shaping advanced ceramics better.

Table 1: *Previous general reviews and technology-specific reviews on the additive manufacturing of ceramic materials in the literature.*

Authors	Year	Title of the review	Focus of the review
J.D. Cawley [33]	1999	Solid freeform fabrication of ceramics	General review
J.W. Halloran [34]	2002	Freeform fabrication of ceramics	EFF, DIP, BJ, LOM, SL
B. Tay *et al.* [35]	2003	Solid freeform fabrication of ceramics	General review
J. Lewis *et al.* [36]	2006	Direct Ink Writing of Three-Dimensional Ceramic Structures	EFF, BJ, DIP
B. Qian, Z. Shen [37]	2013	Laser sintering of ceramics	LS
N. Travitzky *et al.* [38]	2014	Additive Manufacturing of Ceramic-Based Materials	BJ, LS, EFF, SL, LOM
J. Deckers *et al.* [39]	2014	Additive Manufacturing of Ceramics: A Review	LS, LM, SL
B. Derby [40]	2015	Additive Manufacture of Ceramics Components by Inkjet Printing	DIP
A. Zocca *et al.* [41]	2015	Additive Manufacturing of Ceramics: Issues, Potentialities, and Opportunities	General review
J.W. Halloran [42]	2016	Ceramic Stereolithography: Additive Manufacturing for Ceramics by Photopolymerisation	SL
S.L. Sing et al. [43]	2017	Direct selective laser sintering and melting of ceramics: a review	LS, LM

This article aims to provide a detailed, comprehensive overview of the current state-of-the-art in AM of advanced ceramic materials through a systematic evaluation of the capabilities of each AM technology. An in-depth analysis of the advantages, limitations, opportunities, and issues arising with each AM technology when processing advanced ceramics is provided, and the current industrial and commercial market of ceramic AM is also mentioned. First, a brief explanation of what is described in this review as advanced ceramic materials is provided in Section 2. The most extensive list to date of AM technologies that have been used to shape advanced ceramics is provided in Section 3, with extensive details on achievements in terms of density, surface finish, and mechanical properties. These various results are then carefully analysed and the characteristics, advantages and limitations of AM technologies are compared in Section 4. Finally, short-term and long-term objectives for the AM of advanced ceramics are discussed in Section 5, in order to understand the potential future evolutions in the field better. This review focuses on the mould-less additive manufacture of pure advanced ceramic materials and ceramic matrix composites (CMCs). Therefore, PMC (polymer-matrix) and MMC (metal-matrix) composites using ceramic as reinforcement are not discussed, and results on advanced ceramics obtained through negative AM are not presented.

2. Advanced Ceramic Materials

2.1. Oxide and non-oxide advanced ceramics

Ceramics are inorganic, non-metallic materials typically organised into the following categories based on their nature and industrial use: clays, whiteware, cements, glasses, refractories, abrasives, and advanced ceramics. Advanced ceramics, also called "technical", "engineering", or "fine" ceramics, are mainly polycrystalline materials which, unlike traditional ceramics that are produced from natural sources, are almost always synthetic in nature and/or have been engineered (high purity, tailored particle size distribution, small grain size) to meet the service requirements of increasingly more demanding industrial applications in fields as diverse as aerospace, automotive, biomaterials, communications, transport, energy and defence [44]. Their unique set of physical, chemical, and mechanical properties, including high temperature resistance, superior hardness, high stiffness, low coefficient of friction, and excellent chemical inertness, is a direct consequence of their atomic structure based on rigid ionic and covalent bonds [45].

Advanced ceramics are typically categorised according to their chemical nature as *metal oxides,* such as alumina (Al_2O_3) and zirconia (ZrO_2), or *non-oxides,* such as carbides, nitrides or borides [46]. These high-performance ceramic materials can also be subdivided according to their end-use application into *structural* ceramics, *electroceramics* (which include dielectric, piezoelectric and pyroelectric performance), *optoceramics*, *chemical processing* ceramics, ceramic *coatings*, *bioceramics*, and *superconductors* [47][48].

The most commonly investigated oxide ceramics for AM are Al_2O (due to its versatility, low price, and relatively low sintering temperature) and ZrO_2 (due to its high toughness, relatively low sintering temperature, and widespread industrial applications). Although silica (SiO_2) and silicate ceramics are not always considered to be technical ceramic materials, they are included in this review because of their widespread utilisation across several research groups as a cost-effective alternative to alumina and other advanced ceramics in the initial stages of AM research projects or for biomedical applications. Non-oxide ceramics such as silicon carbide (SiC), tungsten carbide (WC), boron carbide (B_4C), silicon nitride (Si_3N_4), aluminium nitride (AlN), and zirconium diboride (ZrB_2) are usually characterised by a higher temperature resistance as well as increased strength and fracture toughness. Furthermore, whilst oxide ceramics are relatively easy to process, with sintering temperatures rarely exceeding about 1550°C, non-oxide ceramics are much more challenging to process due to their higher hardness, sintering temperatures generally well in excess of 1700°C, and the fact that pressure-assisted firing in a controlled inert atmosphere is often also required.

While oxide and non-oxide advanced ceramics are typically processed and shaped according to the powder processing method ~~described in Section 1,~~ – i.e. shaping and sintering of a ceramic component from a dry or wet ceramic powder mix – they can also be obtained from the pyrolysis of preceramic polymers.

2.2. Polymer-derived Ceramics

Polymer-derived ceramics (PDCs) are another class of advanced ceramics, obtained from the pyrolysis under inert atmospheres at temperatures above 800°C of polymeric precursors into ceramic materials [49]. Non-oxide binary advanced ceramics SiC, Si_3N_4, BN and AlN can be obtained through this route, as well as complex ternary, quaternary and even pentanary ceramic systems, such as SiCN, SiCO, SiBCN, and SiAlCN, which are very difficult or even impossible to produce using the conventional powder processing route [50]. The PDC route starts with preceramic polymers such as polyorganosiloxanes, polyorganosilazanes and polyorganosilylcarbodiimides, and typically leads to silicon-based ceramics, with SiC, Si_3N_4, silicon oxynitride (SiON), silicon oxycarbide (SiOC) and silicon carbonitride (SiCN) being the most commonly studied ceramic systems [51]. Some boron-based ceramics, such as boron nitride (BN) and boron carbonitride (BCN), can also be obtained. PDCs can be used to produce ceramic fibres, coatings or ceramic components and usually offer improved thermomechanical properties over other advanced ceramics, with retention of mechanical properties at temperatures up to 2000°C in oxidising atmosphere [52].

The preceramic polymers route offers an alternative to the more conventional powder processing route with the striking advantage that preceramic polymer feedstock can be processed using forming methods used in the plastic industry, such as injection moulding and resin transfer moulding (RTM). Likewise, preceramic polymers offer an interesting opportunity in the ceramic AM field to produce PDC components using AM technologies designed and optimised for polymers, such as inkjet printing and photopolymerisation-based processes [53].

However, the main drawback of the PDC route lies in the polymer-to-ceramic transformation by pyrolysis itself. Indeed, the high-temperature pyrolysis is characterised by the release of substantial amounts of volatile gaseous species (H_2O, CO_2, H_2, CH_4), which results in high mass loss and significant dimensional shrinkage of 40 to 70%. This tends to prevent the use of preceramic polymers for making ceramic components with a bulk volume greater than a few millimetres without the formation of pores and cracks [54].

2.3. Ceramic matrix composites (CMCs)

Despite their many advantageous physicochemical and thermomechanical properties, nearly all advanced ceramic materials are plagued by the same drawback: ceramics are brittle materials that desperately lack toughness and are prone to catastrophic brittle failure. This critical limitation is one of the main factors that have prevented advanced ceramics from replacing their more ductile metallic counterparts in most engineering applications. CMCs are composite materials where ceramic reinforcements such as continuous fibres, whiskers or nanoparticles are embedded into a ceramic matrix phase; CMCs were developed in an attempt to enhance the properties of single-phase ceramics and address their lack of reliability. Some CMCs have significantly better thermomechanical properties than their single-phase ceramic counterpart, in particular improved thermal shock resistance and increased fracture toughness with higher elongation to rupture, leading to uses as thermostructural components for high-performance applications in demanding service conditions, such as high temperature turbomachinery components as shown in **Figure 6** [55]. The specific properties of CMCs make this class of materials highly desirable for a number of high value-added industrial applications in working conditions where single-phase ceramics and metal matrix composites cannot provide the same performance. As a result, the CMC market is expected to grow at a CAGR of 9.5% between 2019 and 2029, from USD 9.4 billion to USD 23.3 billion [56].

Composite ceramic powders can be synthesised through a number of conventional or advanced processing routes, including solid state, sol-gel, co-precipitation, and hydrothermal synthesis routes [57]. However, the most common CMCs that are currently being used commercially mostly use continuous fibres as reinforcement and include carbon fibres/carbon matrix (C_f/C), C_f/SiC matrix, and SiC_f/SiC [58]. Specific processing techniques are required to manufacture CMCs, and gas- or liquid-phase infiltration methods are usually favoured, such as slurry infiltration, sol-gel infiltration, reactive melt infiltration (RMI), polymer infiltration and pyrolysis (PIP), and chemical vapour infiltration (CVI) [59].
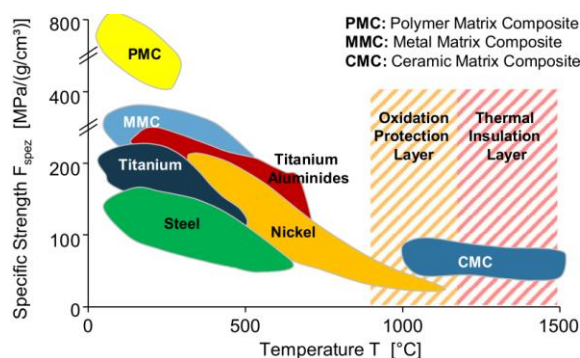

Figure 6: *Specific strength of materials as a function of working temperature for turbomachinery components.* [55]

3. Multi-Step AM Technologies Used to Shape Advanced Ceramics

Although ceramic AM is still considerably less advanced than polymer AM and metal AM due to its many specific challenges, the field has developed considerably in its three decades of existence. Indeed, all AM technologies can be adapted somehow to processes ceramics and most of them have already been demonstrated, although each process has its limitations. This chapter describes in turn each multi-step AM process that has been applied to shape advanced ceramics; both qualitative and quantitative results that have been obtained are presented and discussed.

3.1. Indirect powder bed fusion

The term PBF encompasses AM processes where particles in a powder bed are selectively fused together under the application of a concentrated heat source [60]. Three common AM technologies fall into the general PBF category: laser melting (LM), laser sintering (LS) and electron beam melting (EBM). Whilst the first two technologies can be used to shape ceramics, the latter is generally not applicable as most ceramic materials are not electrically conductive. Several variants of the original LS and LM processes, which were initially created to process polymers and metals respectively, have been developed throughout the years in order to adapt these technologies to the specific requirements of ceramic materials. Local densification of the powder bed can be obtained either by direct laser sintering (dLS) of the advanced ceramic powder itself, which will be presented and discussed in section 4.1, or by indirect laser sintering (iLS) of a sacrificial polymeric or inorganic binder phase that acts as a temporary matrix for the ceramic powder until its removal or conversion by heat treatment. Furthermore, the use of ceramic slurries as feedstock instead of dry powders was introduced in order to enable the use of submicron particles and to reach higher green/sintered densities [61][62][63][64].

3.1.1. Powder-based indirect laser sintering (P-iLS)

In the powder-based indirect LS process (typically referred to in the literature as indirect SLS, iSLS or P-SLS), a coarse[2] ceramic powder, typically 45-90 microns, is mixed with a low melting point polymeric or inorganic binder phase, and local sintering of the powder mix is performed through melting of the binder by the laser beam. The binder provides a solid matrix for the ceramic powder upon its redensification, ensuring the layer-by-layer formation of a green body. P-iLS is usually carried out in a conventional LS machine developed for polymer laser sintering (e.g. Formiga and EOSINT systems by EOS) equipped with a CO_2 laser of wavelength 10.6 μm and power within the range 25-100 W. After completion of the LS process, the green part is transferred into a furnace for heat treatment. When polymeric binders are used, the heat treatment consists of firing the part in an oxidising environment for complete removal of the polymer, followed by furnace sintering at a higher temperature to obtain the final pure ceramic body. P-iLS with organic binders has been used to process a wide range of technical ceramics, including Al_2O_3 [65][66][67][68]–[72], SiO_2 [73], ZrO_2 [73][74], SiC [75][76][77], ZrB_2 [78], as well as apatite-mullite [79] and apatite-wollastonite glass-ceramics [80].

Unlike polymeric binders, low melting point inorganic binders cannot be removed by heat treatment. Instead, they are usually converted by post-LS heat treatment into either a crystalline salt or an oxide ceramic, thus yielding either a single-phase advanced ceramic body or a ceramic composite where a low-strength ceramic acts as the matrix for advanced ceramic particles. Already in 1992, Lakshminarayan *et al.* used 0.43 volume fraction of ammonium phosphate as an inorganic binder to produce a green body composed of alumina particles in an ammonium phosphate matrix [81]. Heat treatment at 850°C for 6h resulted in the conversion of the binder into aluminium phosphate, yielding a composite of unreacted alumina particles in an aluminium phosphate matrix. A very low relative density of 45% and a compressive strength of only ~17 MPa were obtained with a 69 μm average powder size, whereas an 80 μm powder resulted in marginal increase of both relative density and compressive strength to 54% and ~40 MPa, respectively. In 2002, Lee applied a similar approach with monoclinic metaboric acid (HBO_2) as the inorganic binder that converted during post-heat treatment into boron oxide (B_2O_3), which, in turn,

---

[2] The term "coarse powder" is used throughout this review in opposition to colloidal (submicron) powders and few-micron powders (1-10 μm). Coarse ceramic powders typically have an average particle size of several tens of microns up to a few hundreds of microns.

chemically reacted with alumina during firing to form aluminium borate whiskers at the surface of alumina particles [82]. Al_2O_3-B_2O_3 composites fired at 900°C showed a highly anisotropic shrinkage of 2%, 4% and 12% in X, Y and Z, respectively, and an extremely low three-point bending (3PB [3]) flexural strength of ~7.6 MPa. In 1995, Subramanian *et al.* used an aluminium-alumina powder mixture to make pure alumina bodies [83]. The aluminium powder subjected to the laser beam melted to bind the alumina particles and some of the aluminium then reacted with the ambient air to form alumina whilst the residual metal was oxidised by post-heat treatment.

Indirect LS with organic binders has mainly been used to produce highly porous components, but relatively high densities have also been achieved successfully by some research groups using indirect LS with additional pre- and post-processing steps. Several post-processing densification techniques, such as infiltration and isostatic pressing, have indeed been used to further increase green and sintered densities and enhance final mechanical properties. Subramanian *et al.* introduced the infiltration of LSed parts with ceramic colloids, although infiltrated alumina bars had a final density of only 50% TD and highly interconnected porosity resulting in very low 3PB flexural strength of 2-8 MPa [66]. In 2007, Liu *et al.* used ball-milled mixtures of alumina powder and stearic acid binder to manufacture alumina bars with a sintered density of 88% TD and a four-point bending (4PB) flexural strength (ASTM C1161 [84]) of 255 MPa [67]. Similarly, Leu *et al.* prepared 50:50 wt/wt mixtures of ZrB_2 and stearic acid by ball-milling to then manufacture 80% dense samples with a 4PB flexural strength of 195±16 MPa, corresponding to only 44% of the flexural strength of hot pressed ZrB_2 due to the high porosity [85]. The process was later improved to reach 87% theoretical density and 250 MPa flexural strength [78]. Two pre-processing powder preparation methods were developed by Shahzad and Deckers to produce polymer-coated ceramic powders more adapted to the indirect LS process: dispersion polymerisation [71][86] and temperature-induced phase separation (TIPS) [69][68][72][74]. However, the benefits of these methods were limited as the formation of inter-agglomerate pores and cracks still occurred, and sintered densities between 36 and 66% only were achieved without post-processing. The same research team also investigated the influence of several post-LS densification strategies on the final density of complex-shaped alumina parts: laser remelting; cold, warm or quasi isostatic pressing (CIP, WIP and QIP, respectively); and pressure, pressureless or vacuum infiltration of the green or brown body with alumina suspensions [69][71][18]. It was found that several densification strategies involving green or brown infiltration combined with WIPing could significantly increase the final density of LSed parts, although not all could be applied to complex shapes. Relatively higher sintered densities of about 90% were achieved, but crack formation, microstructural irregularities and differential shrinkage often resulted from both the infiltration and pressing steps. In 2013, Liu *et al* reported the use of PVA-epoxy-coated alumina powder prepared by spray drying and blending to manufacture alumina parts by indirect LS [87]. CIPing at a holding pressure of 200 MPa was applied prior to debinding at 1000°C and furnace sintering at 1600°C, and a hot isostatic pressing (HIP) step completed the process. The relative density of alumina gears obtained by the iLS-CIP-sintering-HIP process increased from 32% in the green state to a final density of nearly 96%.

Another approach, based on the selective laser curing (SLC) of an organosilicon preceramic polymer powder mixed with ceramic particles, was developed by Friedel *et al.* at the University of Erlangen-Nuremberg [88]. During SLC, the CO_2 laser beam was irradiated on the 50 volume percent (vol%) polysiloxane/50 vol% SiC powder layer, inducing curing of the polymeric binder phase. Green bodies were then converted into SiOC/SiC ceramic by pyrolysis at 1200°C in argon. This process was characterised by a linear shrinkage of only 3.3% and yielded a 4PB flexural strength of only 17±1.4 MPa due to the formation of microcracks. Parts were subsequently infiltrated with liquid silicon under vacuum at 1500°C, resulting in the decomposition by carbothermal reduction of the SiOC matrix into gaseous SiO and CO, yielding a SiSiC ceramic composite consisting of 65 vol% Si. Final SiSiC parts had no observable porosity and a much higher flexural strength of 220±14 MPa, but also had a visibly rough surface and low SiC content (35 vol%).

---

[3] According to the ASTM Standard C1161-13: "The three-point test configuration exposes only a very small portion of the specimen to the maximum stress. Therefore, three-point flexural strengths (3PB) are likely to be much greater than four-point flexural strengths (4PB). Three-point flexure has some advantages. It uses simpler test fixtures, it is easier to adapt to high temperature and fracture toughness testing, and it is sometimes helpful in Weibull statistical studies. However, four-point flexure is preferred and recommended for most characterization purposes." [84]

One intrinsic limitation of PBF processes in their original form comes from the use of dry powders to deposit layers of ceramic material. Only coarse ceramic particles can be used to form layers in dry PBF processes, because fine ceramic powders are subjected to an increased influence of Van der Waals inter-particle forces during layering, resulting in poor powder flowability and preventing the formation of uniform powder layers – the term "fine powders" typically encompasses powders with an average particle diameter of only a few (1 – 3) microns, but increasingly refers more specifically to submicron- and even nano-powders. Although post-printing densification steps can help improve final density, they only provide a partial and inelegant solution to the low density of laser sintered parts, as the real root of this issue is caused by large inter-particle voids formed within the powder bed during the layer deposition of dry coarse ceramic powders. The low packing density of the powder bed, composed of significant interconnected porosity, is translated to the final part since large voids are not eliminated during the debinding, sintering, and any pressure-based steps. Consequently, increasing the packing density of the powder bed remains the most critical issue to address in order to prevent the formation of inter-agglomerate pores and enable the direct production of fully-dense parts by LS. One approach that researchers have started to investigate is the incorporation of small amounts of nanoparticles into the binder liquid in order to fill the interparticle voids in the powder bed with finer powders, whereas another approach lies in the use of colloidal slurries instead of coarse dry powders.

3.1.2.   Slurry-based indirect laser sintering (S-iLS)

S-iLS was developed to enable the deposition of finer powders by suspending the ceramic powder in a liquid carrier to yield a colloidal suspension. The advantage of using submicron ceramic particles is two-fold. First, fine particles tend to have a wider size distribution than coarser powders, namely a larger relative particle size variation, resulting in improved packing densities, which has a highly positive impact on green density. Second, the driving force of furnace sintering is greatly improved by using finer particles, and the shift from coarse powders to submicron powders therefore results in increased sintered densities. A slurry coating system was designed by Tang *et al.* at the National Taipei University of Technology to pave [4] thin layers of colloidal ceramic slurries using a scraper [89][90]. Using this paving device, Tang *et al.* developed the ceramic laser sintering (CLS) and the ceramic laser fusion (CLF) approaches to process water-based slurries of silica powder and silica sol with clay as low melting point inorganic binder [5] [91][92]. It is the use of clay that is probably key here, as it forms a mouldable mass with water. Although this process only enabled the fabrication of low-strength highly porous silica-clay components, its suitability for manufacturing in a single step ceramic shell moulds for investment casting was demonstrated [93][94]. The CLS process was later modified to produce dense ceramic parts from submicron alumina powders with PVA as the sacrificial polymeric binder [95]. Water-insoluble fully hydrolysed PVA was first coated onto Al_2O_3 particles to act as the main binder. A water-based slurry containing the coated alumina powder as well as small amounts of water-soluble sub-partially hydrolysed PVA as secondary binder was then sequentially paved, dried and laser scanned. Laser irradiation caused both types of PVA to react and form a water-insoluble mixture that bound the alumina particles. The water-insoluble green body could then be easily removed from the water-soluble un-scanned powder bed by immersing in water. Complex-shaped parts with a relative green density of 56.5% could be obtained and, after binder burnout and furnace sintering, the final density reached 98% TD. Besides, parts obtained were free of cracks and delamination, and had a mean flexural strength of 363.5 MPa. Tang also patented in 2004 the ceramic laser gelling (CLG) process [61][96]. CLG is based on the layer-wise selective irradiation by a low power CO_2 laser of a colloidal oxide sol to induce its physical gelling, making it water insoluble whilst the unscanned slurry can be dissolved in water [97][98][99][100].

3.1.3.   Advantages and limitations of iLS

The LS processes is characterised by its self-supporting powder bed, which enables the production of large overhangs and negative hanging features without the need for support structures. PBF processes

---

[4] **Paving** is used here with a similar meaning as in the construction industry, where it means "to cover an area of ground with a hard, flat surface of pieces of stone, concrete, or bricks" (as defined in the Cambridge Dictionary).
[5] **CLS, CLF and CLG** were categorised as "indirect laser sintering" techniques despite producing ceramic components in a single step, due to the fact that an inorganic binder is used as the matrix with the advanced ceramic being only a reinforcement, and therefore the technical ceramic itself is not sintered.

are very well suited to implementing structural grading but they do not enable material (compositional) grading. PBF processes are theoretically scalable, as demonstrated by the many metal LM and polyamide LS industrial machines, although some issues specific to PBF of ceramics need to be taken into account and may render scalability significantly more challenging with ceramics than it is with metals and polymers. Indeed, large amounts of polymeric binder are used in indirect LS, making binder removal difficult for large monolithic cross-sections and resulting in significant shrinkage during furnace densification. Furthermore, relatively coarse powders must be used in PBF processes to ensure a satisfactory powder flowability during layer spreading, because fine powders (monosized few-micron powders and multimodal powders containing submicron particles) do not flow as well due to increased Van-der-Waals interparticle attraction effects [101]. However, using few-microns and submicron ceramic powders is usually preferred in order to reach high sintered densities during furnace densification due to their higher sintering activity.

3.2. Sheet lamination of ceramic tapes

Sheet lamination of ceramic encompasses the laminated object manufacturing (LOM) process and its variant, the computer-aided manufacturing of laminated engineering materials (CAM-LEM) technology. The main difference between these two variants lies in the stack-then-cut approach of LOM whereas CAM-LEM adopts a cut-then-stack approach.

3.2.1. Laminated object manufacturing (LOM)

LOM was developed in the 1980s by Helisys Corporation, with a patent in 1987 and commercialisation in 1991, for the production of 3D objects from sheets of polymer, composite prepregs (pre-impregnated fibre preforms), metal, ceramic green tapes or paper. Ceramic LOM works by sequentially stacking, cutting and bonding ceramic green tapes produced by tape casting [102], extrusion [103][104], or preceramic paper [8], to form the desired geometry. For each layer, the outline of the part is first cut with a computer-controlled knife or CO_2 laser, and a heated roller is then applied onto the surface to thermally activate the binder to promote bonding between adjacent layers. LOM works at low temperature and rolling pressure, which helps minimise issues with warping and delamination. It has been used to produce monolithic components, and the mechanical properties of produced parts have been reported. Monolithic RBSiC parts with a 250 μm layer thickness could be fabricated using a solvent assist spray technique [105]. Unpolished specimens had a 4PB flexural strength of 150 MPa, which was quite low compared with commercial sintered SiC (~400 MPa). SiC/SiC CMCs could also be processed but delamination remained an issue. LOM has also been used to produce Al_2O_3 and SiO_2 ceramic preforms for HIP of tool steel [73]. Biomorphous SiSiC ceramic composite parts were produced by LOM from silicon infiltrated porous biocarbon preforms [103]. First, cellulose-based paper sheets were pyrolysed at up to 800°C in a nitrogen atmosphere and were coated in a LOM device with a phenolic adhesive tape on one side. 18 layers of coated biocarbon paper sheets were then laminated to form 4.5 mm thick samples which were subsequently pyrolysed to convert the phenolic resin into carbon. Finally, highly porous carbonised samples were infiltrated with molten Si at 1500°C in vacuum for 1 h and 7 h. The process was characterised by a low linear shrinkage of only 2% in the XY plane and 1.5% in the Z-direction, and no further shrinkage after infiltration. A 1 h post-infiltration dwell time resulted in a SiSiC ceramic composition of 41 vol% SiC, 33 vol% Si, 26 vol% C, and a 4PB flexural strength of 130±10 MPa. Increasing the infiltration dwell time by 6 h resulted in a higher conversion of carbon into SiC (61 vol% SiC, 23 vol% Si, 16 vol% C) and a similar bending strength at 123±8 MPa. Thus, unreacted residual carbon from the phenolic resin remained in final parts even after a 7 h infiltration. The process was later refined in order to eliminate residual carbon and improve mechanical properties by using SiC powder-rich cellulose hand-sheets instead of commercial filter paper, yielding SiCC sheets upon pyrolysis. By preparing a custom adhesive binder based on polysiloxane and novolac phenolic resin [8], SiSiC ceramics (54.9 vol% Si and 45.1 vol% SiC) were obtained, with no residual carbon and improved 4PB flexural strength of 150-315 MPa depending on testing orientation. Mechanical properties were highly anisotropic due to the layered microstructure of the composites and the presence of silicon-rich layers at the interfaces.

LOM was also used to produce LiO_2-ZrO_2-SiO_2-Al_2O_3 (LZSA) glass-ceramic parts from water-based LZSA sheets prepared by tape casting with polyvinyl alcohol (PVA) as the binder [106]–[108]. Sintered LZSA samples with a 0°/0° stacking orientation had a low 3PB flexural strength of 70 MPa. These laminates were characterised by a high amount of porosity (53-88%) due to internal delamination and a

lower shrinkage in the stacking direction by 5-30%. Adopting a 0°/90° layer stacking resulted in significantly lower porosity since the theoretical density reached 95%, as well as no delamination, leading to an increase of the bending strength to 120 MPa, although a high surface roughness due to stair-casing effect was observed as well as significant warping in the z-direction (**Figure 7**~~Figure 7~~). The effects of small additions of $ZrSiO_4$ were investigated in later experiments [108]. It was found that a 5 wt% $ZrSiO_4$ addition had no impact on the dielectric properties of laminates, but negatively affected density and therefore bending strength too, since LZSA laminates had an 88.55% density and a 3PB flexural strength of 127±6 MPa whilst it was 85.87% and 96±5 MPa, respectively, for LZSA5Zr specimens. However, LZSA5Zr laminates had a nearly constant thermal expansion coefficient (TEC) between 25 and 800°C whereas LZSA laminates were characterised by two main TEC regions within the same temperature range.
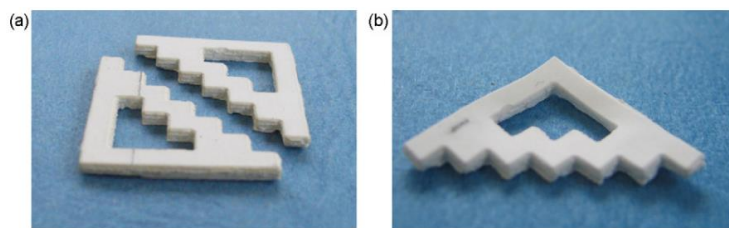

Figure 7: LZSA laminates in stair-like geometry produced by LOM in the green state (a) and after sintering (b). [104]

Rodrigues *et al.* used LOM to process Si_3N_4 tapes containing an acrylic binder [109]. Manufactured samples had a green density of 56% and a sintered density of 97%, and sintering induced a 40% volume shrinkage. Cut, machined and ground mechanical testing specimens exhibited an elastic modulus (ASTM C 1259) of 307GPa, a 4PB flexural strength (ASTM 1161-90) of 918 MPa, a fracture toughness (Single Edge V-Notch Beam method) of 7.45 MPa m$^{1/2}$, and a Vickers hardness (ASTM E 384- 89) of 1457 Kgf/mm^2 were obtained. Zhang *et al.* manufactured Al_2O_3 laminates that had a high green density of 65.4% which translated to a 97.1% sintered density. Linear shrinkage during sintering was highly anisotropic at 34% in the XY plane and 8% in the Z direction, and final specimens had a low hardness of 391 HV, and anisotropic 3PB flexural strength of 228 MPa perpendicular to stacks and 145 MPa when tested parallel to layers [110]. Zhong *et al.* prepared SiC laminates containing B_4C and carbon black as sintering aids [111]. A final density of 98.16% was obtained, 3PB flexural strength of 402±23 MPa, hardness of 19.86±0.17 GPa, toughness of 3.32±0.29 MPa m$^{1/2}$, elastic modulus of 393±41 GPa, and linear shrinkage of 25% in Y direction and 20% in Z. Although no layer interfaces could be observed in sintered bodies, mechanical properties were higher in the stacking direction.

A variant of the LOM process, the "Curved-Layer LOM," uses a non-planar base to specifically produce curved ceramic components and CMC parts with continuous fibres oriented along the curved surface [112][113].

3.2.2. *Computer-aided manufacturing of laminated engineering materials (CAM-LEM)*

The CAM-LEM process is another variant of LOM that uses a "cut-then-stack" approach, where each ceramic green layer is pre-cut before lamination [114][9]. As a result, unlike in LOM, there is no waste material within the build and therefore additional fugitive support material is required for overhanging structures. However, the fact that tapes are pre-cut allows for the production of hollow geometries. It also enables in-layer spatial mixing of materials as well as the implementation of "tangent cutting" [6] for enhanced surface quality [115]. Liu *et al.* used aqueous slurries of Si_3N_4 with 10 wt% sintering aids (3:5 Y_2O_3/Al_2O_3) and PVA as the binder to prepare 150 μm thick tapes that were then dried, cut, and stacked layer by layer under 50 MPa with isostatic pressing at room temperature for 2 min to form green bodies [116]. After debinding and pressureless sintering (1800°C, 60 min, nitrogen atmosphere) a relative density of 93.7% and total linear shrinkage of 23.2% were registered. For each sample, at least 5

---

[6] **Tangent cutting** describes the action of laser cutting the boundary edges of a part tangentially to the physical model surface in order to eliminate stair casing effect usually found in parts manufactured by CAM-LEM.

specimens were cut, ground, polished to 1 μm finish, and chamfered; an average 3PB flexural strength of 475 ±34 MPa was obtained, though this was lower than for injection moulded and extruded parts.

Table 2: Composition of ceramic green tapes used in LOM and CAM-LEM processes.

Ceramic material	Average size or commercial name of the starting powder	Ceramic powder loading	Tape Binder / LOM Adhesive	Binder content	Tape thickness (μm)	Ref.
Al_2O_3	A16	55 vol%	Unspecified thermoplastic	-	254	[73]
	2 μm	63.2 wt%	Polyvinyl butyral (PVB) / Polyvinyl acetate	7 wt%	760	[110]
	A16-SG	69 wt%	Acrylic emulsion binders	15.3 wt%	600	[114]
	-	56.6 vol%	PVB	20.5 vol%	600	[117]
SiO_2	325 mesh	84 wt%	Unspecified	16 wt%	203	[73]
Si_3N_4	0.7 μm	56 vol%	Acrylic binder	-	190	[109]
	GS-44	51.6 vol%	PVB	29.9 vol%	300	[117]
	3–5 μm	49.8 wt%	Polyvinyl alcohol (PVA)	2.75 wt%	150	[109]
SiC	Bimodal 3 μm, 60 μm	-	Unspecified polymeric resin / Butanol solvent assist spray	-	250	[105]
	0.5 μm	23 vol%	PVB / phenolic resin in alcohol	6.06 wt%	150	[111]
RBSiC	4.5 μm	76.8 wt%	Catiofast VFH / Polysiloxane and novolac phenolic resin	7 vol%	240	[8]
LZSA	2 μm	~ 48 wt%	PVA / 5 wt% PVA aqueous solution	10.5 wt%	400, 600	[108]

A16, **A16-SG**, Alcoa, Pittsburgh PA / **GS-44**, AlliedSignal Ceramic Components, Torrance CA / **Catiofast VFH**, Bayer, Germany

3.2.3.   Advantages and limitations of sheet lamination

As listed in ~~Table 4~~Table ~~Table 2~~, LOM and CAM-LEM have been successfully used to manufacture parts from a wide range of oxide and non-oxide advanced ceramic tapes, showing the versatility of sheet lamination regarding the type of ceramic materials that can be processed. However, sheet lamination processes are limited in terms of surface quality due to the creation of surface defects during the decubing [7] step, although this issue can be largely minimised by using adaptive laser crosshatching strategies or surface burnishing [105]. LOMed parts are also usually characterised by a high surface roughness caused by stair casing [8] effects, which are difficult to minimise. The use of non-negligible amounts of binder to promote layer bonding can be detrimental to the final density of sintered parts and results in the formation of pores. As with most lamination methods, the presence of interfacial discontinuity and defects is the main downside of LOM, leading to delamination, differential shrinkage, and interfacial porosity [106][108]. Nevertheless, LOM and CAM-LEM have been used successfully to produce parts with good mechanical properties. As expected, there is usually a significant difference in mechanical properties and shrinkage between stacking direction (Z) and tape plane (XY) [103][106][110][111], and hence this anisotropic behaviour must be taken into account during the design phase.

---

[7] **Decubing** is the step at the end of the LOM process when excess material is stripped away from the part.
[8] **Stair casing** or stair stepping effect is the formation of steps at angled surfaces of 3D printed workpieces due to the limited geometric resolution of layer-by-layer fabrication processes.

3.3. Ceramic material extrusion

Ceramic material extrusion is an AM process in which a ceramic-loaded paste, or a ceramic-loaded filament, or a preceramic polymer filament, is extruded through a nozzle and deposited onto a platform layer-by-layer to form a 3D structure. The many different names used to refer to ceramic material extrusion technologies can be rather confusing. In particular, the terms extrusion freeforming (EFF) [33] and filament-based direct ink writing (DIW) [36] have both been used to refer to the entire family of processes, although the former acronym initially described more specifically a process similar to FDC [118], whilst the latter is now mostly used interchangeably with robocasting. An overview of material extrusion technologies that have been used to shape advanced ceramics is provided in **Table** .

The successful operation of all material extrusion processes relies on the precise control of the rheological properties of the extruded paste or filament. Feedstocks must have a high solid loading of well-dispersed ceramic particles to minimise shrinkage and prevent the formation of porosity and cracks during debinding and sintering heat treatments. They must also have a pseudoplastic (shear-thinning) behaviour to ensure that the very high starting viscosity decreases by several orders of magnitude when subjected to a small increase in shear rate inside the nozzle during deposition [119]. These viscoelastic materials are also designed to have a significant yield stress and can be fitted to the Herschel-Bulkley model for yield-pseudoplastic fluids [120]. Yield stress increases with ceramic solids loading as well as with the addition of a binder/viscosifier such as polyvinylpyrrolidone (PVP) [121], polyethyleneimine (PEI) [122], or Pluronic F-127 [123] or methylcellulose [124], and pastes suitable for extrusion typically have yield stress values ranging between 100 and 1000 Pa [125][126][127][128]. Although thixotropic behaviour can help promote inter-filament bonding, it is usually not desirable as it introduces deposition delays and can result in slumping issues [121]. There are two main types of ceramic material extrusion processes: (i) wax-based extrusion processes, which are discussed in 3.4.1., and (ii) water-based extrusion processes, which are discussed in 3.4.2.

Table 3: *Overview of material extrusion processes used to shape advanced ceramics.*

	Acronym	Technology	Feedstock	Solidification mechanism
Wax-based extrusion processes	**FDC** [129] **EFF** [130]	Fused Deposition of Ceramics Extrusion Freeform Fabrication	Highly loaded filament made of ceramic particles suspended in a thermoplastic polymer or wax.	Glass transition of the polymer binder upon cooling.
	MJS [131]	Multiphase Jet Solidification	Mixture of ceramic and thermoplastic binder powders or pellets.	Glass transition of the polymer binder upon cooling.
	T3DP [132]	Thermoplastic 3D Printing	Highly loaded liquid suspension of ceramic particles in a thermoplastic polymer.	Glass transition of the polymer binder upon cooling.
	PHASE* [133]	Extrusion-Based AM Using Photoinitiated Polymerisation	Medium solids loading photocurable ceramic suspension.	Photo-induced polymerisation of the UV curable binder resin.
Water-based extrusion processes	**RC** [12] **DIW** [36]	Robocasting Direct Ink Writing	Highly loaded aqueous ceramic slurry with low amounts of organic additives (<5 vol%). or Colloidal gel.	Evaporation of the solvent to induce dilatancy of the slurry. or Coagulation by controlled flocculation.
	FEF [11] **ABEF** [134]	Freeze-Form Extrusion Fabrication Aqueous Based Extrusion Fabrication	Highly loaded aqueous paste with low amounts of organics.	Crystallization of the aqueous liquid phase.
	CODE [135]	Ceramic On-Demand Extrusion	Highly loaded aqueous ceramic paste with low amounts of organic additives (<5 vol%).	Partial drying using an infrared lamp, with a liquid oil surrounding the part to prevent non-uniform evaporation from the sides.
	3DGP [136]	3D Gel Printing	Highly loaded aqueous ceramic slurry with gelling agent.	Gelation of HEMA.

*PHASE: acronym suggested by the authors of this review standing, for **Ph**otopolymerisation-**A**ssisted **S**yringe-based **E**xtrusion

3.3.1. Wax-based extrusion processes

In wax-based ceramic material extrusion processes, ceramic powders are suspended in a polymeric dispersion medium, and the resulting polymer/ceramic composite paste or filament is extruded through a small orifice onto a platform.

3.4.1.1. Fused deposition modelling of ceramics (FDC)

In FDC, a highly loaded suspension of ceramic particles in a polymeric binder system similar to injection moulding feedstock is extruded using a standard FDM printer. Sintered ceramics are obtained after subjecting as-printed green parts to debinding and firing. Solids loading range between 45 vol% and 65 vol% depending on the ceramic material. The binder system of a FDC feedstock comprises the base polymer (e.g. PP), an elastomer, a tackifier, and a plasticiser, which respectively provide strength, elasticity, flexibility and plasticity to the filament, whilst a wax is also added to lower the viscosity [10]. FDC has been demonstrated for the fabrication of 3D parts from Al_2O_3 [65], SiO_2 [129], Si_3N_4 [137][138][139], and PZT [140]. A 65 vol% SiO_2 filament was made from SiO_2 powder feedstock with a 70 µm average size. Extruded parts shrank by only 1-4% upon firing, and had a 30% porosity and a flexural strength of 1825±243 psi (12.6±1.7 MPa) [129]. A Si_3N_4 filament (55 vol% AlliedSignal GS-44 powder) was extruded and a green density of 53% was obtained. Sintered parts shrank 16.6±1.3% in XY, 19.3±1.6% in Z, and a sintered density above 98% was obtained [137]. A 4PB flexural strength of 824±110 MPa, Vickers indented 3-Point bend strength of 354±10 MPa, and a tensile strength of up to 3.18 MPa were achieved [138].

Extrusion free-form fabrication (EFF) [118][130][141] and multiphase jet solidification (MJS) [142][131] processes use a similar approach, although MJS feedstock is made of mixtures of ceramic and polymer powders or pellets instead of a filament [143]. Lombardi *et al.* used EFF to process a filament containing 53 vol% Al_2O_3 with 0.5 wt% MgO in liquid acrylic monomers with 200 μm carbon fibres [141]. 60% green density and 90-99% sintered density were achieved, along with a 358 GPa flexural modulus and a 3PB flexural strength of 431-606 MPa. Later, a commercially available Stratasys 3D Modeler retrofitted with a high-pressure extrusion head was used to process a 55 vol% Si_3N_4 filament [130]. Sintering shrinkage was slightly anisotropic at 18±3% in X-Y and 20±5% in Z and a density above 97% was obtained. Polished specimens had a 4PB flexural strength of 613±12 MPa when filaments where deposited in the same direction and the strength was halved (312±71 MPa) when adopting a 0°/90° alternating filament deposition strategy.

These processes have not been used in recent years and most of the research on ceramic material extrusion has moved towards aqueous-based ceramic extrusion processes instead.

3.3.1.2. Thermoplastic 3D printing (T3DP)

Scheithauer *et al.* at the Fraunhofer Institute for Ceramic Technologies and Systems IKTS, Germany, developed a process that combines FDM and robocasting for the additive fabrication of metal, ceramic and metal-ceramic composites [144], and patented the technology in 2015 [145]. In T3DP, ceramic powders are dispersed in a liquefied paraffin-based thermoplastic and suspensions are ball milled at 100°C before being placed in a heated cartridge for extrusion through a nozzle. The process enables the adoption of both continuous and droplet-based deposition strategies, and can also be used to shape hard metals and cemented carbides [146]. Al_2O_3 and ZrO_2 suspensions with solid loadings of 67 vol% and 45 vol%, respectively, could be extruded and simple geometries consisting of stacked lines could be produced and sintered. Densities above 97% and homogenous microstructures with no visible interface between layers were obtained, but photos of printed structures revealed a very low accuracy and poor surface finish [132]. The process was later refined and used to produce a small, well-defined fully-zirconia test component with a much higher accuracy, as well as FGM structures with alternating dense (>99% TD) and porous (~5% porosity) regions by co-depositing a 36 vol% zirconia suspension and a zirconia suspension containing 5 vol% polysaccharide powder as a pore-forming agent, respectively [147]. Thus far, mechanical properties of samples produced by T3DP have not been reported.

3.4.1.3. Photopolymerisation-assisted syringe-based extrusion

A process combining ceramic extrusion and photopolymerisation was developed by Faes *et al.* at KU Leuven, Belgium, in an attempt to combine the respective advantages of each technology [133]. A UV curable ZrO_2 suspension consisting of 30 vol% 3Y-TZP powder in a commercial photopolymeric resin was formulated and could be successfully extruded using a 3Dprinter equipped with a syringe. As-printed layers were only partially polymerised due to the low irradiance of the UV source, which caused slumping of lower layers, so an additional thermal curing step had to be included to complete polymerisation. Sintered samples had a density of 92% TD but, due to the relatively low solids loading (30 vol%), excessive shrinkage during firing resulted in severe cracking.

3.3.2.   Water-based ceramic extrusion processes

In order to address the issues that arise during debinding when using large amounts of polymer as the dispersion medium for ceramic materials, most ceramic extrusion technologies actually use water-based ceramic pastes rather than polymer/ceramic feedstock. These aqueous pastes are typically characterised by a high ceramic powder loading and a low organic content. Several variants of the ceramic extrusion process are based on this approach.

3.4.2.1. Robocasting (RC) / direct ink writing (DIW)

The robocasting process was developed by Cesarano *et al.* at Sandia National Laboratories, USA [12], and was patented in 2000 [148]. In robocasting, which is also often called direct ink writing (DIW), a highly loaded viscous ceramic paste is extruded through a nozzle at ambient temperature and solidifies onto the substrate upon drying in air [119]. Suspension solidification and shape retention after deposition is induced by the pseudoplastic to dilatant transition that occurs upon evaporation of the solvent [119]. The use of a suitable dispersant, mostly acting by electrosteric repulsion, is essential to the formulation

of a homogeneous, well-dispersed paste. Small amounts (0–5 wt%) of other additives, such as thickener, plasticiser and viscosifier, can be added to enhance suspension stability and impart specific rheological properties. Further developments led to the formulation of reversible colloidal gels that can coagulate by controlled flocculation with additions of salts or polyelectrolytes, and set immediately after deposition without drying [149][150][122]. These colloidal inks display improved shape retention properties for the fabrication of free spanning geometries such as lattices without support structures. Instead of extruding in air, deposition can also be carried out into an oil bath, which enables the generation of filaments with diameters under 100 μm [151][127]. It has been suggested that the use of biphasic mixtures instead of colloidal gels could facilitate the use of smaller nozzle orifices to print even finer micro features [152].

DIW has been used to process a very wide range of ceramic materials, including Al_2O_3 [153][126][154][127][155], PZT [156], mullite [157], barium titanate [122], Si_3N_4 [158][159], SiC [160], and B_4C [128][161]. DIW was also used to produce biomedical scaffolds for tissue engineering from tricalcium phosphate (TCP) [31][162][163], hydroxyapatite (HA) [164], HA/β-TCP [165][166][167] [168], wollastonite/TCP [169], C-Al_2O_3 [170], bioactive glass [120][171][172][173], and magnesium aluminate ($MgAl_2O_4$) spinel [174].

Costakis *et al.* fabricated near-net-shaped alumina [126] and boron carbide [128] components from highly loaded aqueous slurries containing respectively 5 vol% PVP and 5 vol% PEI as the binder. Ceramic powder loading had a strong influence on the viscosity and yield stress of slurries as well as on the uniformity of layer height and on slumping and warpage effects. Optimum solids loading was 55 vol% for Al_2O_3 (A-16 SG from Alcoa, d_{50} = 0.48 μm) and 56 vol% for B_4C (HS grade from H.C. Starck, d_{50} = 1.72 μm). A final sintered density of 98% was obtained for alumina specimens, with a 3.17±0.37 μm grain size and a 3PB flexural strength of 156.6±17.5 MPa [126]. B_4C specimens reached an 82% final density after furnace sintering at 2000°C and shrinkage was anisotropic [128].

Feilden *et al.* formulated concentrated hydrogel inks for robocasting of both alumina and silicon carbide [123]. The pastes, which were prepared by adding the fine ceramic powders to a 25 wt% Pluronic stock solution, exhibited the characteristic yield-pseudoplastic rheological behaviour of material extrusion feedstock but they had a higher yield stress, >1k Pa, despite having a slightly lower powder loading (Al_2O_3: 36 vol%, SiC: 39 vol%). Extruded SiC samples were 95% dense whilst Al_2O_3 specimens reached 97% TD. Average 4PB flexural strengths of 300 and 230 MPa, Vickers hardness of 23.4±2 and 18.6±0.8 GPa, and fracture toughness of 3.11±0.17 and 3.31±0.23 MPa√m, were obtained for SiC and Al_2O_3, respectively [123]. However, several critical defects introduced during the printing process, i.e. residual porosity, bubbles, inter-filament delamination, and surface finish, greatly limited the strength and reliability of printed parts depending on the printing direction. Thus, polishing was essential to improve both mechanical strength and reliability.

A 52 vol% Si_3N_4 paste was formulated for robocasting operation and manufactured samples had a 56% green density, which increased to >99% TD after sintering [158]. A linear sintering shrinkage of 16% was observed and a 4PB flexural strength of 737±38 MPa was obtained. Zhao *et al.* also formulated an Si_3N_4 aqueous paste of 62.55 wt% total ceramic loading using Si_3N_4 powder (d_{50} = 0.70 μm) with 6 wt% Y_2O_3 and 4 wt% Al_2O_3 sintering additives, 0.75 wt% TiO_2 colorant, 2.5 wt% high and low molecular weight PEI, respectively, and 0.9 wt% cellulose (HPMC) [159]. They used robocasting to manufacture either macroporous grid-like scaffolds or monolithic parts by using a centre-to-centre spacing between extruded filaments of 910 or 410 μm, respectively. After furnace sintering followed by HIP, monolithic parts experienced a linear shrinkage of 27.8% and a final density (ASTM C373-88) >99% was obtained. 4PB test (ASTM C1674-11) of as-printed unpolished specimens showed a bending strength of 552±68 MPa, and the surface roughness (R_a) measured by AFM was 0.75 μm. Eqtesadi *et al.* manufactured geometrically-complex B_4C components by robocasting followed by pressureless spark plasma sintering (SPS) at 2100°C, and investigated how CIP of the green body at 200 MPa affected densities, shrinkage, and mechanical properties [161]. Without CIP, green densities of 45-53 ±2% were obtained, sintered parts shrank laterally and vertically by 17±1% and 21±2%, respectively, and a 90% TD final density was achieved. With CIP, green densities increased to 51-58 ±2%, a higher sintering shrinkage was observed (20 ±2% laterally and 24 ±1% vertically) as well as a higher sintered density of 95 ±3% TD. A Vickers hardness of 27 GPa and a compressive strength of 1800 MPa were achieved without post-consolidation, whilst applying CIP resulted in lower mechanical properties at 20.5 GPa and 1450 MPa, respectively, showing that on the one hand, CIP induced higher densities and shrinkage, but on the other hand, it probably also created defects and microcracks that were detrimental to the mechanical properties.

To facilitate the manufacture of complex ceramic parts by robocasting, concentrated colloidal inks that act as combustible fugitive support material have been developed; aqueous carbon black-based inks [175] and graphite-based inks [124] have been demonstrated. These inks can be completely removed by combustion during the debinding step without discolouring nor deforming the ceramic part. Besides, Martínez-Vázquez et al. showed that the shrinkage of graphite inks can be engineered to match that of the ceramic ink by adjusting their solid content.

Franchin et al used DIW to manufacture highly-porous CMC structures from preceramic polymer ink loaded with >30 vol% of short carbon fibres. They observed that individual struts did not contain any macro-porosity and noted the good alignment of the short fibres in the extrusion direction, which could be exploited in the future to optimise the microstructural and mechanical properties of printed objects in preferential directions. However, significant residual cracks were observed at the surface of C_{sf}/SiOC struts after pyrolysis, although cracking could be partially mitigated by reducing the amount of short carbon fibres and adding SiC powder as inert filler and SiO_2 as rheology modifier [176].

Feilden also used robocasting to manufacture CMCs using short carbon fibres as the reinforcement, and investigated a number of ceramic matrix systems, including Al_2O_3, SiC (with Al_2O_3-Y_2O_3 sintering aid) and SiC-B_4C as the ceramic matrix [177]. Although sintered samples with appreciable densities could be obtained, all CMC systems showed extensive cracking, either due to thermal expansion mismatch in the case of C_f-Al_2O_3 or due to the fibres reacting with oxides (Al_2O_3, SiO_2 or B_2O_3) at high sintering temperatures and resulting in undesirable grain growth of the ceramic matrix into the fibre.

Chen et al. used DIW of polycarbosilane (PCS)/n-hexane inks to produce various porous structures and scaffolds that were converted into SiC after pyrolysis [178]. The printability of inks as a function of PCS concentration and nozzle diameter was first studied and a stable printing region was determined. Printed parts experienced significant but homogeneous shrinkage during pyrolysis, and feature sizes between 100 and 400 µm were obtained depending on the diameter of the extrusion orifice, although a relatively rough surface and some slumping of spanning struts were observed (Figure 8). To improve the shape retention of printed PDC structures and minimise distortion defects, the addition of SiC whiskers (SiC_w) and particles (SiC_p) reinforcements was then investigated [179]. It was found that both linear shrinkage and weight loss were materially decreased from 18.2% to 8.3% and from 17.5% to 10.6%, respectively, when using a high SiC_p/PCS ratio, and SiC_p content played a determining role in improving the mechanical strength of printed SiC_xO_y-based lattices.
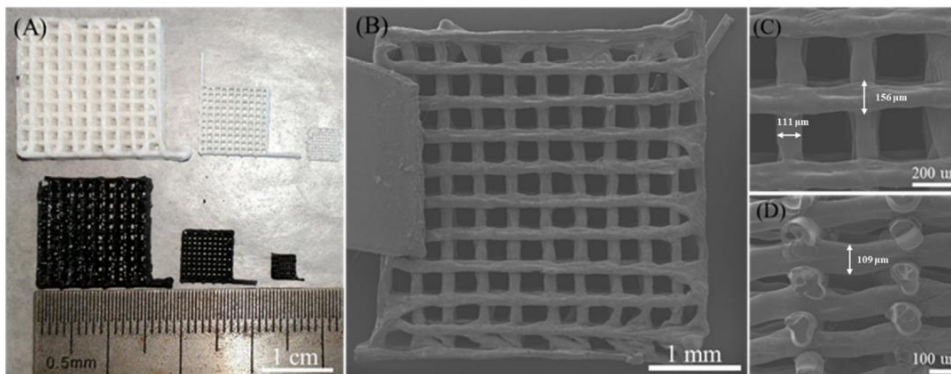
Figure 8: (A) 3D scaffolds (16 layers) assembled from PCS/n-hexane solutions deposited through 400 µm, 200 µm and 100 µm nozzle respectively, before (white) and after (black) pyrolysis. (B to D) SEM images of 3D SiC scaffold assembled through 100 µm nozzle: top view (B-C) and side view (D).

Xia et al. [180] proposed a novel approach involving DIW to produce filaments with a core-shell microstructure where the SiC shell surrounded a highly oriented short C_f core with a core diameter/shell

diameter ratio (d/D ratio) from 0.4 to 0.7 (**Figure 9**). However, the very high porosity of printed parts (52% open porosity, which could be decreased to 31% after several polymer infiltration and pyrolysis steps) severely hindered mechanical properties, showing that there is significant scope for further research and improvement of this promising technique.

Figure 9: (a) Shear rate-dependent viscosity and fitting curve based on the Cross model and (b) Numerical simulation of the co-extrusion process. (c) C_f were highly oriented in the direction of extrusion. (d–g) SEM and CT of Core-Shell filaments with a d/D ratio from 0.4 to 0.7, respectively. [180]
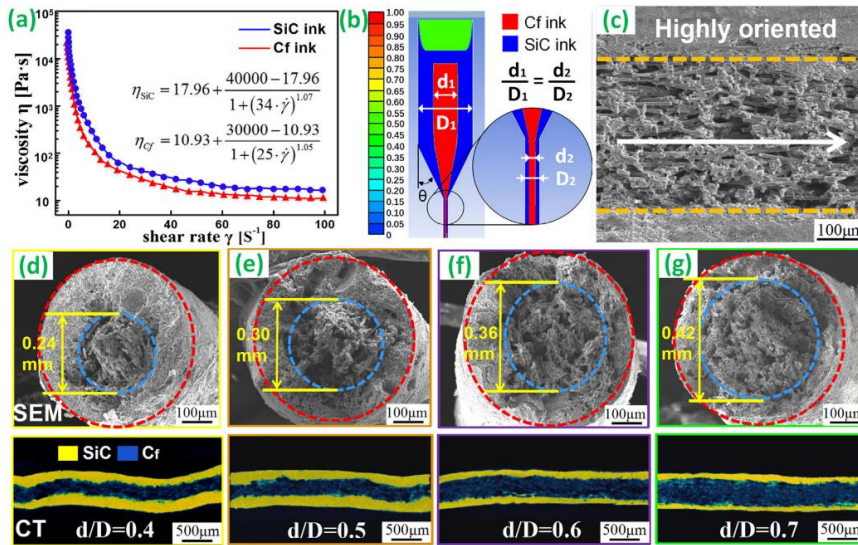
3.3.2.2. Freeze-form extrusion fabrication (FEF)

In FEF, an aqueous ceramic suspension or colloidal gel is extruded through a nozzle and frozen onto the cold substrate as it is deposited [11]. The term aqueous-based extrusion fabrication (ABEF) has also been used to describe the same process for a time [181][134].

FEF has been used to process Al_2O_3 [134], ZrB_2 [182], B_4C [183] and to manufacture bioactive glass (13-93) scaffolds [184]. A triple-extruder FEF system was developed to fabricate parts with functionally graded material (FGM) composition. Test bars with discrete material grading were produced by varying Al_2O_3/ZrO_2 ratios from 100% Al_2O_3 to 50% Al_2O_3-50% ZrO_2 [125]. FGM parts from aqueous-based colloidal suspensions of ZrC and W consisting of a graded composition from 100%ZrC to 50%W- 50%ZrC were also produced [185]. A hybrid extrusion force-velocity controller was implemented to regulate the extrusion flow rate and the deposition velocity better, and obtain a more precise deposition positioning for a more consistent geometry of extruded tracks [186]. Monolithic Al_2O_3 and coloured functionally graded $CaCO_3$ parts were fabricated, although components displayed large surface bumps due to extruded track lines and poor dimensional accuracy (**Figure 10**) [187].
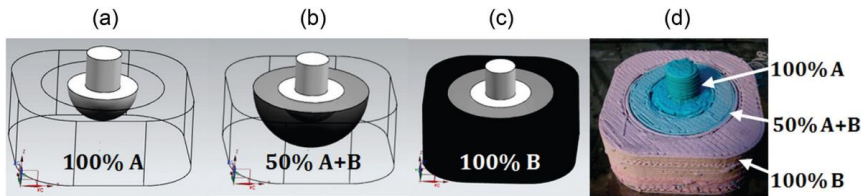
Figure 10: Functionally graded material part fabricated using two CaCO3 pastes. [187]

3.4.2.3. Ceramic on-demand extrusion (CODE)

Ghazanfari *et al.* from the Missouri University of Science and Technology, USA, developed the ceramic on-demand extrusion (CODE) process, in which an aqueous ceramic paste (50-60 vol%) is extruded using an auger valve onto a substrate located in a tank designed to hold a fluid. After each layer is deposited, a mineral oil is pumped into the tank at a controlled-flow rate to a level just below the top surface of the layer. Infrared heating is then applied to partially dry the layer, with the oil precluding undesirable non-uniform water evaporation from the sides, thus preventing warpage and crack formation. To show the capabilities of the technology, Al_2O_3 impellers, gears and spheres were manufactured with sintered densities >98% and uniform microstructures [135]. Smaller components with improved surface finish were also fabricated using a 254 μm nozzle instead of nozzles up to 1.3 mm wide used for larger parts. To manufacture complex parts with overhangs, a calcium carbonate ($CaCO_3$) paste was co-deposited to act as sacrificial support material that was removed by decomposition of $CaCO_3$ into CaO and CO_2 during pre-sintering, followed by dissolving the remaining CaO in acid solution or water before high-temperature sintering. This method was used to produce a 97.5% dense complex Al_2O_3 turbine-blower housing shown in **Figure 11** [188].

The CODE process was also used to produce functional 92% dense alumina components with embedded sapphire optical fibre sensors of 125 μm diameter [189]. It was found that the mechanical integrity and the functionality of the parts were compromised when the sintered density increased or when larger optical fibres were used. Alumina [190] and partially-stabilised zirconia [191] specimens were manufactured with sintered densities of 99% and 98%, respectively. After machining and diamond grinding, Al_2O_3 specimens had a Young's modulus of 371±14 GPa, a 4PB flexural strength of 364±50 MPa, a Weibull modulus of 8.3x0.943, a chevron notch fracture toughness (K_{Ivb}) of 4.5±0.1, and a Vickers hardness of 19.8±0.6 GPa. Linear sintering shrinkage was quasi-isotropic and the microstructure was composed of equiaxed grains <5 μm. These mechanical properties matched or surpassed values obtained using conventional manufacturing techniques in the literature. The mechanical properties of as-printed samples were not measured.

3Y-TZP (d_{50} = 40 nm) was processed by CODE and a maximum relative density of 98.8% was first achieved [192], later improved to 99.2% [193]. A near-isotropic linear sintering shrinkage of ~20% was observed and the average size of zirconia grains was between 0.52 and 0.81 μm. Vickers hardness and fracture toughness were 13.1 GPa and 4.6 MPa $m^{0.5}$, respectively. The flexural strength obtained from 4PB test performed on standard specimens cut from a sintered printed block was 563 MPa, from which the 3PB flexural strength was estimated as 715 MPa. CODE was also used to process 8YSZ (d_{50} = 52 nm) and printed components reached 99% sintered density, with a total volumetric sintering shrinkage of 53.2% [135]. There was no intergranular porosity, whilst intragranular pores under 1 μm were found. A hardness of 14.5±0.2 GPa, an average flexural strength of 278±59 MPa, and a K_{Ivb} fracture toughness of 2.5±0.1 MPa $m^{0.5}$ were measured, the latter comparing to a Vickers indentation fracture (VIF) toughness of 3.61±0.08 MPa $m^{0.5}$. The authors also pointed out that Quinn and Bradt recommended that the VIF toughness method should no longer be used due to its lack of reliability [194].

Finally, the suitability of CODE for manufacturing FGM specimens graded from pure Al_2O_3 to Al_2O_3/ZrO_2 with varying composition gradients was evaluated [195]. A 1% average error in material composition was observed compared to the original design of compositions, and it was found that greater material composition gradients led to larger delamination and curling.
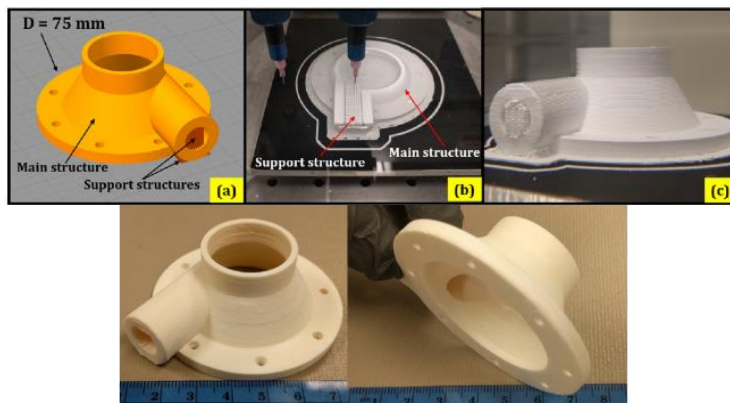
Figure 11: **TOP:** *Sample turbine-blower housing:* **(a)** *CAD model with main and support structures,* **(b)** *part being printed,* **(c)** *completely printed part surrounded by oil.*
BOTTOM: *Final turbine-blower housing part after removal of support and sintering.* [188]

3.3.2.4. 3D gel printing (3DGP)

3DGP was developed by Shao *et al.* at the University of Science and Technology Beijing, China, and relies on the gelation of 2-hydroxyethyl methacrylate (HEMA) to produce green parts [196]. To produce zirconia components, a high solids loading aqueous slurry containing 50 vol% 3Y-TZP powder with 0.3% dispersant was co-extruded through a 500 µm nozzle with a solution containing N,N,N',N'-tetramethylethylenediamine and ammonium persulphate as the catalyst and initiator, respectively [136]. It was found that a 50 vol% ceramic loading was optimal as higher loadings were too viscous to be extruded and settled too rapidly, whilst printed parts experienced significant distortion at lower loadings.

3.3.3. Advantages and limitations of ceramic extrusion

The primary advantages of ceramic material extrusion processes concern their relative ease of operation as well as the low manufacturing costs as a result of the processes not involving any high-energy beams. Furthermore, water-based extrusion techniques DIW, FEF and CODE make use of highly loaded aqueous slurries with minimal binder content, which has a number of additional advantages compared to wax-based extrusion: (i) high green densities, (ii) simplified debinding schedule, (iii) low sintering shrinkage, (iv) environmentally-friendly, (v) low cost of feedstock and hardware [119][153]. Unlike wax-based extrusion processes, DIW and FEF should enable the production of thick cross-sections with appreciable densities due to the very low amounts of organic additives in the feedstock formulation; this has already been demonstrated using CODE [188]. On the other hand, FDC, EFF and other wax-based extrusion processes may provide more freedom than water-based extrusion in terms of geometrical complexity when manufacturing small components due to the use of a thermoplastic polymer as the structural matrix, which enables the formation of stiffer struts for the production of small overhangs without the need for a secondary support material.

However, extrusion-based AM processes still have some major issues. The mechanical properties of extruded parts are typically highly anisotropic and largely depend on the raster printing orientation strategy. Surface bumpiness and stair casing effects remain an aesthetic issue, although **Figure 12** shows that the surface finish can be substantially improved using finer nozzles [188]. The latter have some drawbacks, such as much longer printing times, which increase the likelihood of printing defects occurring, as well as a higher propensity for nozzle clogging. However, they also have several important advantages, including significantly higher resolution, lower surface roughness, improved geometrical accuracy, and enhanced shape retention. Surface roughness is also a source of critical defects that limit the mechanical reliability of as-printed parts, but mechanically strong parts were obtained after post-process machining and grinding [135][123][191] (though this reduces the primary advantage of using

AM). Extrusion-based processes are also inherently restricted in terms of printing throughput, since fabrication time increases linearly with part volume, although this issue can be partially addressed by using a larger extrusion orifice or multiple printing nozzles. However, the nozzle diameter has a direct effect on layer thickness and resolution, and a compromise must thus be made between productivity and resolution, making extrusion-based ceramic AM relatively unsuited to produce large components with a good surface finish without resorting to post-process machining. Instead of using finer and finer nozzles to improve the surface finish of extruded components or resorting to post-AM machining, another approach that has been investigated is the implementation of a hybrid additive-subtractive manufacturing process that combines DIW with *in-situ* machining. Hinton et al. [197] demonstrated the ability of this approach to manufacture near-fully dense alumina components with significantly improved surface finish compared to the same components made without *in-situ* machining, as shown in **Figure 13**, with a decrease in surface roughness (R_a) from 8.09 μm for non-machined parts to 1.11 μm for machined components. The process yielded monolithic alumina components with densities above 99.8% and 3PB flexural strength of 218 MPa [198], although this value is low compared to conventionally processed alumina. This hybrid additive-subtractive approach is therefore promising but further research is needed to better evaluate the influence of *in-situ* green machining on the introduction of surface defects that could adversely affect the mechanical properties of 3D printed parts. Moreover, the additional machining step results in decreased manufacturing throughput as well as increased manufacturing cost. However, calculations of manufacturing throughput and cost would have to consider that *in-situ* machining would prevent the need to use a smaller extrusion orifice, therefore increasing extrusion throughput, and potentially removing the need for post-sintering machining, therefore reducing costs substantially.
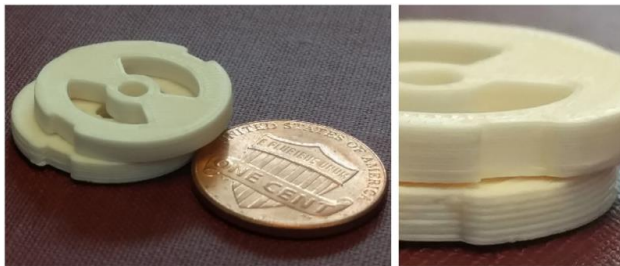

Figure 12: *A part printed by CODE with a fine nozzle on top of the same part printed with a large nozzle.* [188]
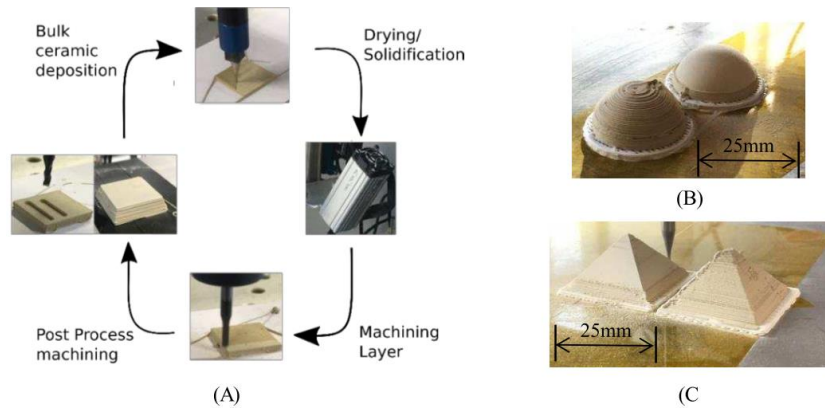
Figure 13: *Process flow for the hybrid additive-subtractive manufacturing of ceramics (A). The surface finish of 3D printed components is significantly improved when using the hybrid manufacturing approach, as demonstrated by hollow hemispheres (B) and pyramids (C)* [197]

3.4. Direct inkjet printing (DIP)

Material jetting is defined by ISO/ASTM standard 52900:2015(E) as an AM process in which droplets of build material are selectively deposited to directly shape 3D parts onto a substrate [60]. In the context of ceramic AM, material jetting is usually called direct inkjet printing (DIP). In DIP, the jetted ink is either *(i)* a well-dispersed suspension of submicron ceramic particles in water or an organic solvent, or *(ii)* a wax-based ink containing submicron ceramic particles. DIP can be performed either by jetting a constant flow of ceramic ink or by adopting a drop-on-demand (DoD) approach [199]. In continuous inkjet printing (CIJ), an uninterrupted flow of individual droplets of electrically charged ink is generated, and unwanted droplets are caught before hitting the substrate using deflecting electrodes. These unprinted droplets are then redistributed to the ink reservoir to be reused. DoD on the other hand is a non-continuous approach where individual droplets are generated by the pressure pulses induced by the excitation of a piezoelectric or thermal actuator at controlled frequencies. As a result, ink droplets are deposited only when and where required. Whilst the building rate of DoD is slower than that of CIJ, its wider range of jettable materials, lower risk for ink contamination, higher resolution, and better accuracy make it more suited to the fabrication of 3D objects [200]. Besides, piezoelectric actuators are suited to a larger variety of solvents than thermal actuators, the latter being restricted to water-based inks only [201]. DoD inkjet printing performance is highly dependent on the physical properties of the ink, particularly its viscosity and surface tension [202][203]. The jettability of a printing ink is often determined using the dimensionless Z parameter, inverse of the Ohnesorge number Oh, which is a function of the density, viscosity and surface tension of the fluid as well as the diameter of the printing nozzle. The range 1< Z < 10 was first suggested by Reis and Derby for a stable drop generation without satellite droplets formation nor excessive viscous dissipation [204], whereas Jang *et al.* suggested the range 4 < Z < 14 [205]. Beside ink properties, printing parameters such as jetting frequency, travel speed, acoustic wave speed, and nozzle-substrate distance also have a strong influence on the jettability [204][206]. The use of optimised quantities of dispersants, surfactants, humectants, and plasticisers is key to formulate stable ceramic suspensions suitable for inkjetting with physical properties adjusted within the required range for jettability. Furthermore, because jetting nozzles typically have a diameter between 10 and 60 μm, only fine submicrometric or nanopowders must be used in order to avoid nozzle clogging and improve suspension stability. It is vital that the ceramic solid loading be high enough so that a high green density can be obtained as well as to avoid issues with excessive shrinkage and cracking, whilst ensuring viscosity remains low enough for the ink to be printable. Therefore, powder loading is usually formulated in the range 20-30 vol% [207], although paraffin wax-based inks containing up to 45 vol% Al_2O_3 powder were successfully jetted by applying a slight overpressure of ~10 kPa to the ink reservoir and using a higher piezoelectric driving voltage [208][209].

3.4.1. DIP of solvent-based suspensions (solvent-DIP)

Solvent-DIP has been used to process a broad range of advanced ceramic materials, from alumina and zirconia to silicon carbide and silicon nitride, as detailed in **Table 4**.

Mott and Evans studied the jetting behaviour of suspensions of polycarbosilane preceramic polymer with submicrometric SiC particles in n-paraffin solvents of various molecular weight, with polyisobutene succinimide as a dispersant [210]. The molecular weight of the solvent had a strong influence on its evaporation rate and therefore on ink printability: whilst compositions based on n-heptane (0.684 g cm^{-3}) could not be printed due to fast evaporation at the nozzle tip and n-decane (0.730 g cm^{-3}) required at least 1 min drying time between adjacent rows, n-octane (0.703 g cm^{-3}) could be jetted reliably and required 5 s delay. A low volume shrinkage of 8.2% was obtained after pyrolysis, but a high porosity of 34% could not be avoided.

Zhao *et al.* demonstrated the use of DIP to produce dense zirconia pillar arrays [211] and thin walls [212]. The ceramic ink was a 14.2 vol% suspension of fine ZrO_2 (450 nm) in a 4:1 octane-IPA solution. The diameter of printing nozzles was 15 microns, printing was performed with a 500 mm/s travel speed and a resolution of 180x180 dpi, and each layer was dried for 20s by hot air blowing at 45°C. 2mm-high walls made up of 4900 layers were printed, giving an average layer thickness of only 0.4 microns due to the small droplet size, solvent evaporation, and mispositioning of the printing table leading to accuracy and repeatability issues. Nevertheless, well defined fully dense features with smooth surfaces could be obtained, although a higher than expected linear sintering shrinkage as well as non-uniform pillar height and wall width were observed because of residual solvent and faster drying at the edges.

Table 4: *Ceramic suspensions that have been successfully jetted by solvent-DIP.*

Ceramic material	Particle size (μm)	Solids loading (vol%)	Solvent	Dispersant	Other additives	Nozzle diam. (μm)	Viscosity (mPa.s)	Year [Ref.]
SiC	~0.6 (d$_{50}$)	10	n-Octane	3.1 vol% ADX201, polyisobutene succinimide diluted in 30 wt% mineral oil	6.9 vol% Polycarbosilane	65	~ 1.6	2001 [210]
Si$_3$N$_4$	0.3-0.4 (d$_{50}$)	30.2	Distilled water	0.2 wt% polyacrylic and carboxylic acid-based polyelectrolyte	Ethanol, Glycerol, PEG 400,	30	9.1	2011 [213]
MoSi$_2$	0.3-0.4 (d$_{50}$)	26.7	Distilled water	Dolapix CE64	Ethanol, Glycerine, PEG 400	30	6.9	2011 [213]
3Y-TZP (ZrO2)	0.45 (d$_{50}$)	14.21	1:4 IPA-octane	Solsperse 13940	2.84 vol% wax	15	-	2002 [211]
	0.683 (d$_{90}$)	24.2	Water	1 wt.% Dolapix CE64	10 wt.% ethylene glycol	30	10	2009 [214]
	0.6 (d$_{50}$)	27	Distilled water	Dolapix CE64	Glycerol, Ethanol, Inorganic binder	30		2014 [15]
	0.2 (d$_{90}$)	21	Water	0.5 vol% DolapixCE64	Ethanol, Ethylene glycol, PEG 400, Anti-foaming agent	24	4.8	2015 [215]
PZT	0.4 (d$_{50}$)	10	Water	-	High molecular weight binder, Surfactant	52	10	2009 [216]
TiO$_2$	0.4 (d$_{50}$)	15	Water	-	High molecular weight binder, Surfactant	52	10	2009 [216]
Al$_2$O$_3$	0.193 (d$_{90}$)	21	Water	-	Ethanol, Ethylene glycol, PEG 400, Anti-foaming agent	24	4.5	2015 [215]
	< 0.6	15	Water	-	-	36	15.94	2016 [217]

Chen and Brandon at Imperial College London inkjet-printed a water-based Al_2O_3 suspension ($d_{50} <$ 0.6 µm) to manufacture defect-free porous alumina multilayers [217]. The mechanical properties, calculated from nano-indentation measurements, and microstructure obtained from two different sintering schedules were compared. After sintering at 1300°C, an average grain size of ~241 nm was observed, and a very high porosity of 41% was obtained, which resulted in poor mechanical properties (E = 92 GPa and indentation hardness H = 1.46 GPa). Specimens sintered at 1500°C had coarser grains of ~1.5 µm, but porosity was significantly reduced, although still relatively high at 14%, and mechanical properties were much higher as a result (E = 250 GPa, indentation hardness H = 6.57 GPa).

Cappi *et al.* from RWTH Aachen University used DIP to jet highly-loaded aqueous ceramic suspensions of Si_3N_4 [218]. After pressureless sintering, they measured a mean grain size of 0.75 µm (a-axis) and 3.0 µm (c-axis), a fracture toughness K_{Ic} (ICL method) of 4.4 MPa m$^{0.5}$, which was low due to the small c/a ratio of the grains, and a hardness value (HV 0.2) of 17. At the same university, Mareike *et al.* used solvent-DIP to manufacture 3D components from both oxide and non-oxide ceramics [15]. 3Y-TZP zirconia ($d_{50} =$ 0.28 µm) components had a sintered density of 97% and experienced an isotropic linear firing shrinkage of 20%. Small specimens (3 x 4 x 0.3 mm^3) had a biaxial flexural strength of up to 1393 MPa (ball-on-three-balls (B3B) test), a Weibull modulus of 10.4, and a VIF fracture toughness of up to 8.9 MPa m$^{0.5}$. With Si_3N_4 ($d_{50} =$ 0.5 µm), a green density >50% and a sintered density of 96.4% were achieved. A B3B flexural strength of 643.8 MPa and a Weibull modulus of 1.8 were measured, as well as a Vickers hardness and fracture toughness of 15.1 GPa and 8.7 MPa m$^{0.5}$, respectively. $MoSi_2$ ($d_{50} =$ 2.8 µm) specimens were fabricated with a green density of <50%, which resulted in a lower sintered density of 87.9%, with the formation of amorphous SiO_2 at triple points. B3B flexural strength, Weibull modulus, Vickers hardness, and fracture toughness were measured at 677.6 MPa, 3.3, 10.8 GPa, and 4.7 MPa m$^{0.5}$, respectively.

Another technology that can be broadly classified as DIP is the pressurised spray deposition (PSD) technology developed by HotEnd Works LLC (Ohio, USA), where a proprietary slurry formulation of fine ceramic powder with a binder is heated and pressurised for deposition by spraying. A second material that they call the binder, which is in fact the support material, is co-deposited from a second nozzle. Polymeric phases are then removed by thermal debinding at temperatures below 150°C before furnace sintering. The American start-up, founded in 2012, claimed to commonly achieve fired densities >98% with alumina, zirconia, and other ceramics [219]. Alumina disks produced using the PSD technology had a sintered density above 99.7% TD, but very large voids several millimetres long severely limited the mechanical properties of the samples [220]. Alumina tiles manufactured by PSD had a density of 3.89 g cm^{-3}, corresponding to ~98% TD, a flexural strength (ASTM C1684 [221]) of 130±38 MPa, and a Knoop hardness (ASTM C1326 [222]) of 17.7±1.0 GPa [223]. These tiles were tested for ballistic impact and were compared to both commercially available tiles manufactured by die pressing [224]. Despite having mechanical properties similar to that of the reference material, additively manufactured tiles were 13% less effective against ballistic penetration, most likely due to the slightly lower sintered density and the presence of flaws generated during PSD fabrication. They also had lower mechanical properties than tiles made using direct ink writing [225].

3.4.2.   DIP of wax-based inks (wax-DIP)

Wax-DIP is based on the hot-melt or phase-change printing approach: ceramic powders are suspended in a low melting point wax which, after ejection from the printing nozzles at a temperature above its melting point, solidifies onto the substrate upon impact cooling. There is therefore no solvent drying cycle in wax-DIP. **Table**   shows the composition of alumina suspensions that were successfully processed using this technique.

Table 5: Ceramic suspensions that have been successfully jetted by wax-DIP.

Ceramic material	Average particle size (µm)	Solid loading (vol%)	Wax system	Dispersant	Nozzle diameter (µm)	Viscosity (mPa.s)	Ref.
Al_2O_3	0.44	30	Paraffin wax	2% Hypermer FP1 / 4% Sterylamine	-	14.5	[207]
Al_2O_3	0.3	35	2:1 paraffin wax-kerosene	Hypermer LP1 / 1-octadecylamine	75	22	[226]

3.4.3. Advantages and limitations of DIP

DIP is characterised by a high resolution thanks to the deposition of droplets with a volume of a few picoliters. Moreover, fully dense components with an excellent surface finish can be obtained. Solvent-DIP enables the fabrication of green parts containing very low amounts of organics, providing improved sintering behaviour and a lower linear shrinkage upon firing. Aqueous-DIP in particular is desirable for a more environmentally friendly and less hazardous alternative to organic solvent-based DIP.

The unique advantage of DIP over all other AM technologies lies in the ability to deposit droplets of multiple materials simultaneously, enabling the fabrication of FGMs and voxel-wise microstructure tailoring. Mott and Evans fabricated a one-dimensional ZrO_2/Al_2O_3 FGM but experienced issues with differential sintering and cracking [227]. Gingter *et al.* manufactured 3Y-TZP/Al_2O_3 FGMs cylinders with a diameter of 10 mm [215]; cylinders made of 800 individual layers with a 2 µm thickness were printed on a substrate at 80℃. A high sintered density was obtained (97.5% TD). Simultaneous jetting is also useful for the deposition of droplets of support material, and it has already been used to print sacrificial support structures based on carbon black to enable the fabrication of complex shapes and overhangs such as dental bridge frameworks [228]. Furthermore, the suitability of DIP for manufacturing dense fully ceramic parts from both oxide and non-oxide ceramic materials has already been demonstrated. DIP can *a priori* be used to shape any ceramic material as long as a stable suspension of submicron powders with the required physical properties for jetting can be formulated. The fact that the use of submicron or nanoparticles is required for the ceramic ink to be jettable results in a higher particle packing during deposition and a higher furnace sintering activity, which are both highly beneficial to the final density of printed products.

One of the main disadvantages of the DIP process is its relatively slow building rate, which is the trade-off for its high resolution. Indeed, each pass of the printhead depositing picoliter droplets results in the formation of a very thin layer leading to a height increment rate of only about 2 mm/h at best. Besides, defects are easily generated in DIP because of the difficulty to ensure printing consistency and reliability. Nozzle clogging is still a major issue when jetting ceramic suspensions, which can easily cause missing features, uneven layer thicknesses, or deposition inaccuracies.

XJet (XJet Ltd., Rehovot, Israel) recently unveiled a line of AM systems for metals and ceramics based on the NanoParticle Jetting™ (NPJ) technology [229]. The process effectively uses well-dispersed non-aqueous suspensions of ceramic nanoparticles as build material for DIP. The technology has so far been demonstrated for zirconia, with final densities reaching 99.9% TD, a hardness of 12.3 GPa, and a roughness between N10 and N7 (12.5 > R_a > 1.6) [230]. It is claimed that complex geometries can be fabricated by simultaneously jetting a second material to build sacrificial support structures that can be dissolved in water, although printed parts with overhangs have yet to be demonstrated. By jetting picoliter size droplets and building layers as thin as 10 µm, resolution and accuracy of 20-100 µm are achieved, so that complex parts such as those in **Figure 14**~~Figure 14~~~~Figure 13~~ can be built almost free of stair casing effect. The trade-off, however, is a relatively slow building rate of only 1 to 1.5 mm height increment per hour, despite the use of 24 printhead each equipped with 512 jetting nozzles, showing that significant hardware complexity is required for scale-up.

Figure 14: *Fully-zirconia demonstration parts manufactured with XJet's NPJ technology (Images provided as a courtesy by Mr. Avi Cohen, VP Healthcare & Education at XJet).*

3.5. Binder jetting

The original binder jetting process was invented by Emanuel M. Sachs, John S. Haggerty, Michael J. Cima, and Paul A. Williams from the MIT in the late 80s, with a patent filed in December 1989 [231]. The technology, coined three-dimensional printing (3DP) at the time, a term that is now usually used to refer to all AM processes, has been licensed to several companies. The BJ process manufactures 3D structures by selectively depositing droplets of a liquid binding agent onto a powder bed of coarse ceramic powder. As the binder penetrates into the powder bed by capillarity, ceramic particles are joined to form a pattern as defined by the STL file. This process is repeated layer after layer until a printed ceramic green body is obtained. After its removal from the unprinted powder bed, the green part is subjected to debinding and sintering schedules, which are potentially preceded by a binder activation heat treatment and/or followed by additional densification steps.

3.5.1. Powder-based binder jetting (P-BJ)

In P-BJ, a coarse ceramic powder is used as feedstock and is typically spread into thin layers by a roller. This technology has thus been extensively used to additively manufacture porous ceramic components, especially for biomedical applications such as scaffolds for tissue engineering [232][233][234][235][236]. However, P-BJ does not enable the manufacture of monolithic ceramic parts since coarse powders result in a highly porous powder compact upon spreading, and it usually yields final relative densities of between 20 and 70% [234][237][238][239], although higher densities have been achieved using either high binder saturations [240][241], WIP [242], uniaxial and cold isostatic pressing [243] or infiltration [244].

WIP was applied to 3D printed Al_2O_3 and MgO-doped Al_2O_3 [242]. Whilst as-printed Al_2O_3 green parts had a low density of 36%, a high fired density of 97.8% was obtained after WIP, with a 4PB flexural strength (ASTM C1961-90) of 231.5 MPa. Doping Al_2O_3 with MgO resulted in even better properties: despite a lower green density of 34%, a fired density as high as 99.2% was obtained, as well as a 40% higher 4PB flexural strength of 324 MPa.

Carrijo *et al.* studied the effect of uniaxial pressing and CIP on the density of titanium silicon carbide (Ti_3SiC_2) parts manufactured by binder jetting with dextrin as the binder [243]. They showed that high uniaxial or CIP pressures were beneficial in increasing the density and flexural strength of sintered parts. The remaining porosity in sintered specimens CIPed at 180 MPa was only 3.6% and was even lower at 1.7% for samples uniaxially pressed under 726 MPa, whilst porosity of sintered specimens not subjected to a post-densification step was as high as 48%.

Zocca *et al.* have used the preceramic polymer approach to manufacture SiOC parts with ordered porosity [245] and porous wollastonite-based silicate bioceramic scaffolds [246]. SiOC parts were manufactured from a preceramic polymer powder and, by using a mixture of 1-hexanol and hexylacetate as the printing solvent, a relative density of 80% could be achieved both in the as-printed polymeric state and in the post-firing ceramic state.

Gonzales *et al.* from The University of Texas at El Paso investigated the effect of powder particle size, layer thickness and sintering time on the density and mechanical properties of binder jetted Al_2O_3 samples [241]. They showed that powder particle size had a significant influence on final density, and found that fired density increased from < 70% to > 90% by decreasing the powder size from 53 μm to 30

μm or by using a blend of powders (53, 45, and 30 μm) for a larger particle size dispersion. However, sintering shrinkage was highly anisotropic, at 8.75% in the X direction, 10.92% in Y, and 15.37% in Z. Furthermore, despite having a relatively low effect on final density, the sintering profiles strongly affected final mechanical properties. Indeed, by increasing sintering time from 2 h to 16 h, the maximum compressive strength (ASTM C773-88) was nearly doubled, from 77.86 to 146.60 MPa, Young's modulus increased by 70% from 31.25 GPa to 54.14 GPa, and Vickers hardness experienced a six-fold increase from 240 MPa to 1.51 GPa.

Zhang *et al.* fabricated Al_2O_3/glass composites by P-BJ of Al_2O_3 preforms followed by pressureless infiltration of LAS glass into sintered porous preforms at 1100°C for 2 h [244]. An alumina/dextrin powder blend (0.1 to 150 μm freeze-dried granules) was used as feedstock. By reducing the layer thickness of powder layers from 150 μm to 90 μm, the porosity of alumina preforms decreased from 39 vol% to 19 vol%, inducing an increase of the bending strength from 29±11 to 98±6 MPa and of the Young's modulus from 55±24 to 178±23 GPa. After LAS glass infiltration, Al_2O_3/glass composites exhibited the following mechanical properties: fracture toughness of 3.6 MPa $m^{1/2}$, 4PB flexural strength of 175 MPa, Young's modulus of 228 GPa, and Vickers hardness of 12 GPa.

Fu *et al.* at the University of Erlangen-Nuremberg [247] used BJ to manufacture SiSiC components from powder blends of Si (d_{50} = 19.4 μm), SiC (d_{50} = 16.2 μm), and 18 vol% dextrin (d_{50} = 109 μm). Parts were infiltrated in the green state with liquid silicone resin and, after conversion into SiC, the following mechanical properties were measured: 4PB flexural strength (DIN EN 843-5), SEVNB fracture toughness (DIN CEN/TS 14425-5), and Young's modulus (DIN EN 843-2). On the one hand, it was found that when using a powder blend made of 40% SiC, printed components had a green density of ~39% and a final porosity of 1.1% after sintering, with an elastic modulus of 225 GPa, a 4PB flexural strength of 183 MPa, and a fracture toughness K_{IC} of 2.0 MPa $m^{0.5}$. On the other hand, a 49% SiC powder content resulted in a higher green density of ~43% and a lower final porosity of 0.5%, which in turn led to higher mechanical properties, with a 256 GPa elastic modulus, 4PB flexural strength of 208 MPa, and fracture toughness of 2.5 MPa $m^{0.5}$.

3.5.2. Slurry-based binder jetting (S-BJ)

Slurry-based binder jetting (S-BJ) was developed to enhance the binder jetting process by introducing colloidal ceramic processing into the technology. The powder bed is formed by making layers of ceramic slurries instead of dry powders, thus enabling the use of submicron powders to improve the powder bed packing density, therefore increasing the green and sintered densities. The slurry-based three-dimensional printing (S-3DP) process was developed by the same group that invented the binder jetting process at the MIT in the late 90s [231][248][249]. The group last reported working on the technology in 2007 [250]. Ceramic green layers were deposited by inkjet printing a ~30 vol% water or water-alcohol-based ceramic colloidal suspension over a substrate. Each individual jetted layer was then slip cast onto the previous layer, resulting in much denser powder compacts than in traditional binder jetting. Grau showed that doctor blading was also suitable for making thin and smooth layers with 30 vol% ceramic slurries [248]. After completion of the printing process, the powder bed was first heat treated at 150°C in argon to crosslink the binder and was then immersed in water or ethanol and sonicated to remove the unbound powder from the insoluble green part. The implications of using ceramic slurries instead of dry powders and powder beds of submicron particles on the infiltration of various types of polymeric binders was studied by Grau [248] and Holman [251]. It was found that whilst latex and wax emulsion binders did not readily penetrate powder beds, homogenous solution-phase binders of 10 vol% styrene-acrylic copolymer in water or 10 vol% furfuryl resin in acetone were suitable binders [252]. By using DoD jetting instead of CIJ to print the binder, the resolution could be improved and the minimum feature size reduced from 300 μm to under 150 μm [253].

In 1998, Baskaran *et al.* demonstrated that the gelation of sodium alginate by divalent metal cations, which has since then been extensively used in gelcasting [254][255][256], could be used as a binding mechanism in the S-BJ process [257]. Ceramic slurries containing ~50 vol% Al_2O_3 powders and small amounts of sodium alginate were selectively gelled upon contact with droplets of a saline solution. High-density alumina components with fine-grained microstructures and flexural strengths above 400 MPa could be produced. More recently, a research group at the BAM Federal Institute for Materials Research and Testing in Germany has developed and perfected its own version of the process under the name LSD-print [64]. This S-BJ process has been used to produce fully-dense alumina as well as Si-SiC parts with

mechanical properties comparable to those of conventionally manufactured ceramics. An aqueous slurry of fine Al_2O_3 powders containing 0.3 wt% alginic acid sodium salt was paved into 50 μm layers using a doctor blade. Each layer was then dried and crosslinked by selectively jetting a binder solution consisting of copper sulphate pentahydrate dissolved in ethylene glycol; the Cu^{2+} ions in the binder inducing the gelation of the sodium alginate. The alginate also improved the rheological properties of slurries for paving and, more importantly, acted as a binder in green layers, preventing the formation of cracks which would otherwise appear during drying. Sintering shrinkage was anisotropic, but reproducible, and fully dense sintered alumina components with a fine-grained homogeneous microstructure and without any visible interphase between layers were obtained. However, neither mechanical properties nor surface roughness data were reported.

3.5.3.   Advantages and limitations of binder jetting

The binder jetting process holds a number of distinct advantages, including scalability, material selection, design freedom, and throughput [258]. Indeed, P-BJ is one of the most scalable AM technologies and has already been used extensively to produce large parts from a variety of materials, including sands, polymers, metals, and ceramics [259]. Furthermore, much like laser sintering, the self-supporting powder bed in BJ enables the production of geometrically complex parts and overhanging features without the need for secondary support structures. P-BJ also provides appreciable fabrication throughput since the technology works by laying down a whole layer of ceramic powder at once coupled to the advantage of depositing the binder using inkjet printing, which is fast and can easily be scaled up by using several jetting heads with hundreds of nozzles each to increase throughput. Furthermore, unlike DIP, the jetting head is used to process low concentration binders rather than relatively concentrated colloidal ceramic suspensions, therefore significantly minimising the occurrence of nozzle clogging issues.

The downsides of P-BJ applied to advanced ceramics mostly stem from the requirement to use powders with an average particle size well above 10 μm to enable layer spreading during the recoating step, which limits the resolution of the process, results in high surface roughness, and leads to high porosity and poor sintering densification. Therefore, the best applications for this technology used with ceramics remain the production of non-structural porous components such as scaffolds for tissue engineering [232][246] and investment casting cores and moulds [260]. Nevertheless, post-processing densification steps, such as CIP, WIP, and infiltration can be used to increase density and mechanical properties, although these additional steps result in increased labour, manufacturing time, and overall costs.

Finally, the main issues of P-BJ may be overcome by taking a colloidal slurry-based approach, which has been shown to enable the production of near-fully dense parts without the need for pressure-assisted post-processing thanks to the use of submicron powders. The resolution of the process and surface roughness of as-printed parts are also greatly improved for the same reason [64]. However, S-BJ results in longer manufacturing time due to the need to dry out the powder bed before jetting the binder for each recoated layer. Moreover, careful consideration must also be given to the chemical and physical properties of ceramic slurries to ensure they have the correct viscosity for layer spreading, to prevent drying cracks, and ensure that parts can be successfully removed from the unbound powder bed.

3.6. Vat photopolymerisation

Vat photopolymerisation is a lithography-based process,   defined by ISO/ASTM standard 52900:2015(E) as "an additive manufacturing process in which a liquid photopolymer in a vat is selectively cured by light-activated polymerisation" [60]. To manufacture ceramic parts using lithography-based processes, fine ceramic powders are dispersed into the liquid photopolymer, which is usually based on acrylate or epoxy monomers, to form a UV-curable slurry [13][261][262]. Alternatively, the process can be based on the photopolymerisation of UV-curable liquid preceramic polymers [263].

3.6.1.   Lithography-based additive technologies

The reactive colloidal system consists of monomer, photoinitiator, submicron ceramic particles, dispersant, and additional additives such as diluent and solvent. Upon curing, the photopolymer acts as a matrix for the ceramic particles and provides shape, cohesion, and strength to the green part. Subsequent thermal treatments are performed on the green body: first binder burnout to ensure complete removal

of the polymer matrix and then sintering to yield the final properties of the ceramic part. In order to prevent deformation and cracking during debinding as well as excessive shrinkage during sintering, it is crucial to minimise the organic content of the ceramic slurry by formulating suspensions with a solid loading of at least 50 vol% [264][265]. A high solid loading is also beneficial to the density and mechanical properties of the green body and usually enables to achieve near-fully-dense sintered parts. However, too high a solid loading may yield a slurry with rheological properties unsuitable for SL, namely too high a viscosity or a transition from shear thinning to dilatant behaviour [266]. Other critical parameters that must be well controlled are the cure depth and cure width of polymerisation, which relate to the adhesion between layers and the dimensional resolution, respectively [13]. Cure depth and width are greatly affected by light scattering phenomena caused by the presence of submicron ceramic particles in the reactive medium [267][268]. Furthermore, it is reported that the most influential parameters affecting the UV reactivity of ceramic slurries are powder concentration, mean diameter of particles, particle size distribution, refractive index of the ceramic material, and difference between refractive indices of the monomer and ceramic powder. Colloidal systems must therefore be optimised to the specific ceramic material being used in order to yield slurries with appropriate viscosity and limited light scattering. Optimisation of colloidal processing and influence of concentration of dispersant, photoinitiator, and diluent on the rheology and reactivity of specific alumina suspensions at different solid loadings have been widely investigated [261][267][268][269]. Increasing the refractive index of the UV-curable system in order to reduce the difference with the refractive index of the ceramic material has been shown to limit scattering effects and increase the depth of cure [270][271][272]. The effect of particle size on photopolymerisation kinetics has also been investigated, showing that a decrease in particle size towards the laser wavelength tends to increase scattering effects, thereby reducing the reactivity of suspensions [13][269]. The rheology of photocurable suspensions as a function of particle size dispersion was also investigated in detail [273]. Finally, the energy density, spot size and scanning speed of the laser must also be optimised to ensure an adequate cure depth (higher than 200 μm [13]), dimensional resolution and accuracy whilst minimising manufacturing time and power consumption.

Several technological variants of the vat photopolymerisation process exist for the layerwise freeform fabrication of ceramic components: stereolithography (SL), Digital Light Processing (DLP), and two-photon photopolymerisation (2PP).

In SL, selective solidification of the liquid photocurable resin suspension is induced by a UV laser that is steered using a scanning galvanometer mirror positioning system to scan selectively the resin surface at the locations specified by the STL file [274]. Wu *et al.* [275] used SL to fabricate zirconia-toughened alumina (ZTA) ceramics with a mass ratio of 4:1 Al_2O_3:ZrO_2. A sintered density of 99.5% TD and grains with an average size of 0.35 μm were obtained. They measured a Vickers hardness of 17.76 GPa, a 3PB flexural strength of 530.25 MPa, and a fracture toughness of 5.72 MPa m$^{1/2}$. Tian *et al.* [276] processed a photocurable resin consisting of phenolic epoxy acrylate, phenolic resin, triethylene glycol as pore forming agent, and benzoin dimethyl ether as photoinitiator. The UV laser had a 350 nm wavelength and a power of 200 mW, whilst a hatch spacing of 0.1 mm and a 50 mm/s scan speed were used. The fabricated resin prototypes were pyrolysed at 850°C for 1 h to obtain porous carbon preforms that were then infiltrated with molten silicon and converted to RBSiC with a maximum bending strength of 127.8 MPa.

DLP, which has also been called Direct Photo Shaping [277], Large Area Maskless Photopolymerisation (LAMP) [278] or Mask-Image-Projection-based Stereolithography (MIP-SL) [279], has at its core the digital micromirror device (DMD) technology. A DMD chip is a digitally controlled micro-opto-electro-mechanical system (MOEMS) invented at Texas Instruments in 1987 made of a 2D array composed of several hundred thousand individually switchable micromirrors producing a dynamic image that is projected onto the photopolymer surface. The main advantage of DLP over laser-based SL is its much greater manufacturing speed, because the entire surface of the polymer is cured at once, whilst SL provides a point-based photopolymerisation method.

In 2015, Schwentenwein and Homa [280] presented the Lithography-based Ceramic Manufacturing (LCM) technology, a commercial DLP technology developed by Lithoz GmbH. They used a CeraFab 7500 commercial printer to manufacture Al_2O_3 specimens with a 99.3% TD and 4PB flexural strength of 427 MPa, as well as small complex-shaped components with smooth surfaces such as the parts shown in **Figure 15**. Indeed, the roughness was comparable to injection moulded parts since an R_a of 0.84 μm along

the layer boundaries, 1.08 μm perpendicular to individual layers, and only 0.36 μm in the plane of an individual layer was measured.

Harrer *et al.* [281] used LCM to fabricate 3Y-TZP samples from a photosensitive slurry containing 42 vol% ZrO_2. A 99.6% sintered density was achieved, with a Vickers hardness of 13.4 GPa, and a SEVNB fracture toughness of 4.9 MPa $m^{0.5}$. The 4PB flexural strength of as-fired and ground specimens was 845 and 878 MPa, respectively, and fracture originated from pores, agglomerates, or handling defects.

He *et al.* [282] fabricated 97.1% dense zirconia parts from an acrylate-based photocurable suspension of zirconia particles (0.2 μm). Mixtures were ball milled at 200 rot/min for 6 h with 5 mm zirconia grinding balls to achieve a good state of dispersion. Specimens experienced significant anisotropic shrinkage upon sintering, and displayed a Vickers hardness of 13 GPa and a fracture toughness of 6 MPa $m^{1/2}$.
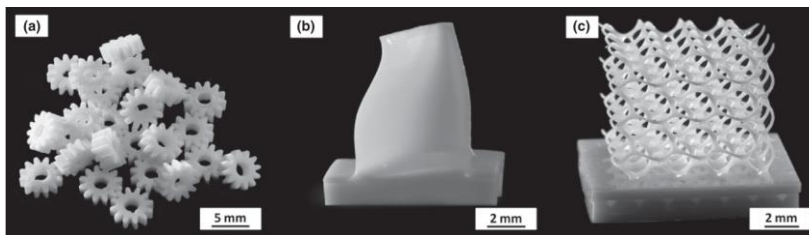
Figure 15: *Sintered alumina parts fabricated using the LCM technique: (a) gear wheels; (b) a turbine blade; and (c) a cellular cube.* [280]

SL can also be used to produce SiC and Si_3N_4 ceramic structures by processing photocurable preceramic polymers instead of the more commonly used ceramic suspensions [283]. This has the advantage of avoiding issues with light scattering and limited depth of penetration that can occur when working with highly-loaded SiC suspensions in particular. Complex SiC-rich structures, depicted in **Figure 16**, were manufactured from commercially-available liquid allylhydridopolycarbosilane (AHPCS) mixed with a (meth)acrylate monomer and a photoinitiator; it was noted that the structures where characterised by a relatively high level of microporosity, which was not quantified, but would hinder mechanical properties.

Figure 16: Examples of SiC ceramic parts produced by STL of preceramic polymer (top). Comparison of as-printed and pyrolised/sintered samples (bottom).

Hundley *et al.* produced a number of small geometrically-complex amorphous silicon oxycarbide structures from a UV-curable siloxane preceramic resin using a commercial Autodesk Ember DLP system equipped with a 405 nm source [284]. They then used X-ray micro-computed tomography (µCT) to precisely measure the dimensions of the 3D printed components before and after pyrolysis. Uniform linear and volumetric shrinkages of 29.7% ± 1.2% and 64.9% ± 1.6%, respectively, were obtained across various geometries, showing the repeatability of the process, albeit the shrinkages were high. Furthermore, SEM and TEM observations showed that the pyrolysis conversion did not induce porosity or cracking, although it was noted that the pyrolysis did not promote void migration and therefore, if flaws already existed in the preceramic polymer, they are likely to result in crack propagation in the final ceramic product.

Schmidt and Colombo [285] used a commercial DLP printer, with a light source in the 400-500 nm range, to manufacture dense, pore-free and crack-free SiOC ceramic scaffolds from a physical blend of preceramic polymers containing a proprietary commercial liquid photocurable acrylic siloxane mixed with two non-photocurable high ceramic yield silicone resins having phenyl and phenyl-methyl side groups. Toluene was used as the solvent and the mixture also comprised a photoinitiator and a photoabsorber. Complex scaffold structures with a resolution of 30 µm and a maximum ceramic yield of 60.2 wt% could be produced. It was found that the ceramic yield as well as the pyrolysis shrinkage were mainly controlled by the preceramic polymer/acrylic polymer ratio.

Two-photon photopolymerisation (2PP or TPP) is yet another lithography-based AM process characterised by its extreme resolution and accuracy, making it ideal for the manufacture of microscopic structures. Pham et al. reported the fabrication of complex SiCN ceramic microstructures with a 210 nm resolution via nano-stereolithography of a preceramic polymer [263]. The process is based on the two-photon absorbed crosslinking of a 2-isocyanatoethyl methacrylate-functionalised polyvinylsilazane precursor and its subsequent pyrolysis at 600°C under a nitrogen atmosphere. However, a highly anisotropic shrinkage was obtained, which is detrimental to the accuracy of the process. A significantly lower and quasi-isotropic shrinkage could be obtained by adding to the photoresist up to 40 wt% colloidal silica particles with a diameter of ~10 nm as filler. It was found by measuring the Young's modulus at increasing temperatures that the UV-cured polymer films pyrolysed at 600°C with further increase in strength at 800°C, although the authors pointed out that such high pyrolysis temperatures caused severe volume shrinkage due to additional weight loss and densification.

3.6.2.   Self-propagating photopolymer waveguide technology (SPPW)

Lattices are one of the most commonly additively manufactured structures, either from polymers, metals or ceramics and even glass, AM enables the fabrication of complex lattice structures that could not be manufactured before the emergence of the technology. However, AM processes are usually characterised by their relatively slow building rate due to being based on the layer-by-layer fabrication method. To address this issue as well as to increase the fabrication rate of ceramic microlattices and honeycombs, Schaedler et al. invented in 2011 the self-propagating photopolymer waveguide (SPPW) technology [286]. The mode of operation of SPPW is entirely based on a self-focusing effect enabled by the careful selection of the starting monomer, which must undergo a change in its index of refraction upon polymerisation resulting in internal reflection of the UV light. The polymer therefore effectively becomes a waveguide, tunnelling the light in a straight line to induce polymerisation further down into the vat. The process, due to its layerless nature, enables the fabrication of lattice structures from preceramic polymers up to 1000 times faster than conventional SL. After SPPW had been demonstrated for the indirect manufacture of ultralight metallic microlattices, Eckel et al. [14] reported in 2016 its use for processing a UV curable siloxane preceramic resin system and producing fully-dense, pore-free and crack-free amorphous silicon oxycarbide microlattice structures (**Figure 17**).
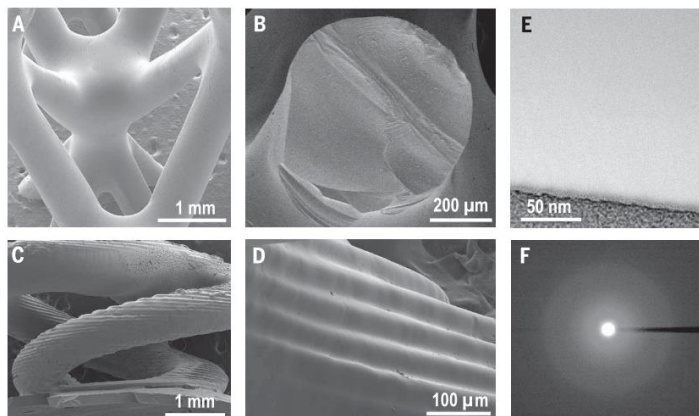

Figure 17: Electron microscopy characterization of SiOC microlattice and cork screw. *(A) SPPW-formed lattice node showing smooth surface and (B) Fracture surface of a strut. Compare with (C) SLA printed corkscrew showing undulations on the surface. (D) 3D printing step size is 50 mm. (E) Bright-field TEM image showing no porosity. (F) TEM diffraction indicating amorphous structure.* [14]

3.6.3.   Advantages and limitations of vat photopolymerisation

The first advantage of vat photopolymerisation technologies, in particular SL and DLP, is their industrial readiness level. Light-activated polymerisation is indeed currently by far the most established process on the AM market for the manufacture of monolithic advanced ceramic components. The main industrial manufacturers of machines based on this approach are Lithoz [287], Prodways [288], 3DCeram and Admatec [289]. 3DCeram machines are based on the original design of the stereolithography process, using a top-down approach where a UV laser hits the top surface of a large resin vat into which the build platform is lowered for recoating and layerwise fabrication. Lithoz uses the bottom-up DLP technology called Lithography-based Ceramic Manufacturing (LCM) [280][281], whilst another manufacturer, DDM Systems, also employs a bottom-up DLP approach [290]. Prodways' patented MOVINGLight® technology uses a DLP head that moves over the entire surface of the ceramic suspension, allowing it to maintain a resolution of 40 microns per pixel even for large build areas [291]. Admatec also uses a bottom-up DLP approach but, instead of using a vat, doctor blading is used to produce a fine layer of the ceramic-filled resin on a moving foil that transports the slurry layer to the building area.

Photopolymerisation-based AM technologies enable the fabrication of near-net-shape fully-dense parts with a high geometrical complexity and an excellent surface finish comparable to that of injection

moulded parts [280]. The first drawback concerns the limited types of ceramic materials that can be produced using the photopolymerisation of ceramic slurries. These technologies have been widely demonstrated and are now used commercially to manufacture near-fully-dense pure ceramic components from oxide ceramics that are relatively transparent to UV light, such as silica [278], alumina [292], hydroxyapatite, zirconia [282][293] and silicon nitride [294], although the last two are a bit more challenging to process due to their higher refractive indices, as listed in

Table . However, ceramic materials with even higher refractive index and higher coefficient of extinction have been more challenging to shape due to excessive light scattering and light absorption, resulting in poor resolution and insufficient polymer curing [278]. Non-oxide ceramics such as SiC, TiC, ZrB_2 and B_4C fall into this category and are therefore difficult to shape into monolithic components using current technologies and methods, in particular the last two since they are "black ceramics". There is now tremendous interest to expand the range of processable materials to these more challenging ceramics; SiC is first on the list being a "grey ceramic" with lower absorbance and refractive index than B_4C and ZrB_2. Some success has already been achieved in producing porous green SiC parts, from both the ceramic powder processing [295] and the polymer-derived ceramic [283][276] routes, often combined with post-processing infiltration and pyrolysis. However, as Ding *et al.* rightly pointed out, further work is required to improve the density of final components [296].

Photopolymerisation-based processes may also be limited in terms of maximum wall thickness that can be manufactured without the formation of porosity or cracks. Indeed, the composition of photocurable ceramic slurries used in SL and DLP is very similar to that of injection moulding suspension feedstock, and usually consists of no less than 40-60 vol% polymeric binder as suspension medium, to which other organic compounds such as dispersants and photoinitiator are added. These large amounts of organics can first result in very significant shrinkage that can lead to part deformation, and, second, tend to complicate the debinding stage due to the release of gaseous species that must slowly escape the bulk of the component by diffusion. As a result, processing thick-walled parts without excessive porosity and cracking in the brown body is challenging [297]. Besides, the use of high amounts of toxic photopolymers also results in H&S issues and is not environmentally friendly. Nevertheless, photolithography-based AM technologies are highly suited to the manufacture of small complex-shaped oxide ceramic and polymer-derived ceramic components with high resolution and excellent surface finish for precision applications.

***Table 6:** Refractive index of common advanced ceramics and full range of refractive index of photosensitive polymer (data available at refractiveindex.info, Accessed [09/5/2020]).*

Lithography-based AM of advanced ceramic materials			
Material	**Refractive index *n* at 405 nm**	**Extinction coefficient *k* at 405 nm**	**Readiness level as of 2019**
Photopolymers	1.3 – 1.8	-	-
SiO_2	1.47 – 1.57	0.003	Commercially available at industrial scale
HA	1.65	-	
Al_2O_3	1.70 – 1.79	0.019	
YAG	1.86	-	
Si_3N_4	2.07 – 2.10	-	
ZrO_2	2.22 – 2.32	-	
SiC	2.69 – 2.83	0.66	Academic and industrial R&D
TiC	2.75	-	Challenging, early-stage research
B_4C	3.131	0.76	

4. Single-Step AM of Advanced Ceramics

4.1. Direct powder bed fusion

4.1.1.   *Direct laser sintering (dLS)*

The PBF AM approach, where a laser selectively scans a powder bed layer-by-layer to fuse material, can also be applied in the form of direct laser sintering (dLS) to obtain sintered ceramic parts in a single step directly out of the AM process. Here, it is the ceramic material itself rather than a low melting point binder that is sintered/melted by the laser beam. Alternatively, the laser beam can induce a chemical reaction from a non-ceramic feedstock resulting in the formation of a ceramic material in the brown or sintered state. Ideally, there is no need for post-thermal treatment nor additional densification steps after dLS. However, the inherent properties of advanced ceramic materials (i.e. their very high melting point, poor thermal shock resistance and low ductility) make dLS of ceramics significantly more challenging than with metals [298]. Indeed, the very short laser-powder interaction time during the dLS process, combined with the extreme temperature gradients, tend to result in poor ceramic sintering, incomplete densification and high thermal residual stress causing crack formation [19][299].

Nevertheless, dLS process has been applied to the following technical ceramics: Al_2O_3 [300], SiO_2, reaction-bonded silicon carbide (RBSiC) [301], Al_2O_3-SiO_2 [302] and Al_2O_3-ZrO_2 mixtures [303][304], 3 vol% yttria-stabilised tetragonal zirconia (3Y-TZP), HA–silica [305] lithium aluminosilicate (LAS) glass [306], and tri-calcium phosphate (TCP). Higher laser scanning temperatures are necessary to achieve direct laser sintering of technical ceramic powders without using any sacrificial binder due to the very high melting point of this class of materials. Solid-state fibre lasers such as the Nd:YAG laser with a wavelength of ~1μm are often used for dLS of ceramic powders because of their higher power and smaller beam spot size compared to CO_2 lasers. Less technical ceramics such as silicates (e.g. SiO_2 and $ZrSiO_4$) can be sintered using a CO_2 laser to manufacture low-strength porous parts, such as ceramic moulds for metal investment casting [307][308].

Bertrand *et al.* (2007) processed fine yttria-stabilised zirconia (YSZ) by dLS in a Phenix Systems PM100 equipped with a roller to deposit the powder layers and a 50W fibre laser to selectively sinter the particles [309]. The final density remained low at only 56% TD and furnace sintering could not increase the density, showing that partial melting of the YSZ powder had occurred.

Wissenbach's research group (2010-2013) at the Fraunhofer Institute for Laser Technology investigated the dCLM of an alumina/zirconia powder mixture [310][311][312][304]. They used the eutectic ratio of 58.5:41.5 wt/wt Al_2O_3/ZrO_2 which has a significantly lower melting point (1860°C) than the single phases (2072°C and 2710°C, respectively). The process is based on the development of a new top-down high temperature preheating strategy to minimise extreme thermal gradients and prevent the formation of cracks: a CO_2 laser was used to preheat the entire surface of the powder bed above 1700°C whilst a continuous-wave (cw) Nd:YAG laser beam selectively melted the powder. They were able to manufacture small 100% fully-dense sintered ceramic parts in a single-step as well as demonstration dental restoration frameworks, shown in **Figure 18**. However, several limitations still remained: a very poor surface quality was obtained (R_Z of 100-150 μm) and micro-cracking occurred due to the extreme temperature gradients. Scalability was also an issue as parts with height > 3mm could not be processed without severe crack formation. In 2011, an alternative preheating strategy combining bottom-up inductive heating at a temperature of 1400°C with top-down selective (instead of areal) laser preheating using a diode laser beam was proposed as a potential solution for manufacturing larger parts, but the outcome of this modification was not reported.

Figure 18: *Dental restoration bridges produced by dLS of Al_2O_3-ZrO_2 showing the potential of the process for manufacturing complex parts in a single step, but with a very poor surface finish* [311].

RBSiC parts were produced by LS from a 67:33 wt/wt SiC/Si powder mixture [301]. The average particle size of SiC and Si powders was 25 μm and 45 μm, respectively. A 100 W cw fibre laser was used to selectively melt the Si in argon atmosphere, resulting in a porous SiSiC preform that was subsequently impregnated with a graphite suspension and infiltrated with molten Si at 1450°C. Highly dense RBSiC parts (95% TD) could be obtained after infiltration of the preform produced with a large scan spacing (77 μm), but over-infiltration resulted in surface protrusions and parts contained only 40% SiC. Whether this should be considered a single-step AM process may be up for debate since the post-AM infiltration was an essential step of the manufacturing process to increase the density of SiSiC parts. However, the AM process still resulted in a fully ceramic part before infiltration was carried out, albeit a very porous one; in principle this process is single-step though it is multi-step in practice due to current limitations that may be overcome in the future.

The slurry-based approach has also been used for the direct LS of ceramic components. Liu *et al.* fabricated silicate-hydroxyapatite (HA) bioceramic scaffolds for bone tissue engineering by direct LS via a 25 W CO_2 laser with a 300 μm spot size [305]. The build material was an aqueous slurry containing 28 wt% SiO_2 and 30 wt% HA with a viscosity of 3Pa s and paved into 0.1 mm layers by a scraper. Small porous bone scaffolds with hollow shell structure could be obtained in 120 min with a laser power of 13 W, scan speed of 150 mm/s, and laser frequency of 10 kHz. As specimens obtained out of the AM process were only partially sintered, a furnace sintering schedule at 1200°C for 90 min was applied to reduce the pore size and improve mechanical properties. Here again, we still consider this process to be single-step despite the need for a post-AM heat treatment, since the AM process resulted in a partially sintered, fully ceramic component that simply required a relatively short heat-treatment to homogenise the microstructure, which could be considered similar to the heat treatment that may follow SLM of metal alloys [313]. Fired specimens had a high apparent porosity of 27-30% with surface pores in the range 5-25 μm, a surface roughness (R_a) of 25 μm, but a maximum bending strength of only 4.7 MPa. Furthermore, it was found that scaffold composition (HA particles surrounded by solidified silica) and surface macroporosity were both beneficial to cell attachment and proliferation, confirming the suitability of the process for the fabrication of bioactive hollow bone scaffolds.

A slurry-based dLS process combining a layer-wise slurry deposition (LSD) paving system with laser sintering was developed at Clausthal University of Technology in Germany [62][63]. The technology has been used to manufacture porous porcelain [314], SiO_2-Al_2O_3 [315] and lithium aluminosilicate (LAS) glass [306] parts. The process was later renamed LSD-laser [64]. LSD-laser enables the freeform fabrication of porous ceramic parts by pumping into a hollow doctor blade an aqueous ceramic suspension with less than 2% organic additives that is paved onto a preheated ceramic tile to form a thin layer that is then dried and selectively laser sintered [316]. Whilst a CO_2 laser (wavelength = 10.6 μm) was used to process the SiO_2-Al_2O_3 system, more recent works on porcelain and lanthanum-alumino-silicate (LAS) glass were carried out using a 100 W single mode YAG:fibre laser beam (wavelength = 1.064 μm). Multilayer LAS glass samples could not be produced without excessive bubble formation originating from the binder burn-out. It was suggested that replacing the fibre laser with a CO_2 laser could result in a better sintering behaviour due to the wider absorption band of the material around 10 μm than 1 μm wavelength [317]. SiO_2-Al_2O_3 slurries with 34 wt% deionised water could be processed when alumina amounted to 25.5 wt% of the solid loading. After optimisation of the laser parameters, the density of laser sintered multilayer samples was 86-92% TD, with formation of mullite needles within an amorphous aluminosilicate phase [302]. After post-heat treatment at 1600°C, all the alumina disappeared and the

Commented [YL(aM3)]: It was suggested by a reviewer to move this to section 3.1.1. on indirect laser sintering since the process was followed by an infiltration step. A short sentence was added to explain why we would keep this in the direct LS section.

Commented [YL(aM4)]: Reviewer's comment was: "Also, the laser sintering of slurry-based silicate-HA followed by additional sintering shouldn't be considered as a one-step ceramic AM process."

Much like in the previous comment, the AM process still resulted in a fully-ceramic composite directly out of the AM machine. It simply required a heat-treatment, not to remove any binder, but to homogenise the microstructure and increase mechanical properties, which is somehow similar to what may be done with metallic components out of SLM. A short sentence was added to explain this.

density reached ~96% TD. Although the LSD deposition method enabled the formation of powder compacts with a density >60%, the density of fired porcelain bodies did not exceed 80% due to bubble formation induced by excessive laser heating [318]. After post sintering in a furnace at 1380°C for 1 h, the strength of laser sintered porcelain samples was only half that of biscuit-fired[9] specimens, but high enough for handling, glazing and gloss firing [319].

4.1.2.   Advantages and limitations of dLS

The most significant advantage of dLS in particular over most other ceramic AM processes is its single-step nature, where the ceramic material is directly melted and sintered as it is shaped, removing the need for the lengthy post-AM thermal debinding and furnace sintering steps.

However, thermal stresses that occur during dLS remain a critical issue for ceramic materials, resulting in cracking and porosity, and as a result no large monolithic ceramic parts have been demonstrated to date. So far, dLS has been demonstrated mostly with some oxide ceramic materials or specific ceramic blends such as the eutectic Al_2O_3-ZrO_2 mixture, but there may however be some limitations regarding material selection: some high-performance oxide and non-oxide ceramics may remain extremely challenging to shape by dLS due to their very high melting point, poor resistance to thermal gradients, and low plasticity.

4.2. Directed energy deposition (DED)

DED, also known as laser cladding, direct laser fabrication or Laser Engineered Net Shaping™ (LENS®), is defined as an additive manufacturing process in which focused thermal energy is used to fuse materials by melting as they are being deposited [60]. DED has the striking advantage over most other ceramic AM processes of being a single-step AM process, meaning that the final geometry of the part and its final physicochemical properties are defined directly during the AM process, removing the need for post-processing heat-treatment. During fabrication, ceramic powder particles are fed from a nozzle into the focal point of a laser beam, where the powder is fully melted and solidifies onto the substrate. **Figure 19** shows how a combination of ceramic and/or metal powder and wire can also be used to manufacture composite structures, and feed rates can be adjusted during fabrication to generate composition gradients [320].
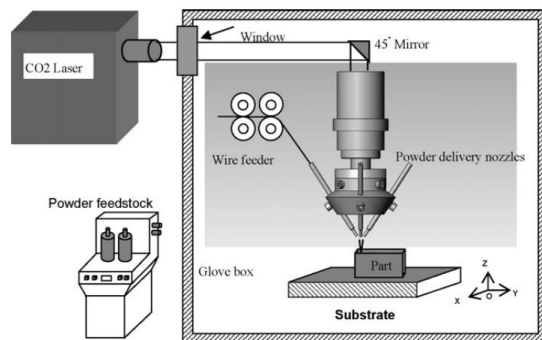
Figure 19: Schematic of a DED system with simultaneous powder and wire feed. [320]

Balla *et al.* used a commercial LENS® machine equipped with a Nd:YAG laser (1.5 mm beam diameter) to fabricate dense, crack-free, near-net-shape bulk alumina components from 99.9% pure α-Al_2O_3 powder with a particle size in the range 44-74 μm [20]. Parts without any macroscopic defects could be produced using the optimal laser parameters listed in **Table 2**~~Table 7~~. They investigated the influence of post-heat

---

[9] **Biscuit-firing** is "the first firing given to pottery, before it is glazed." (as defined in the Collins English Dictionary)

treatment on the density, microstructure, compressive strength, fracture toughness and microhardness of test parts, and the results are summarised in **Table 3**. It was found that whilst a 5-hour heat treatment at 1000°C resulted in marginal changes of the measured properties, heat treatment at 1600°C led to an increase in density from 94% to 98% TD and to significant grain growth from 6.6±2 to 207±90 μm, but, nonetheless, with slightly improved mechanical properties. The formation of columnar grains along the build direction during part formation, however, resulted in strength anisotropy.

Niu *et al.* used LENS® to manufacture pure α-Al$_2$O$_3$ samples [321][322] as well as Al$_2$O$_3$–ZrO$_2$ (Y$_2$O$_3$) [323] and Al$_2$O$_3$–Y$_3$Al$_5$O$_{12}$ (YAG) [324] eutectic ceramic structures. The formation of macro-cracks perpendicular to the scanning direction could not be avoided when processing pure alumina, even when DED process parameters were optimised, due to the fast cooling rates of the DED process resulting in thermal stresses. However, the use of eutectic compositions, coupled with optimised laser parameters, enabled the fabrication of high density, crack-free thin walls and cylinders with fine microstructures. Vickers microhardness measurements listed in **Table 3** showed that hardness values were comparable to that of eutectic ceramics made by directional solidification or laser-heated floating zone [325].

Table 2: Starting materials and optimal laser parameters used in several studies of ceramic DED.

Ceramic powder materials	Range of particle size (μm)	Laser power (W)	Scan speed (mm/min)	Powder feed rate (g/min)	Z increment (mm)	Year [Ref.]
α-Al$_2$O$_3$	44-74	175	600	14	0.254	2008 [20]
α-Al$_2$O$_3$	42–90	350	300	1.36	0.22	2015 [322]
Al$_2$O$_3$–ZrO$_2$ (Y$_2$O$_3$) eutectic ratio	42–90	410	400	1.22 (Al$_2$O$_3$) / 0.87 (ZrO$_2$)	0.25	2015 [323]
Al$_2$O$_3$–Y$_3$Al$_5$O$_{12}$ (YAG) eutectic ratio	42–90	300-350	350	1.65	0.21	2016 [324]

4.2.1. Advantages and limitations of DED

The fact that DED is a single-step process, so post- heat treatmentAM furnace sintering is usually not required, combined with its fast deposition rates and the minimal materials pre-processing required, make it the quickest AM method for producing sintered ceramic parts. Furthermore, by using several nozzles, DED also enables depositing multiple materials at a time, allowing for the direct fabrication of ceramic-ceramic [323] and metal-ceramic [320] composites. Besides, material composition can also be adjusted by varying the powder feed-rate, thus enabling a fine level of control over both material grading and composition grading. However, this process also has a few significant limitations. Directed energy deposition methods have been widely used with to shape metals and even then often result in significant residual stresses and thermal cracking [7]. In the case of ceramics, Hhigh thermal gradients and extremely fast cooling rates invariably result in the development of thermal stresses, which usually induce delamination and cracking. if Therefore, laser parameters are notthe energy density of the laser beam – which is a function of laser power, beam spot size, scan spacing and scan speed – must be perfectly controlled and optimised [324]. Much like other AM processes, this process parameter optimisation is largely material dependent and must be carried out every time the composition or morphology of the ceramic powder/wire feedstock is modified. Other disadvantages of the process are the limited geometrical complexity achievable, limited resolution, poor control over the shape of manufactured parts, and its low dimensional and geometrical accuracy, resulting in the need for post-machining to achieve net-shape (**Figure 20**Figure 20Figure 16). Support structures cannot be generated and there is no self-supporting bed, so some form of 5-axis capability is required to manufacture complex geometries and overhangs. This can be easily implemented, however, and has already been done industrially with metals. Nevertheless, DED is one of the few AM processes that enable the fabrication of fully-closed empty cavities, although a small amount of ceramic particles would always remain trapped in any closed cavity

because not all of the feedstock powder is caught under the laser beam. Similarly to dLS, there could be limitations regarding material selection, and high melting point non-oxide ceramics in particular could prove challenging. The DED process involves complex melting/solidification behaviour, and a better understanding of the relationship between starting material composition, process parameters, microstructure, and final properties is required.
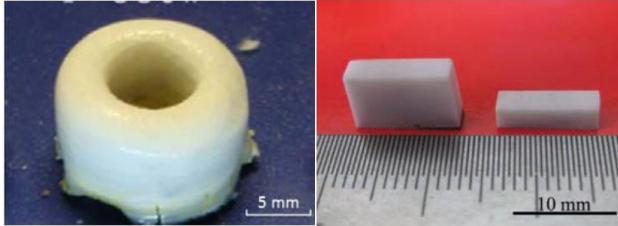
Figure 20: *Hollow cylinder structure fabricated by LENS (LEFT) and rectangular samples machined from the fabricated specimen (RIGHT).* [324]

Table 3: *Mechanical properties of ceramic samples manufactured by DED.*

Ceramic material	Final density (% TD)	Microhardness (GPa)	Vickers hardness (HV)	Fracture toughness (MPa m$^{1/2}$)	Compressive strength (MPa)	Year [Ref.]
Al$_2$O$_3$ as-fabricated	94	-	1556 ±90	2.1 ±1.3	229 ±11	2008 [20]
Al$_2$O$_3$ heat treated 1600°C, 5h	98	-	1700 ±36	4.4 ±1.4	276 ±5	2008 [20]
Al$_2$O$_3$–ZrO$_2$ (Y2O3) 58.5:41.5	"fully dense"	17.15	-	4.79	-	2015 [323]
Al$_2$O$_3$	-	-	1800	-	-	2015 [322]
Al$_2$O$_3$–Y$_3$Al$_5$O$_{12}$ (YAG) 66.5:33.5	-	-	1575	-	-	2015 [322]
Al$_2$O$_3$–Y$_3$Al$_5$O$_{12}$ (YAG) 45:55	98.6	17.35	-	3.14	-	2016 [324]

5. Comparison of AM Processes for Advanced Ceramics

5.1. Criteria for selecting AM processes for ceramic materials

Whilst ceramists can take advantage of the entire spectra of AM processes to shape advanced ceramic materials, end-results and performances vary widely from one process to another, and each AM technology is characterised by its own advantages and limitations. Therefore, there is not a "best overall" ceramic AM process, but rather the selection of the most suitable AM technology to be used to manufacture a particular component directly depends on the material of choice and end-use application of said component. As a result, the following requirements need to be identified and specified before deciding which AM process to use:

i. **Type of ceramic material**: Identifying which ceramic material is to be processed, given the application and desired properties of the final component, is arguably the first step in the selection of any process and this is also true of AM processes. Indeed, whilst most oxide ceramics can usually be shaped using any AM process, as long as proper material pre-processing is performed and printing parameters are optimised, some restrictions can apply to non-oxide and polymer-derived ceramics due to some of their specific physical properties. For instance, non-oxide ceramics with high refractive index and absorption at UV and daylight wavelengths (e.g. B_4C and TiC) may prove significantly more difficult to shape using photopolymerisation-based processes than more transparent ceramics (e.g. Al_2O_3, ZrO_2, HA) because of excessive light scattering and insufficient cured depths. The use of dLS and DED with some non-oxide ceramics may also be hindered by the very high melting point, low toughness, and poor thermal shock resistance resulting in cracking. On the other hand, other AM processes such as ceramic extrusion, inkjetting, binder jetting and sheet lamination have already been successfully used to process all types of advanced ceramics since part shaping is relatively independent from the physical properties of the ceramic material.

ii. **Final density**: Arguably, the property that has the biggest influence on the physical properties and mechanical strength of ceramic parts, final sintered density is directly dependent upon green density and powder size, as well as on sintering method and schedule. Before choosing an AM process for manufacturing, it is important to consider carefully the requirements in terms of in-service mechanical properties of the end-use component, because these will directly impact the required part density. Dry powder-bed processes P-BJ and P-LS are not suitable for producing high density parts due to the use of dry coarse powders that have a low sintering activity and provide a poor packing density, thus resulting in high residual porosity. Post-densification steps such as WIP and infiltration can help improve density but they result in extra manufacturing time, added cost, and only partially solve the issue. High sintered densities can be achieved using the slurry-based variants of these processes, namely Slurry-LS and Slurry-BJ, as well as other AM processes that use liquid ceramic feedstock such as aqueous-based extrusion (robocasting, CODE), inkjetting and stereolithography. Both single-step processes dLS and DED have also been used to produce monolithic specimens, although issues with cracking and limited geometrical freedom still need to be addressed. One must also keep in mind that, in single-step processes, densification is performed in a very different manner than with the more conventional solid-state sintering carried out at very low heating rates in a furnace with dwell times of several hours at maximum temperature. Instead, sintering in dLS and DED is carried out through the formation of a liquid phase, the ceramic powder being melted in-situ under a high temperature laser and then resolidified within a fraction of a second. As a result, the microstructure of monolithic ceramics produced using single-step AM technologies most likely differs significantly from that of identical ceramics densified by furnace sintering, resulting in potentially very different final physical, chemical, and mechanical properties.

iii. **Resolution and part dimensions**: The overall dimensions of the component to manufacture have a deciding influence on the ceramic AM process selection. On the one hand, some AM processes may be better suited to manufacture small components for which high precision is paramount. On the extreme side of the spectrum, 2PP enables to produce micron-sized objects with a resolution of a few hundred nanometres. SL, DLP and DIP are also very well suited to manufacturing small

components for high precision applications thanks to their excellent resolution and accuracy in the order of a few tens of microns. Although all AM processes probably have the technical potential to eventually be scaled-up for the production of large parts, processes that tend to have a lower accuracy but a higher throughput, such as powder-bed processes, may be easier and more cost-effective to scale-up for the production of medium to large parts. In particular, powder-based binder jetting is highly suited to producing large-sized ceramic parts. In this regard however, direct laser sintering does not (yet) offer the same capability as other powder-bed processes due to the extreme thermal gradients that limit the height that can be manufactured without the formation of pores and cracks. Processes that use extensive amounts of polymeric binder such as SL and FDC may also experience limits regarding the maximum wall thickness that can be manufactured for two reasons. First, because binder burnout must be carried out at very slow heating rates, it may not be economically viable to run debinding schedules that could potentially take weeks to fully complete for thick-walled parts. Second, because the high amounts of volatile gaseous species trying to escape the bulk volume by diffusion are likely to result in the formation of pores and cracks.

iv. **Surface finish**: Usually strongly correlated to process resolution, surface roughness is mostly a function of two parameters: open porosity at the surface and stair casing effect. On the one hand, roughness resulting from open pores is directly related to the inability of some AM processes to produce fully-dense parts and to mitigate residual porosity, and on the other hand stair casing effects arise when printing relatively thick layers and is acerbated by poor interlayer merging. Whilst it is commonly accepted that the best surface finish from AM processes can be achieved using SL and DLP vat photopolymerisation technologies, excellent results have also been demonstrated with DIP and S-BJ. Parts manufactured using these two processes usually do not display any open porosity and can be optimised to be seemingly free of stair casing effect. Slurry-based processes S-BJ and S-iLS also provide a good surface finish compared to their powder-based counterparts due to the significant reduction of residual open porosity and the ability to form thinner layers. The often poor surface quality obtained with ceramic extrusion technologies is caused by stair casing and bumpiness due to poor surface merging of successive individual struts caused by stair casing and bumpiness due to poor surface merging of successive individual struts and is exacerbated when using large extrusion nozzles. As discussed in 3.3.3, surface finish of extruded parts can be greatly improved by using smaller orifices (**Figure 12**), although higher resolution comes at the cost of reduced manufacturing throughput. A comparison of dental crowns and frameworks produced using a number of AM technologies is provided in **Figure 21**, and shows the disparities in terms of surface finish that can be achieved currently.

v. **Geometrical complexity**: It is important to realise that not all AM processes have the same capabilities and potential regarding geometrical complexity. The process with the most limited potential for improvement in this regard is without doubt directed energy deposition (DED) due to the fact that neither self-supporting material nor support structures are present to accommodate overhangs. This, however, can be partly addressed by enhancing the DED process with a 5-axis deposition system. Conversely, LS and BJ powder-bed processes, both in their dry powder-based and slurry-based variants, are naturally well-suited to the manufacture of complex-shaped parts thanks to their self-supporting powder bed that allows for the production of intricate geometries and large overhangs without the need for additional support structures. However, these processes do not allow the fabrication of fully-closed volumes since any excess support powder cannot be removed from enclosed cavities and would remain trapped. Whilst the same limitation applies to LOM because the ceramic tape that acts as support would remain trapped inside any closed volume, CAM-LEM addresses the issue thanks to its cut-then-stack approach. Bedless AM processes, such as DIW, DIP, and DLP, may in theory allow the production of fully-enclosed volumes without the need for support structures by following specific design rules, although support material is most likely often going to be needed. Designers must keep in mind that any support structures built inside an enclosed volume are not removable, unless the enclosed cavity is porous, in which case the support material could be dissolved or burnt-out. SL and DLP

technologies are already well developed for AM of ceramics and have been widely used in the industry to produce complex-shaped monolithic components, mostly from oxide ceramics.

vi.   ***Manufacturing costs and time***: Costs incurred and/or time taken by equipment, materials, pre-processing, production, and post-processing must be taken into account. Equipment costs include the purchase price of the AM equipment, running costs (electricity, gases), and maintenance charges from the equipment manufacturer. Materials costs include the price of feedstock materials as well as additional pre-processing costs for material preparation. Processing costs depend mostly on the degree of complexity of the AM process and whether costly equipment is required to run the process, such as high-power lasers and inert gases. Finally, post-processing costs can amount to a significant share of the total production costs due to high-temperature heat-treatments for debinding and sintering, as well as potential consolidation processes such as CIP or HIP, and machining or polishing steps. Such calculations are difficult to run accurately, even more so in the context of ceramic AM. For instance, whilst DIW is a relatively low-cost process overall, it still requires post-processing heat-treatment at high temperature to sinter ceramic parts to full density, which can become relatively expensive for some advanced ceramics such as high melting point carbides requiring inert gas flow in furnace chambers and temperatures in excess of 2000 ᵒC. On the other hand, dLS is in theory a significantly more expensive process due to the use of high-power laser(s) and argon gas, but post-sintering would typically not be required since parts are already sintered to full-density in-situ. Therefore, the time saved and lower amount of post-processing steps (see **Figure 5**) may in fact result in overall manufacturing cost savings. It thus becomes obvious that estimating and contrasting the overall manufacturing costs of each process is a difficult task, and further research dedicated to this topic is required.
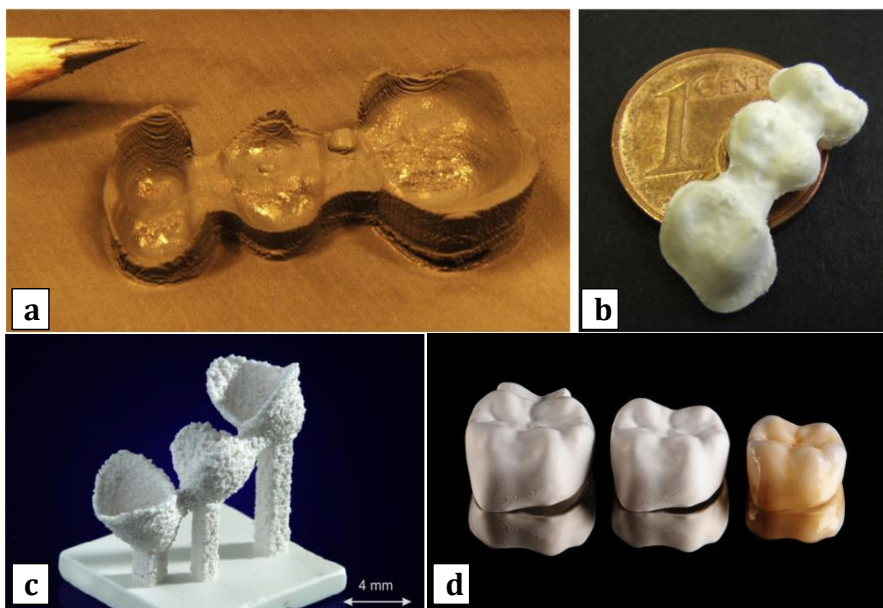
***Figure 21**: Comparison of dental crowns and frameworks produced using a number of AM technologies. A supportive base made of carbon black (a) and the corresponding sintered 3Y-TZP bridge framework (b) produced using DIP, showing an appreciable surface finish despite some surface defects caused by the support materials* [228]. *Dental restoration frameworks manufactured by dLS have a very high surface roughness (c)* [311], *while dental crowns made by DLP (d) display an excellent surface finish and a high level of detail, from the as-printed state to the stained and sintered state (image provided as a courtesy by Dr Johannes Homa, CEO of Lithoz GmbH).*

5.2. Overview of the characteristics and performances of ceramic AM technologies

In this section, we briefly review the main characteristics and capabilities of additive manufacturing In this section, we briefly review the main characteristics and capabilities of additive manufacturing In this section, we briefly review the main characteristics and capabilities of additive manufacturing processes that have been used to shape advanced ceramic materials (**Table 4**).

Powder-based binder jetting (P-BJ) was the first AM process used for shaping ceramics. As it turned out to be a powerful tool for the fast and cost-effective fabrication of highly porous ceramic components from coarse powders, it started being used in the manufacture of porous moulds for investment casting and biomedical scaffolds for tissue engineering. However, the P-BJ process is also characterised by its inability to produce dense struts and monolithic parts, always yielding high levels of residual porosity, which on the one hand tends to be beneficial for the aforementioned applications but on the other hand is highly detrimental to mechanical properties. This issue was addressed by adopting a **slurry-based binder jetting (S-BJ)** approach where coarse dry powders are replaced by fine submicron particles in suspension. The smaller size and higher surface/volume ratio of submicron particles have the double advantage of increasing particle packing during paving and providing a higher sintering activity, respectively, which are both beneficial to obtaining higher final densities. The adoption of the slurry-based approach also resulted in significant improvements of the surface quality of binder jetted components, whilst the ability to produce very large parts economically was not affected. However, an additional concern that arises from using slurries is the prevention of cracks during drying, which requires precise optimisation of the slurry formulation, paving parameters, and drying rates.

A similar evolution happened when **slurry-based indirect laser sintering (S-iLS)** was introduced to improve the **powder-based iLS process (P-iLS).** However, some disadvantages of Slurry-LS compared to Slurry-BJ are the use of expensive lasers and inert environment, which increase the overall manufacturing cost and require more stringent health and safety measures. Besides, whilst multiple nozzles can easily be used in BJ for a faster green layer processing, implementing multiple lasers is more complex and significantly more expensive. Ceramic-laser interactions also have to be considered and can vary widely from one advanced ceramic material to another, potentially affecting the effectiveness of the LS process with some ceramic materials.

Direct laser sintering (dLS) uses similar expensive high-power lasers, but the part is shaped by directly processing the ceramic material itself rather than a binder, making it a single-step AM process, since ceramic materials are sintered as they are being shaped, removing the need for post-process binder burn-out and furnace firing. However, the extreme temperature gradients ceramics arising from the laser have so far prevented the fabrication of crack-free parts taller than a few millimetres, and have also limited the materials investigated to a few specific oxide ceramics. Furthermore, poor control over dimensions of the melt pool typically result in high surface roughness.

Directed energy deposition (DED) is the other single-step AM method and has the potential to enable the rapid additive fabrication of simple ceramic shapes. Extreme temperature gradients are also an issue with DED and usually result in thermal cracking. Some advanced ceramics, in particular non-oxide ceramics with high melting temperature, may not be processable using the current technology.

Sheet lamination (LOM/CAM-LEM) has been used to produce monolithic parts of both oxide and non-oxide ceramics of medium to large dimensions with acceptable mechanical properties, but the surface quality and resolution achievable are limited.

Stereolithography (SL) and **digital light projection (DLP)** can be used to manufacture monolithic components with an excellent surface finish and a very high precision. SL is ideal for fabricating very fine features with a precision of under 1 μm, but it does not permit the economical fabrication of thick walls due to the substantial amounts of binder needed. This process may also be intrinsically unsuited to processing non-oxide ceramic materials whose high absorbance at wavelengths used in the SL process result in insufficient cure depth and partial photocuring. Indeed, whilst SL and its variants are now widely used industrially to shape white ceramics, including alumina, zirconia and hydroxyapatite, it has not yet been demonstrated for light absorbing non-oxide ceramics such as boron carbide and titanium carbide, although demonstration parts made of silicon carbide have been showcased.

Direct inkjet printing (DIP) is another high-precision additive technology that may be used when high resolution and accuracy are required. Although higher resolutions are achievable using stereolithography, DIP has the striking advantage of allowing the simultaneous deposition of micron-size droplets of multiple materials for the production of complex material gradients at the microscopic level, and is the AM process that allows the finest control over microstructural composition grading.

Ceramic material extrusion processes (RC, DIW, CODE, FDC...) have the advantage of being the cheapest ceramic AM technologies, the most versatile, and the easiest to scale, enabling the fabrication of very small components as well as much larger ones. Material grading is also possible using extrusion processes with multiple deposition orifices, although not with the same level of microstructural control as with DIP. Surface finish however is directly dependent upon the shape and size of the deposition nozzle, giving rise to a direct conflict between surface quality and fabrication throughput. Both DIP and extrusion technologies do not suffer the limitations of SL concerning the range of ceramics that can be shaped, and a wide range of oxide and non-oxide ceramics have already been demonstrated with both processes.

5.3. Density and mechanical properties

The ability for AM processes to produce porous components is essential to a vast number of applications and has been widely demonstrated. However, for AM of advanced ceramics to further develop and reach the same technological maturity as metal AM, it is essential that it enables the manufacture of high-performance ceramic materials into monolithic components with adequate mechanical properties. Values of mechanical properties for various advanced ceramic materials obtained using each AM technology were detailed throughout Sections 3 and 4 of this review. In this section, we propose to compare the highest mechanical properties reported for alumina using various AM processes, as reported in **Table 5**, where a high sintered density was achieved and mechanical properties were assessed. First, high sintered densities above 97% TD could be obtained using each one of the AM technology listed in the table, although P-iLS and P-BJ both required post-process WIP to increase density. Second, the wide variation in mechanical properties that were obtained indicates that some AM processes may be more suited to manufacturing mechanically strong parts than others. For instance, a 3PB flexural strength of only 156.6 MPa was achieved using robocasting [126], whilst stereolithography yielded a bending strength more than twice as high at 367.9 MPa [326] and DLP resulted in a 4PB flexural strength comparable to that of parts made by slip casting [271]. Vickers hardness values from AM parts produced by LENS, RC, CODE, and SL compared well with the hardness of tape cast alumina [327] and relatively high values of fracture toughness could be achieved with alumina shaped by LENS and CODE. Comparing processes in this way to evaluate their respective ability to produce high mechanical strength is limited due to the low amount of mechanical data available. More data on the mechanical properties of AM parts is needed; as such mechanical testing needs to be more systematically investigated, and always in accordance with the relevant ASTM testing standards for meaningful comparision.

Table 49: Current characteristics and capabilities of advanced ceramic AM technologies.

AM technology	Ceramic feedstock	Ideal powder size	Amount of binder and organics in green part	Resolution	Large monolithic parts enabled	Ideal part dimensions	Geometrical complexity	Surface finish	Can 3D material grading be enabled?	Single-step or multi-step AM	Overall manufacturing costs, including machine, feedstock, processing, post-processing	Preferred and/or potential applications
RC / DIW / CODE	Highly-loaded aqueous slurry or paste	Submicron	Low	High	Yes	1 mm – 1 m	Medium [1]	Low - High	Yes	Multi-step	Low	Structural parts, functional ceramics, precision components, scaffolds,
FDC	Highly-loaded thermoplastic polymer filament	Submicron	High	Medium	No	1 cm – 10 cm	Medium [1]	Low-Medium	Yes	Multi-step	Medium	Functional ceramics
Solvent-DIP	Organic solvent- or water-based suspension	Submicron	Low	High	Yes	1 mm – 10 cm	Medium [1]	High	Yes	Multi-step	Medium	Structural parts, functional ceramics, precision components
Wax-DIP	Wax-based suspension	Submicron	High	High	No	1 mm – 10 cm	Medium [1]	Medium-High	Yes	Multi-step	Medium	Structural parts, functional ceramics, precision components
BJ	Dry powder	Coarse	Medium	Medium	No	1 cm – 1 m	High	Low	No	Multi-step	Medium	Casting moulds, infusion preforms, microporous scaffolds
Slurry-BJ	Aqueous slurry	Submicron	Low	High	Yes	1 cm – 1 m	High	High	No	Multi-step	Medium	Structural parts, large monolithic parts
iLS	Dry powder	Coarse	Medium	Medium	No	1 cm – 10 cm	High	Medium	No	Multi-step	High	Casting moulds, infusion preforms, microporous scaffolds
Slurry-iLS	Aqueous slurry	Submicron	Medium	Medium	No	1 cm – 10 cm	High	Medium-High	No	Multi-step	High	Casting moulds, infusion preforms, microporous scaffolds
dLS	Dry powder	Coarse	None	Medium	No	1 cm – 10 cm	High	Low	No	Single-step	Medium [2]	Casting moulds, infusion preforms, microporous scaffolds
Slurry-dLS	Concentrated aqueous slurry	Submicron	Low	Medium	No	1 cm – 10 cm	High	Medium	No	Single-step	High [2]	Casting moulds, infusion preforms
DED	Dry powder	Coarse	None	Low	Yes	1 cm – 10 cm	Low	Low	Yes	Single-step	Medium [2]	Structural parts, large monolithic parts
SLA / DLP	Highly-loaded photopolymer	Submicron	High	High	No	1 mm – 1 cm	High	High	No	Multi-step	Medium	functional ceramics, dentistry, precision components,
2PP	Liquid preceramic polymer	Submicron	High	Very High	No	1 µm – 1 mm	High	High	No	Multi-step	High	Very high precision components
LOM / CAM-LEM	Ceramic green tape	Submicron	Medium	Low	Yes	10 cm – 1 m	High	Medium	No	Multi-step	Medium	Structural parts, large parts

[1] Some geometries such as negative overhangs cannot be created when using extrusion and DIP without a support material; high geometrical complexity can be achieved if a soluble support material is used.

[2] The overall manufacturing cost of single-step ceramic AM processes (dLS and DED) is difficult to evaluate and compare to multi-step technologies; despite being energy-intensive AM processes, significant time and cost savings can be expected nonetheless since post-AM debinding and densification steps are not required.

Table 510: *Comparison of the mechanical properties of additively manufactured Al$_2$O$_3$ standard specimens, contrasted to the mechanical properties obtained using conventional forming techniques.*

Manufacturing Process	Remarks	Sintered Density (% TD)	Bending Strength (MPa) 3PB	Bending Strength (MPa) 4PB	Vickers Hardness (GPa)	Fracture Toughness K$_{Ic}$ (MPa m$^{1/2}$)	Year
P-iLS [242]	WIP	>98	400	400	-	-	1993
P-iLS [67]	-	88	255	-	-	-	2007
LOM [110]	Highly anisotropic shrinkage and mechanical properties	97.1	228	-	3.8 *	-	2001
LENS [20]	As-fabricated	94	-	-	15.3 *	2.1 ±1.3	2008
LENS [20]	Heat treatment (1600°C, 5h)	98	-	-	16.7 *	4.4 ±1.4	2008
DIW [126]	3.17 ±0.37 μm grain size	98	156.6	-	-	-	2016
RC [123]	1.40 μm average grain size	97	232	232	18.6	3.31 ±0.23	2016
DIW [328]	Al$_2$O$_3$ obtained from boehmite precursor	97	591	-	-	-	2017
DIW [329]	Pressureless sintered	98	252	-	15.0	-	2018
CODE [190]	Equiaxed grains <5 μm. Quasi-isotropic shrinkage.	98	364	364	19.8	4.5 ±0.1	2017
PSD [224]	1.6 ± 0.3 GPa compressive strength	93.7	-	-	14.0	4.7 ±0.3	2018
P-BJ [242]	WIP	97.8	231.5	231.5	-	-	1993
P-BJ [242]	MgO-doped, WIP	99.2	324	324	-	-	1993
SL [330]	Liquid desiccant drying and a two-step debinding process	99.3	-	-	~17.5	-	2016
SL [326]	m = 10.2	98.1	367.9	-	-	-	2017
DLP [280]	3.05 ±0.29 μm grain size	99.3	427	427	-	-	2015
Slip casting [331]	-	>99.7	408 - 531	408 - 531	-	3.7	2005
Tape casting [327]	-	98.1	-	-	15.91	4.29 ±0.06	2015

* converted from HV to GPa by multiplying the value in HV by the standard gravity g=9.80665 and dividing by 1000.

5.4. Post-processing

The three critical aspects that ceramists endeavour to modify and improve through post-processing of advanced ceramics are the final density, microstructure and surface quality. Indeed, these three properties directly affect the overall performance of ceramic components and in particular their mechanical properties. The microstructure and density of advanced ceramics are highly influenced by the sintering method, in particular whether post-densification is performed by pressureless or pressure-assisted sintering, but also by the selection of temperature schedule [332] and atmosphere [333]. These considerations are essential since improving the final density by a few percentage points closer to 100% TD, and reducing the average grain size, can result in a double or even triple digit percentage increase in the mechanical properties [242][247]. Furthermore, a high surface roughness is also undesirable, first for aesthetic reasons, and second because surface features may initiate the formation of cracks under mechanical load, thus resulting in significantly lower elastic modulus, flexural strength and hardness [334].

Ideally, ceramic parts produced by AM should be fully dense, have a fine microstructure and a low surface roughness without the need for additional pressure-assisted densification and surface modification, since these extra-steps significantly increase manufacturing complexity, time and costs. Fully-dense ceramics were demonstrated using single-step AM processes dLS and DED, although in both cases careful consideration of material selection by choosing eutectic ratios of oxide ceramics was necessary to produce crack-free dense parts. Both processes, however, currently come with severe limitations regarding part size, as well as extremely high surface roughness for dLS [311] and limited geometrical complexity for DED [323]. Some multi-step AM processes (followed by a suitable pressureless sintering schedule) may already enable the production of complex-shaped, crack-free, near-fully dense parts with specific ceramic materials, such as, for instance, vat photopolymerisation of alumina [280] and material extrusion of silicon nitride [158], alumina [190], or zirconia [193]. Other AM processes, or even the AM processes listed above but applied to different ceramic materials, would result in porous structures that require additional densification steps to increase the density. For instance, while Costakis et al. could produce 98% dense alumina samples using DIW followed by pressureless sintering, boron carbide parts made using the same process reached only 82% TD without post-AM densification [126][128].

Therefore, in the current context of ceramics AM, it remains essential to consider and investigate post-densification methods and surface modification post-processing to produce highly dense ceramic components with a suitable microstructure and the desired surface roughness.

5.4.1.   Surface modification

Significant progress has been made in the past 20 years in developing the processing routes to enhance the surface quality of ceramics shaped using AM without the need for post-processing. Indeed, the surface finish of oxide ceramics produced by vat photopolymerisation is now on par with that of injection-moulded parts [280], while the optimisation of paste formulation and the use of smaller extrusion orifices have enabled a reduction in the surface roughness of ceramics shaped by material extrusion [188]. The introduction of a slurry-based approach to improve dry powder-based AM processes also resulted in a significant improvement in the surface finish of parts produced by binder jetting [64] and laser sintering [318]. Nevertheless, most AM processes still result in relatively high surface roughness and the formation of surface imperfections. Post-AM surface modification therefore remains a key step in additive manufacturing of ceramics.

Due to the extreme hardness of sintered advanced ceramics, machining, grinding, lapping, and polishing after firing are generally performed with diamond tools, making post-processing extremely expensive [1]. In fact, hard machining can account for up to 75% of the overall manufacturing cost of advanced ceramics components, compared to 5-15% for metallic components [3]. Green machining is preferable as a much more economical alternative to hard machining and it enables significantly higher material removal rates. However, green parts must be thick enough and have sufficient strength to enable green machining, and some machining operations such as tapping and threading are difficult to perform in the green state without forming critical defects and cracks [335]. The use of machining is also subject to the conventional manufacturing and design limitations imposed by available paths for cutting tools and restricted access

to internal features. This limitation can often be overcome by implementing *in-situ* machining of green parts as they are being manufactured rather than carrying out the machining as a post-process, thus enabling almost any surface to be machined as it is being manufactured, even for the most complex parts. This method enabled a reduction in the R_a of alumina components shaped by ceramic extrusion from 8.09 μm to 1.11 μm, although it also resulted in the introduction of surface defects that adversely affected the mechanical properties [198].

5.4.2.   Post-AM densification

Pressure-assisted densification in the green or sintered state is a common and effective way to increase the density of advanced ceramics after shaping. Cold, warm, and hot isostatic pressing (CIP, WIP, and HIP, respectively) are preferred over uniaxial hot pressing (HP) since they since they can be used to make complex-shaped parts. Liu *et al.* shaped SIC by laser sintering followed by CIP of the green body and reaction sintering to increase the density and green strength of fabricated specimens [336]. They used a CIP pressure of 130 MPa, with a pressure holding time of 5 min, boost rate of 2 MPa/s, and pressure relief rate of 1 MPa/s.

Eqtesadi *et al.* showed that firing temperature had a significant impact on the densification of B_4C parts produced by robocasting, as would be expected: the density increased by ~20% when the sintering temperature was increased from 1900°C to 2100°C [161]. As shown in **Figure 22**, densification was then further improved from 90% to 95% TD by applying an addition CIP step before firing at 2100°C, which resulted in a 35% and 24% increase in Vickers hardness and compressive strength, respectively.

WIP was applied to 3D printed Al_2O_3 and MgO-doped Al_2O_3 [242]. Whilst as-printed Al_2O_3 green parts had a low density of 36% TD, a high final density of 97.8% TD was obtained after WIP and furnace sintering, with a 4PB flexural strength of 231.5 MPa. The final density and bending strength of WIP-ed specimens were further improved to 99.2% TD and 324 MPa, respectively, by doping the Al_2O_3 with MgO.

Carrijo *et al.* showed that high uniaxial or CIP pressures were beneficial to increase the density and flexural strength of sintered Ti_3SiC_2 parts manufactured by binder jetting [243]. While the porosity of sintered specimens not subjected to a post-densification step was as high as 48%, CIP at 180 MPa and uniaxial pressing under 726 MPa enabled the residual porosity to be lowered to 3.6% and 1.7%, respectively. However, one must keep in mind that the high efficacy of uniaxial pressuring for improving densification is counterbalanced by the limitations it brings in terms of geometrical design freedom, while isostatic pressing enables the densification of complex-shaped parts.

Another method commonly employed to increase the density of advanced ceramics is infiltration. Zhang *et al.* fabricated Al_2O_3/glass composites by shaping Al_2O_3 preforms using P-BJ followed by pressureless infiltration of LAS glass into sintered porous preforms at 1100°C for 2 h [244].

Infiltration is also often used in the manufacture of RBSiC, either by liquid silicon infiltration (LSI), where molten silicon is fed into the pores of the SiC or C preform [301][276], or by precursor infiltration and pyrolysis (PIP), where a low viscosity liquid preceramic polymer is used to fill the pores of a C preform and then pyrolysed to form SiC [295].

RBSiC parts were produced by indirect laser sintering from a 67:33 wt/wt SiC/Si powder mixture to shape a porous SiSiC preform that was subsequently impregnated with a graphite suspension and infiltrated with molten Si at 1450°C to finally produce 95% dense RBSiC parts [301]. Tian *et al.* used SL to shape a photocurable resin consisting of phenolic epoxy acrylate, phenolic resin, triethylene glycol as pore forming agent, and benzoin dimethyl ether as photoinitiator [276]. The fabricated resin prototypes were pyrolysed at 850°C for 1 h to obtain porous carbon preforms that were then infiltrated with molten silicon and converted to RBSiC. Fu *et al.* used binder jetting to manufacture SiSiC components from powder blends of Si, SiC, and dextrin [247]. Parts were infiltrated in the green state with liquid silicone resin and converted into SiC parts with a final residual porosity of only 0.5%, a 256 GPa elastic modulus, a 4PB flexural strength of 208 MPa, and fracture toughness of 2.5 MPa m$^{0.5}$. He *et al.* used stereolithography to manufacture highly porous complex-shaped SiC preforms that were infiltrated after polymer burnout with a polycarbosilane preceramic polymer. After 8 cycles of PIP treatment, SiC ceramics with a final density between 79.2% and 84.8% TD were obtained [295].
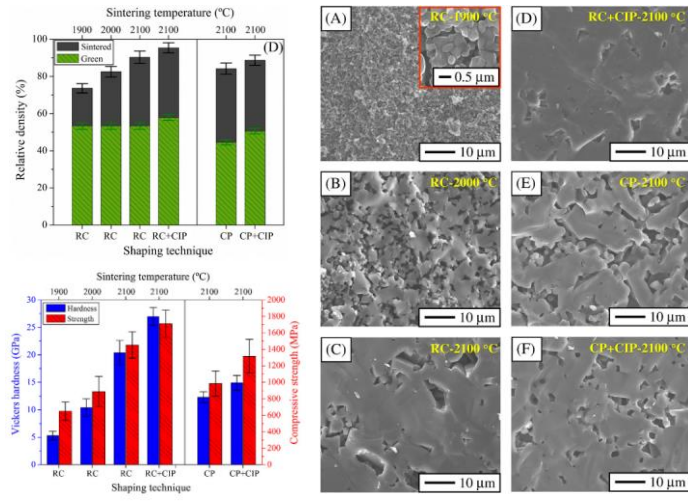
Figure 22: *Effect of SPS firing temperature and of CIP on the density and mechanical properties of sintered B$_4$C samples produced by robocasting* [161]

6.   Short and Long-Term Goals for the Development of Advanced Ceramic AM

When looking at the recent evolution of AM in the metal industry, which is now well developed and used to produce functional parts for high-performance applications, it is clear that the three main factors that will drive the mainstream adoption of AM to manufacture ready-to-use technical ceramic parts are performance, reliability, and cost.

6.1. Benefits and applications of AM in the ceramic industry

Being a near-net-shape manufacturing process, AM could help reduce the need for machining, which can account for more than 70% of total manufacturing costs [3], especially in the case of ultra-hard ceramics such as SiC and B_4C . Furthermore, being a mould-free manufacturing solution, AM can lead to significant cost reductions as well as much shorter production lead times. Indeed, mould and die tooling required for formative ceramic manufacturing processes are extremely costly and time-consuming to manufacture. As a result, AM is the most cost effective solution for prototyping and low volume production series, whilst even enabling the rapid fabrication of fully-personalised and custom ceramic components. A faster turnaround – typically days instead of weeks – also means that new products can be commercialised more quickly (reduced time to market), or on the other hand that more time is available during the product design phase to produce more prototypes, and thus provide a better end-product. This will be even truer in the future when – or if – single-step ceramic AM technologies start to be used commercially since further time savings would then be realised. Moreover, AM provides enhanced design freedom at no extra-cost, whereas complex geometries can be difficult and expensive to produce using conventional manufacturing processes, requiring complex moulds to be made or extremely costly machining to be performed. Besides, this enhanced design freedom can result in new functionalities and designs that cannot be produced using subtractive or formative technologies, such as conformal cooling channels for cutting tools and randomised yet repeatable mesoporous filter geometries. Applications where AM could prove particularly useful to the ceramics industry are listed in **Table 6**Table 11.

*Table 6*11*: Industrial applications where ceramic AM could provide significant added value.*

Application	Ceramic materials	Potential benefits of AM
Dentistry, dental crowns	Al_2O_3, ZrO_2, $Li_2Si_2O_5$	V, P, C, L
Scaffolds for tissue engineering	TCP, HA, Bioglass	V, P, M, F, C, L
Orthopaedic implants, femoral heads, acetabular cups, shoulder buttons, radial heads, spinal components	TCP, HA, Al_2O_3, ZrO_2, Bioglass	V, P, C, L
Cranial segment	TCP, HA	V, P, C, L
Blood valves	Al_2O_3	V, C, L
Investment casting cores	SiO_2	G, C, L, A
Blades, gear wheels, bearings	Al_2O_3, SiC, Si_3N_4	G, V, L, A
Ballistic armour, vehicle panels and personal protection	Al_2O_3, TiB_2, SiC, B_4C	V, P, M, F, C, L, A
Cutting tools	Al_2O_3, Si_3N_4, B_4C	G, M, C, L
Nozzles for slurry pumping, grit blasting and water jet cutting	B_4C	G, V, M, L
High performance valve components for corrosive and abrasive fluid flows	ZrO_2, Si_3N_4	V, M, L
Electrical components, substrates, connectors, spark plug insulators	Al_2O_3, SiC	G, V, C, L
Filters	Al_2O_3, ZrO_2	G, V, F, L
Waveguides for microwave applications	Al_2O_3	V, C, L
Laser reflectors, tubes, waveguides, chambers and spacers	Al_2O_3, AlN	V, C, L
Shielding, control rods, and shut down pellets in nuclear power plants	B_4C	V, L

G: geometrical complexity; **V**: single-unit/low-volume production; **P**: personalised design; **M**: material grading; **F**: functional grading; **C**: lower cost; **L**: reduced lead-times; **A**: less assembly

57

In future, this range of applications could be further expended and strengthened by the improvement and refinement of single-step AM processes. Indeed, when the scientific and technical challenges associated with dLS and DED of advanced ceramics are fully understood and have been overcome, these processes will provide a faster and more effective path to full-scale industrialisation due to their never-seen-before ability to produce near-net-shape ceramic components directly in the sintered state.

6.2. Current limitations to the industrial adoption of ceramic AM

Although ceramic AM has made tremendous progress in its near 30 years of existence, it still counts several limitations that have so far prevented its widespread adoption by industrial product manufacturers.

• **Single-step ceramic AM processes**. Although dLS and DED have the potential to become game-changers in the industrial ceramic manufacturing landscape, there is currently a limited understanding of laser-material interactions and of the steps that need to be implemented in order to prevent the formation of critical defects (porosity and cracking). Careful material feedstock selection and systematic optimisation of printing parameters have been essential to shape defect-free, fully dense ceramics using both dLS and DED; these techniques have been demonstrated for the single-step fabrication of fully dense Al_2O_3-ZrO_2 eutectic compositions [311][323]. Future efforts should focus on increasing the range of materials as well as on lowering the surface roughness of as-printed parts, improving dimensional accuracy, and enabling the production of larger components. Significant developments are needed in this research area in order to increase the performance and reliability of single-step AM processes.

• **Multi-material AM**. There is significant interest in the ability to additively manufacture components made of several materials, not only ceramic-ceramic but also ceramic-metal, ceramic-polymer, and even ceramic-metal-polymer combinations, where dissimilar materials are deposited in turn to fabricate as-printed fully functional devices. However, there are significant challenges associated with this approach, the most notable being the requirement for ceramics to undergo post-fabrication high-temperature furnace sintering, or pyrolysis in the case of PDCs. Indeed, most polymers and metals would not survive pyrolysis temperatures above 800°C, and even less so firing temperatures required to sinter ceramics (e.g. 1500°C for alumina and up to 2400°C for boron carbide). This is the fundamental reason why as-printed multi-material functional devices where ceramics act as structural materials are not currently feasible and may well never be. However, multi-material components can be manufactured by first 3D printing and firing the structural ceramic, followed by metal, polymer or ceramic infiltration [337][338][339], and AM deposition of additional materials onto ceramic components using either extrusion-based processes (DIW) or inkjet printing (DIP).

• **The occurrence of bulk and surface defects** is not always well-controlled and most processes still require further research and optimisation to consistently yield crack-free parts with high final densities. The most common issues across AM processes include excessive surface roughness, lumps, internal porosity, and surface micro- and macro-cracks, which are caused by material feedstock inhomogeneities such as particle agglomerates and trapped air bubbles, part deformation during AM operation, uncontrolled drying and non-isotropic shrinkage.

• **Materials-process-microstructure-properties relationship**. There is a limited understanding of the relationships between material feedstock, process parameters, final microstructure, and mechanical properties, especially in the case of single-step AM processes, although some ceramic AM processes including SL, DLP, and DIW have been investigated more in-depth than others.

• **Monolithic and mechanically-strong ceramic components** are still challenging to manufacture reliably and consistently. Comprehensive mechanical testing need to be performed more systematically.

• **Limited material selection**. So far, most of the research efforts have focused on oxide ceramics, with a strong emphasis on silicates, alumina, and zirconia, since they are the most widely used advanced ceramics and are relatively inexpensive. Silicon nitride has been demonstrated with LOM and a number of extrusion-based processes, whilst both SiC and RBSiC have been processed using either LS, LOM, BJ, or RC, and mechanical properties were studied. There is still limited reported results on AM of B_4C, the most notable attempts thus far were made using robocasting, whereas a number of other advanced non-oxide ceramics are yet to be investigated. Polymer-derived ceramics have been shaped using LS, DIW, binder jetting, vat photopolymerisation, LOM, and SPPW, and this class of ceramic materials provides a significant opportunity to expand the range of ceramics that can be shaped using AM.

• **Scalability**. Small components with acceptable properties can already be manufactured and a number of industrial AM machines exist on the market, mostly based on vat photopolymerisation processes, but also on DIW, BJ, and DIP. However, large 3D printed ceramic parts with high density and low surface roughness still haven't been demonstrated to this day.

6.3. Improving performance

In the context of ceramic AM, performance relates mostly to density, mechanical properties, surface finish, geometrical complexity, and scalability. For the widespread use of AM to become a reality in the ceramic industry, the performance of additively manufactured components must be comparable to at least those of parts fabricated using well established conventional manufacturing technologies such as uniaxial pressing, slip casting and injection moulding. A high sintered density and an absence of cracks is required for ceramic parts to display high mechanical properties, neither of which are straightforward to obtain using AM processes. The most important parameters during AM fabrication that impact final density are particle size distribution and powder packing density. To obtain higher packing densities, research has moved from dry powder-based AM processes to focus on slurry-based approaches, which provide the triple advantage of *(i)* allowing for the use of submicron/nano powders, which result in a better packing density and have a higher sintering activity than coarse powders, *(ii)* enabling the free settling of ceramic particles into the liquid medium for a more effective packing, and *(iii)* enabling the formation of thinner layers, which greatly improves resolution and helps minimise stair casing effects. Both macro-cracks and micro-cracks are initiated either at internal irregularities, such as pores and particle agglomerates, or at surface defects. Cracks are propagated in ceramic materials by mechanical stresses, fast drying kinetics and thermal gradients.

It is well known that various levels of porosity can be introduced in AM parts, either on purpose or involuntarily. On the one hand, macro- and micro-porosity are usually introduced into parts by design to provide enhanced functionality for specific applications, such as scaffolds for tissue engineering or filters. On the other hand, residual porosity, which typically consists of pores with a diameter of from several hundred nanometres to a few micrometres, is inherent to ceramic processing and must be minimised as much as possible to improve the mechanical and chemical performance of ceramic parts.

Expanding the range of advanced ceramic materials that can be processed reliably using AM technologies is also a crucial step for the development of ceramic AM. A list of ceramic materials that have already been successfully processed by AM is provided in **Table 7**.

Good mechanical properties that are comparable to those obtained using conventional forming processes have already been achieved with several AM technologies. However, reported results vary significantly between research groups and several AM processes have yet to be used to produce samples for mechanical testing, showing the need for further systematic mechanical characterisation.

Table 7: Advanced ceramic materials that were successfully demonstrated for each of the main AM technologies.

AM technology	Ceramic materials demonstrated in the literature
Powder-iLS	Al_2O_3 [40-47], SiO_2 [73], ZrO_2 [73][74], SiC [75][76][77], ZrB_2 [78], apatite–mullite [79]
Slurry-iLS	Al_2O_3 [95], Silica-clay [64-67]
Powder-dLS	Al_2O_3 [300], RBSiC [301], Al_2O_3-SiO_2 [302], Al_2O_3-ZrO_2 [304], ZrO_2 [309], HA-silica [305], LAS glass [306]
Slurry-dLS	Porcelain [314], SiO_2-Al_2O_3 [315], LAS glass [306]
DED	Al_2O_3 [20], Al_2O_3-ZrO_2 [323], Al_2O_3-$Y_3Al_5O_{12}$ [324]
LOM/CAM-LEM	Al_2O_3 [73][114][110][117], SiO_2 [73], SiC [105][111], RBSiC [8], Si_3N_4 [117][109], LZSA [108]
FDC	Al_2O_3 [65], SiO_2 [129], Si_3N_4 [137][138][139], PZT [140]
T3DP	Al_2O_3 [132], ZrO_2 [147]
RC/DIW	Al_2O_3 [153][126][154][127][155], PZT [156], mullite [157], $BaTiO_2$ [122], Si_3N_4 [159], SiC [160], B_4C [128][161]. TCP [31][162][163], HA [164], HA/β-TCP [165][166][167][168], wollastonite/TCP [169], C-Al_2O_3 [170], bioactive glass [120][171][172][173]
FEF	Al_2O_3 [134], $CaCO_3$, ZrB_2 [182], B_4C [183], bioactive glass (13-93) [184]
CODE	Al_2O_3 [135][185-187], ZrO_2 [191], $CaCO_3$ [188]
Solvent-DIP	Al_2O_3 [215], TiO_2 [216], $MoSi_2$ [213], ZrO_2 [214], Si_3N_4 [213], SiC [210]
Wax-DIP	Al_2O_3 [226][207]
Powder-BJ	Al_2O_3 [241][242], Ti_3SiC_2 [243], Al_2O_3/glass [244], SiOC [245], wollastonite [246], SiSiC [247]
Slurry-BJ	Al_2O_3 [257][64]
SL/DLP	Al_2O_3 [280], SiO_2 [278], ZrO_2 [282][281], ZTA [275], HA [340], RBSiC [276]
2PP	SiCN [263]
SPPW	SiOC [14]

6.4. Increasing reliability

The exceptional physicochemical and mechanical properties that typically characterise advanced ceramic materials are governed by the occurrence of flaws such as porosity, cracks and inhomogeneity that are introduced during part fabrication. It is essential that these defects be well controlled and predictable so that high-performance ceramic components can be obtained and behave in a repeatable and reproducible manner. Indeed, high manufacturing reliability is equally as important as performance for industrial organisations to fully embrace additive manufacturing for the fabrication of technical components for high value applications. Yet, research groups working on AM of ceramics too often did not and still do not provide either qualitative or quantitative information on the effective reliability and consistency of their manufacturing method, too often presenting and discussing their best results whilst leaving aside failed attempts. For instance, a technology that would enable to produce only one component out of four with the desired properties – i.e. giving a failure rate of 75% – would obviously not be acceptable to most manufacturers, but it is likely that several current ceramic AM processes provide such low levels of manufacturing reliability. Therefore, it is essential that research efforts focus not only on improving the performance of additively manufactured ceramics, but also on enhancing the reliability

of AM processes in order to prevent the creation of critical defects during fabrication. Besides, a common way of characterising and quantifying the reliability of brittle materials is by performing a Weibull Analysis, where the Weibull distribution is a continuous probability distribution providing the probabilities of occurrence of different outcomes; A two-parameter Weibull distribution is typically used to describe the strength distribution of ceramics and is usually determined using the four-point bending method. The Weibull modulus is used to describe the strength variability of ceramics and other brittle materials and directly relates to the distribution of physical flaws, whilst the scale factor describes the stress level below which 63.2% of the samples fail. A low Weibull modulus would show that flaws are not uniformly distributed in the ceramic material, thus indicating a poor reliability and a broad distribution of strengths from one specimen to another. Despite being an extremely important component of ceramics manufacturing and testing, Weibull Analysis has been scarcely carried out by research groups investigating AM of ceramics. Therefore, more systematic description and discussion of the reasons behind possible inconsistent manufacturing quality, combined with Weibull analysis of AM specimens, are required to gain a better and more comprehensive understanding of the factors affecting the reliability of ceramic AM processes.

6.5. Reducing costs

Costs savings is one of the most important potential high-value upside of additive manufacturing for the ceramic industry. Indeed, the mouldless nature of AM means that substantial cost savings can be made on the manufacture of advanced ceramic components, especially in the case of low-volume production. Negative AM also provides the ability to reduce production costs by 3D printing moulds for ceramic casting, thus lowing the costs and shortening the lead-times associated with manufacturing investment casting or gelcasting moulds. In the long-term, if single-step AM processes can be improved so as to provide the same performances and reliability as multi-step AM processes and conventional ceramic forming technologies, they would then undoubtedly take over to become the primary AM method to shape functional advanced ceramic parts due to the very significant time and cost savings that would ensue. However, such developments are unlikely to occur in the near future due to the currently limited choice of suitable ceramic materials, low performance of single-step AM technologies, and the limited understanding of the science underpinning these processes.

7. Conclusions

Additive manufacturing has the potential to significantly disrupt the ceramics manufacturing industry by providing a wide range of new opportunities such as increased design freedom, functional and materials grading, mould-free fabrication, and cost-effective low-volume production. AM is therefore particularly well suited to replace injection moulding for low-volume production of complex-shaped ceramic components.

However, AM of advanced ceramics has proved to be significantly more challenging than AM of polymers or metals due to the high melting points, brittleness and hence low tolerance to processing defects of this class of materials. Although considerable progress has already been achieved throughout the past 20 years, further research and development is still needed to accelerate the adoption of ceramic AM. Whilst it was widespread practice in the early days of ceramic AM to improve the additive fabrication of ceramics by only adapting the feedstock to existing AM machines, the approach that consists in combining the optimisation of material formulations and processing routes with the development of AM machines specifically designed to process ceramic materials has shown to be a more effective way to tackle the processing challenges specific to ceramic materials.

Since each AM process has its own advantages and limitations, AM process selection is dependent upon the requirements set by the targeted application in terms of ceramic material, final density, surface finish, part size, etc. Each one of these parameters can have a strong influence on the suitability of an AM process to provide the required manufacturing performance.

With the steady improvement of the performance and reliability of additively manufactured ceramic components, interest in ceramic AM is growing rapidly and industrial adoption is slowly increasing, with more and more AM machines becoming commercially available, although the actual industrial uptake of commercial AM machines for end-use applications is still rather low. Nevertheless, mechanical properties comparable to that obtained using conventional manufacturing processes have been reported using several AM technologies and with various advanced ceramic materials. Lithography-based processes already provide the same surface finish as injection moulding and are already well established as a strong competitor to forming processes; other technologies such as DIP and DIW are starting to become commercially available too.

The development of a single-step AM process able to produce defect-free, fully-dense ceramic parts whilst retaining the freeform fabrication feature that characterises AM, can be considered the ultimate goal, although such an objective, if not utopic, is probably far from being realistically achievable in the near future. Instead, most research teams currently focus on the development and optimisation of viable ceramic systems and processing methods for exploitation in multi-step additive manufacturing. Research has mostly moved towards the use of slurry-based processes instead of dry powders to enable the fabrication of pore-free and crack-free components with a high surface finish and a fine microstructure.

References

[1]   F. Klocke, "Modern approaches for the production of ceramic components," *J. Eur. Ceram. Soc.*, vol. 17, no. 2–3, pp. 457–465, 1997.

[2]   Y. Yang, E. Laarz, S. Kaushik, E. Mueller, and W. Sigmund, "3.1 Forming and Drying," in *Handbook of Advanced Ceramics*, Elsevier, 2003, pp. 131–183.

[3]   I. D. Marinescu, Ed., *Handbook of Advanced Ceramics Machining*, 1st Editio. Boca Raton, FL, United States: CRC Press, 2007.

[4]   R. E. Cowan, "Slip Casting," in *Treatise on Materials Science & Technology*, vol. 9, 1976, pp. 153–171.

[5]   M. J. Edirisinghe and J. R. G. Evans, "Review: Fabrication of engineering ceramics by injection moulding. I. Materials selection," *Int. J. High Technol. Ceram.*, vol. 2, no. 1, pp. 1–31, Jan. 1986.

[6]   G. Tari, "Gelcasting ceramics: A review," *Am. Ceram. Soc. Bull.*, vol. 82, no. 4, pp. 43–46, 2003.

[7]   I. Gibson, D. Rosen, and B. Stucker, *Additive Manufacturing Technologies*. Springer Science+Business Media New York, 2015.

[8]   H. Windsheimer, N. Travitzky, A. Hofenauer, and P. Greil, "Laminated object manufacturing of preceramic-paper-derived Si-SiC composites," *Adv. Mater.*, vol. 19, no. 24, pp. 4515–4519, 2007.

[9]   J. D. Cawley, "Computer-Aided Manufacturing of Laminated Engineering Materials (CAM-LEM) and its Application to the Fabrication of Ceramic Components Without Tooling," in *ASME 1997 International Gas Turbine and Aeroengine Congress and Exhibition*, 1997, p. 6.

[10]   S. Onagoruwa, S. Bose, and A. Bandyopadhyay, "Fused Deposition of Ceramics (FDC) and Composites," in *Proceedings of Solid Freeform Fabrication Symposium*, 2001, pp. 224–231.

[11]   T. Huang, M. S. Mason, G. E. Hilmas, and M. C. Leu, "Freeze-form Extrusion Fabrication of Ceramic Parts," *Virtual Phys. Prototyp.*, vol. 1, no. 2, pp. 93–100, 2006.

[12]   J. Cesarano, B. H. King, H. B. Denham, J. Cesarano III, and H. B. Denham, "Recent Developments in Robocasting of Ceramics and Multimaterial Deposition," in *Proceedings of Solid Freeform Fabrication Symposium*, 1998, pp. 697–703.

[13]   T. Chartier, C. Chaput, F. Doreau, and M. Loiseau, "Stereolithography of structural complex ceramic parts," *J. Mater. Sci.*, vol. 37, no. 15, pp. 3141–3147, 2002.

[14]   Z. C. Eckel, C. Zhou, J. H. Martin, A. J. Jacobsen, W. B. Carter, and T. A. Schaedler, "Additive manufacturing of polymer-derived ceramics," *Science (80-.).*, vol. 351, no. 6268, pp. 58–62, 2016.

[15]   A. Mareike Wätjen, P. Gingter, M. Kramer, and R. Telle, "Novel Prospects and Possibilities in Additive Manufacturing of Ceramics by means of Direct Inkjet Printing," *Adv. Mech. Eng.*, vol. 6, pp. 1–12, 2014.

[16]   B. Leukers *et al.*, "Biocompatibility of ceramic scaffolds for bone replacement made by 3D printing," *Materwiss. Werksttech.*, vol. 36, no. 12, pp. 781–787, 2005.

[17]   J. Grau and J. Moon, "High green density ceramic components fabricated by the slurry-based 3DP process," in *Proceedings of Solid Freeform Fabrication Symposium*, 1997, pp. 371–378.

[18]   J. Deckers, K. Shahzad, P. L. Cardon, M. Rombouts, J. Vleugels, and J. P. Kruth, "Shaping ceramics through indirect Selective Laser Sintering," *Rapid Prototyp. J.*, vol. 20, no. 4, p. status: accepted, 2016.

[19]   E. Juste, F. Petit, V. Lardot, and F. Cambier, "Shaping of ceramic parts by selective laser melting of powder bed," *J. Mater. Res.*, vol. 29, no. 17, pp. 2086–2094, 2014.

[20]   V. K. Balla, S. Bose, and A. Bandyopadhyay, "Processing of bulk alumina ceramics using laser engineered net shaping," *Int. J. Appl. Ceram. Technol.*, vol. 5, no. 3, pp. 234–242, 2008.

[21]   M. Khan, "Novel indirect additive manufacturing for processing biomaterials," Newcastle University, 2015.

[22]   R. Lu, S. Chandrasekaran, W. L. Du Frane, R. L. Landingham, M. A. Worsley, and J. D. Kuntz, "Complex shaped boron carbides from negative additive manufacturing," *Mater. Des.*, vol. 148, pp. 8–16, 2018.

[23]   S. Bose, J. Darsell, M. Kintner, H. Hosick, and A. Bandyopadhyay, "Pore size and pore volume effects on alumina and TCP ceramic scaffolds," *Mater. Sci. Eng. C*, vol. 23, no. 4, pp. 479–486, 2003.

[24]   G. Franchin and P. Colombo, "Porous Geopolymer Components through Inverse Replica of 3D Printed Sacrificial Templates," *J. Ceram. Sci. Technol.*, vol. 6, no. 2, pp. 105–112, 2015.

[25]   R. Detsch, F. Uhl, U. Deisinger, and G. Ziegler, "3D-Cultivation of bone marrow stromal cells on hydroxyapatite scaffolds fabricated by dispense-plotting and negative mould technique," *J. Mater. Sci. Mater. Med.*, vol. 19, no. 4, pp. 1491–1496, 2008.

[26]   A. Ortona, C. D'Angelo, S. Gianella, and D. Gaia, "Cellular ceramics produced by rapid prototyping and replication," *Mater. Lett.*, vol. 80, pp. 95–98, 2012.

[27]   D. Guo, L. T. Li, K. Cai, Z. L. Gui, and C. W. Nan, "Rapid prototyping of piezoelectric ceramics via selective laser sintering and gelcasting," *J. Am. Ceram. Soc.*, vol. 87, no. 1, pp. 17–22, 2004.

[28]   Y. Haiqing, S. Kirihara, and Y. Miyamoto, "Fabrication of Ceramic Photonic Crystals with Diamond Structure for," *J. Am. Ceram. Soc.*, vol. 601, no. 4, pp. 598–601, 2004.

[29]   A. Woesz *et al.*, "Towards bone replacement materials from calcium phosphates via rapid prototyping and ceramic gelcasting," *Mater. Sci. Eng. C*, vol. 25, no. 2, pp. 181–186, 2005.

[30]   S. Yang *et al.*, "Rapid prototyping of ceramic lattices for hard tissue scaffolds," *Mater. Des.*, vol. 29, no. 9, pp. 1802–1809, 2008.

[31]   J. Franco, P. Hunger, M. E. Launey, A. P. Tomsia, and E. Saiz, "Direct-Write Assembly of Calcium Phosphate Scaffolds Using a Water-Based Hydrogel," *Acta Biomater.*, vol. 6, no. 1, pp. 218–228, 2010.

[32]   J. Maurath and N. Willenbacher, "3D printing of open-porous cellular ceramics with high specific strength," *J. Eur. Ceram. Soc.*, vol. 37, no. 15, pp. 4833–4842, 2017.

[33]   J. D. Cawley, "Solid freeform fabrication of ceramics," *Curr. Opin. Solid State Mater. Sci.*, vol. 4, no. 1999, pp. 483–489, 1999.

[34]   J. W. Halloran, "Freeform fabrication of ceramics," *Br. Ceram. Trans.*, vol. 98, no. 6, pp. 299–303, Jun. 1999.

[35]   B. Y. Tay, J. R. G. Evans, and M. J. Edirisinghe, "Solid freeform fabrication of ceramics," *Int. Mater. Rev.*, vol. 48, no. 6, pp. 341–370, 2003.

[36]   J. A. Lewis, J. E. Smay, J. Stuecker, and J. Cesarano, "Direct ink writing of three-dimensional ceramic structures," *J. Am. Ceram. Soc.*, vol. 89, no. 12, pp. 3599–3609, 2006.

[37]   B. Qian and Z. Shen, "Laser sintering of ceramics," *J. Asian Ceram. Soc.*, vol. 1, no. 4, pp. 315–321, 2013.

[38]   N. Travitzky *et al.*, "Additive Manufacturing of Ceramic-Based Materials," *Adv. Eng. Mater.*, vol. 16, no. 6, pp. 729–754, 2014.

[39]   J. Deckers, J. Vleugels, and J.-P. Kruth, "Additive Manufacturing of Ceramics: A Review," *J. Ceram. Sci. Tech*, vol. 05, no. 04, pp. 245–260, 2014.

[40]   B. Derby, "Additive Manufacture of Ceramics Components by Inkjet Printing," *Engineering*, vol. 1, no. 1, pp. 113–123, 2015.

[41]   A. Zocca, P. Colombo, C. M. Gomes, and J. Günster, "Additive Manufacturing of Ceramics: Issues, Potentialities, and Opportunities," *J. Am. Ceram. Soc.*, vol. 98, no. 7, pp. 1983–2001, 2015.

[42]   J. W. Halloran, "Ceramic Stereolithography: Additive Manufacturing for Ceramics by Photopolymerization," *Annu. Rev. Mater. Res.*, vol. 46, no. 1, pp. 19–40, 2016.

[43]   S. L. Sing *et al.*, "Direct selective laser sintering and melting of ceramics: A review," *Rapid Prototyp. J.*, vol. 23, no. 3, pp. 611–623, 2017.

[44]   D. W. Richerson, *Modern Ceramic Engineering: Properties, Processing, and Use in Design*, Third Edit. CRC Press, 2006.

[45]   M. Bengisu, *Engineering Ceramics*. New York: Springer-Verlag Berlin Heidelberg GmbH, 2001.

[46]   C. Drouet *et al.*, *Types of ceramics: Material class*. Elsevier Ltd, 2017.

[47]   R. Riedel, E. Ionescu, and I. W. Chen, "Modern Trends in Advanced Ceramics," in *Ceramics Science and Technology*, vol. 1: Structu, Weinheim: WILEY-VCH Verlag GmbH & Co, 2008, pp. 1–38.

[48]   P. Frischholz, "The Breviary Technical Ceramics," *Fahner Verlag, Selb/Germany*, p. 283, 2004.

[49]   W. Verbeek, "Production of shaped articles of homogeneous mixtures of silicon carbide and nitride," US3853567, 1974.

[50]   P. Colombo, G. Mera, R. Riedel, and G. D. Sorar, "Polymer-derived ceramics: 40 Years of research and innovation in advanced ceramics," *J. Am. Ceram. Soc.*, vol. 93, no. 7, pp. 1805–1837, 2010.

[51]   R. Riedel, G. Mera, R. Hauser, and A. Klonczynski, "Silicon-Based Polymer-Derived Ceramics: Synthesis Properties and Applications-A Review," *J. Ceram. Soc. Japan*, vol. 114, no. 1330, pp. 425–444, 2006.

[52]   R. Riedel, A. Kienzle, W. Dressler, L. Ruwisch, J. Bill, and F. Aldinger, "A silicoboron carbonitride ceramic stable to 2,000°C," *Nature*, vol. 382, no. 6594. pp. 796–798, 1996.

[53]   P. Colombo, J. Schmidt, G. Franchin, A. Zocca, and J. Günster, "Additive manufacturing techniques for fabricating complex ceramic components from preceramic polymers," *Am. Ceram. Soc. Bull.*, vol. 96, no. 3, pp. 16–23, 2017.

[54]   R. Riedel, "Advanced Ceramics from Inorganic Polymers," in *Materials Science and Technology*, 2006, p. 50.

[55]   F. Klocke *et al.*, "Turbomachinery component manufacture by application of electrochemical, electro-physical and photonic processes," *CIRP Ann. - Manuf. Technol.*, vol. 63, no. 2, pp. 703–726, 2014.

[56]   Markets and Markets, "Ceramic Matrix Composites Market by Matrix Type (Oxide/Oxide, C/SiC, C/C, SiC/SiC), End-Use Industry (Aerospace & Defense, Automotive, Energy & Power, Industrial), Region (North America, Europe, APAC, Middle East & Africa,) - Global Forecast to 2029," 2019. [Online]. Available: https://www.marketsandmarkets.com/PressReleases/ceramic-matrix-composites.asp. [Accessed: 16-Jul-2019].

[57]   N. Singh, R. Mazumder, P. Gupta, and D. Kumar, "Ceramic matrix composites: Processing techniques and recent advancements," *J. Mater. Environ. Sci.*, vol. 8, no. 5, pp. 1654–1660, 2017.

[58]   R. R. Naslain, "Ceramic Matrix Composites: Matrices and Processing," in *Encyclopedia of Materials: Science and Technology*, Elsevier, 2001, pp. 1060–1066.

[59]   D. Kopeliovich, "5 - Advances in the manufacture of ceramic matrix composites using infiltration techniques," in *Advances in Ceramic Matrix Composites*, I. M. B. T.-A. in C. M. C. Low, Ed. Woodhead Publishing, 2014, pp. 79–108.

[60]   ISO/ASTM Standard 52900:2015(E), "Standard Terminology for Additive Manufacturing – General Principles – Terminology." ASTM International, West Conshohocken, PA, USA, 2015.

[61]   H.-H. Tang, "Method for rapid forming of a ceramic green part," US20040075197A1, 2004.

[62]   J. Gunster, S. Engler, and J. G. Heinrich, "Forming of Complex Shaped Ceramic Products via Layer-wise Slurry Deposition (LSD)," *Bull. Eur. Ceram. Soc.*, vol. 1, pp. 25–28, 2003.

[63]   T. Krause, S. Engler, J. Gunster, and J. G. Heinrich, "Process and a Device for Producing Ceramic Molds," US 2003/0001313 A1, 2003.

[64]   A. Zocca, P. Lima, and J. Günster, "LSD-based 3D printing of alumina ceramics," *J. Ceram. Sci. Technol.*, vol. 8, no. 1, pp. 141–148, 2017.

[65]   E. a Griffin and S. McMillin, "Selective laser sintering and fused deposition modeling processes for functional

ceramic parts," *Solid Free. Fabr. Proc.*, pp. 25–30, 1995.

[66]   K. Subramanian, N. K. Vail, J. W. Barlow, and H. Marcus, "Selective laser sintering of alumina with polymer binders," *Rapid Prototyp. J.*, vol. 1, no. 2, pp. 24–35, 1995.

[67]   Z. H. Liu, J. J. Nolte, J. I. Packard, G. Hilmas, F. Dogan, and M. C. Leu, "Selective Laser Sintering of High-density Alumina Ceramic Parts," in *Proceedings of the 35th International MATADOR Conference: Formerly The International Machine Tool Design and Research Conference*, 2007, pp. 351–354.

[68]   K. Shahzad, J. Deckers, S. Boury, B. Neirinck, J. P. Kruth, and J. Vleugels, "Preparation and indirect selective laser sintering of alumina/PA microspheres," *Ceram. Int.*, vol. 38, no. 2, pp. 1241–1247, 2012.

[69]   J. Deckers, J.-P. P. Kruth, K. Shahzad, and J. Vleugels, "Density improvement of alumina parts produced through selective laser sintering of alumina-polyamide composite powder," *CIRP Ann. - Manuf. Technol.*, vol. 61, no. 1, pp. 211–214, 2012.

[70]   J. Deckers, K. Shahzad, J. Vleugels, and J. P. Kruth, "Isostatic pressing assisted indirect selective laser sintering of alumina components," *Rapid Prototyp. J.*, vol. 18, no. 5, pp. 409–419, 2012.

[71]   J. Deckers, J.-P. Kruth, L. Cardon, K. Shahzad, and J. Vleugels, "Densification and Geometrical Assessments of Alumina Parts Produced Through Indirect Selective Laser Sintering of Alumina-Polystyrene Composite Powder," *Stroj. Vestnik-Journal Mech. Eng.*, vol. 59, no. 11, pp. 646–661, 2013.

[72]   K. Shahzad, J. Deckers, J. P. Kruth, and J. Vleugels, "Additive manufacturing of alumina parts by indirect selective laser sintering and post processing," *J. Mater. Process. Technol.*, vol. 213, no. 9, pp. 1484–1494, 2013.

[73]   M. Agarwala, D. Klosterman, N. Osborne, and A. Lightman, "Hard metal tooling via SFF of ceramics and powder metallurgy," in *Proceedings of the SFF Symposium*, 1999, pp. 759–766.

[74]   K. Shahzad, J. Deckers, Z. Zhang, J.-P. Kruth, and J. Vleugels, "Additive manufacturing of zirconia parts by indirect selective laser sintering," *J. Eur. Ceram. Soc.*, vol. 34, no. 1, pp. 81–89, 2014.

[75]   J. C. Nelson, N. K. Vail, J. W. Barlow, J. J. Beaman, D. L. Bourell, and H. L. Marcus, "Selective Laser Sintering of Polymer-Coated Silicon Carbide Powders," *Ind. Eng. Chem. Res.*, vol. 34, no. 5, pp. 1641–1651, May 1995.

[76]   R. S. Evans, D. L. Bourell, J. J. Beaman, and M. I. Campbell, "Rapid manufacturing of silicon carbide composites," *Rapid Prototyp. J.*, vol. 11, no. 1, pp. 37–40, 2005.

[77]   B. Y. Stevinson, D. L. Bourell, and J. J. Beaman, "Support-free infiltration of selective laser sintered (SLS) silicon carbide preforms.," in *Solid Freeform Fabrication Symposium Proceedings*, 2006, pp. 359–365.

[78]   M. C. Leu, S. Pattnaik, and G. E. Hilmas, "Investigation of laser sintering for freeform fabrication of zirconium diboride parts," *Virtual Phys. Prototyp.*, vol. 7, no. 1, pp. 25–36, Mar. 2012.

[79]   R. D. Goodridge, D. J. Wood, C. Ohtsuki, and K. W. Dalgarno, "Biological evaluation of an apatite–mullite glass-ceramic produced via selective laser sintering," *Acta Biomater.*, vol. 3, no. 2, pp. 221–231, 2007.

[80]   K. Xiao, K. W. Dalgarno, D. J. Wood, R. D. Goodridge, and C. Ohtsuki, "Indirect selective laser sintering of apatite-wollostonite glass-ceramic," *Proc. Inst. Mech. Eng. Part H J. Eng. Med.*, vol. 222, no. 7, pp. 1107–1114, 2008.

[81]   U. Lakshminarayan and H. L. Marcus, "An Experimental Study of the Relationship between Microstructure and Mechanical Properties of a Ceramic Composite Fabricated by Selective Laser Sintering," in *Proceedings of the Solid Freeform Fabrication Symposium*, 1992, pp. 44–53.

[82]   I. Lee, "Influence of heat treatment upon SLS processed composites fabricated with alumina and monoclinic HBO2," *J. Mater. Sci. Lett.*, vol. 21, no. 3, pp. 209–212, 2002.

[83]   P. K. Subramanian and H. L. Marcus, "Selective Laser Sintering of Alumina Using Aluminum Binder," *Mater. Manuf. Process.*, vol. 10, no. 4, pp. 689–706, 1995.

[84]   ASTM Standard C1161-13, "Standard Test Method for Flexural Strength of Advanced Ceramics at Ambient Temperature." ASTM International, West Conshohocken, PA, USA, 2013.

[85]   M. C. Leu, E. B. Adamek, T. Huang, G. E. Hilmas, and F. Dogan, "Freeform fabrication of zirconium diboride parts using selective laser sintering," in *Proceedings of the Solid Freeform Fabrication Symposium*, 2008, pp. 194–205.

[86]   L. Cardon *et al.*, "Polystyrene-coated alumina powder via dispersion polymerization for indirect selective laser sintering applications," *J. Appl. Polym. Sci.*, vol. 128, no. 3, pp. 2121–2128, 2013.

[87]   K. Liu, Y. Shi, W. He, C. Li, Q. Wei, and J. Liu, "Densification of alumina components via indirect selective laser sintering combined with isostatic pressing," *Int. J. Adv. Manuf. Technol.*, vol. 67, no. 9–12, pp. 2511–2519, 2013.

[88]   T. Friedel, N. Travitzky, F. Niebling, M. Scheffler, and P. Greil, "Fabrication of polymer derived ceramic parts by selective laser curing," *J. Eur. Ceram. Soc.*, vol. 25, no. 2-3 SPEC. ISS., pp. 193–197, 2005.

[89]   H. Tang, "Method for rapid forming of a ceramic work piece," US6217816B1, 2001.

[90]   H. C. Yen and H. H. Tang, "Developing a paving system for fabricating ultra-thin layers in ceramic laser rapid prototyping," *Int. J. Adv. Manuf. Technol.*, vol. 36, no. 3–4, pp. 280–287, 2008.

[91]   H.-H. Tang, "Building Ultra-Thin Layers by Ceramic Laser Sintering," *Mater. Trans.*, vol. 47, no. 3, pp. 889–897, 2006.

[92]   H.-H. Tang, "Direct laser fusing to form ceramic parts," *Rapid Prototyp. J.*, vol. 8, no. 5, pp. 284–289, 2002.

[93]   H. C. Yen and H. H. Tang, "Study on direct fabrication of ceramic shell mold with slurry-based ceramic laser fusion and ceramic laser sintering," *Int. J. Adv. Manuf. Technol.*, vol. 60, no. 9–12, pp. 1009–1015, 2012.

[94]   H.-H. Tang and H.-C. Yen, "Ceramic Parts Fabricated by Ceramic Laser Fusion," *Mater. Trans.*, vol. 45, no. 8, pp. 2744–2751, 2004.

[95]   H. H. Tang, M. L. Chiu, and H. C. Yen, "Slurry-based selective laser sintering of polymer-coated ceramic powders to fabricate high strength alumina parts," *J. Eur. Ceram. Soc.*, vol. 31, no. 8, pp. 1383–1388, 2011.

[96]   H. H. Tang and F. H. Liu, "Ceramic laser gelling," *J. Eur. Ceram. Soc.*, vol. 25, no. 5, pp. 627–632, 2005.

[97]   H. C. Yen, "A new slurry-based shaping process for fabricating ceramic green part by selective laser scanning the gelled layer," *J. Eur. Ceram. Soc.*, vol. 32, pp. 3123–3128, 2012.

[98]   H. C. Yen, H. H. Tang, and C. H. Wu, "Improving Staircase Effect in the Process of Ceramic Laser Gelling," *Adv. Mater. Res.*, vol. 284–286, pp. 43–47, 2011.

[99]   F. H. Liu and Y. S. Liao, "Fabrication of inner complex ceramic parts by selective laser gelling," *J. Eur. Ceram. Soc.*, vol. 30, no. 16, pp. 3283–3289, 2010.

[100]   F. H. Liu, "Manufacturing porous multi-channel ceramics by laser gelling," *Ceram. Int.*, vol. 37, no. 7, pp. 2789–2794, 2011.

[101]   J. H. Tan, W. L. E. Wong, and K. W. Dalgarno, "An overview of powder granulometry on feedstock and part performance in the selective laser melting process," *Addit. Manuf.*, vol. 18, pp. 228–255, 2017.

[102]   X. Cui, S. Ouyang, Z. Yu, C. Wang, and Y. Huang, "A study on green tapes for LOM with water-based tape casting processing," *Mater. Lett.*, vol. 57, no. 7, pp. 1300–1304, 2003.

[103]   L. Weisensel, N. Travitzky, H. Sieber, and P. Greil, "Laminated Object Manufacturing (LOM) of SiSiC Composites," *Adv. Eng. Mater.*, vol. 6, no. 11, pp. 899–903, Nov. 2004.

[104]   Y. Zhang, X. He, J. Han, and S. Du, "Ceramic green tape extrusion for laminated object manufacturing," *Mater. Lett.*, vol. 40, no. 6, pp. 275–279, Sep. 1999.

[105]   D. Klosterman, R. Chartoff, B. Priore, N. Osborne, and G. Graves, "Automated fabrication of structural polymer and ceramic matrix composites via Laminated Object Manufacturing (LOM)," in *Proceedings of Solid Freeform Fabrication Symposium*, 1997, pp. 537–550.

[106]   C. M. Gomes, A. P. N. Oliveira, D. Hotza, N. Travitzky, and P. Greil, "LZSA glass-ceramic laminates: Fabrication

and mechanical properties," *J. Mater. Process. Technol.*, vol. 206, no. 1–3, pp. 194–201, 2008.

[107]   C. M. Gomes *et al.*, "Colloidal Processing of Glass–Ceramics for Laminated Object Manufacturing," *J. Am. Ceram. Soc.*, vol. 92, no. 6, pp. 1186–1191, 2009.

[108]   C. Gomes *et al.*, "Laminated object manufacturing of LZSA glass-ceramics," *Rapid Prototyp. J.*, vol. 17, no. 6, pp. 424–428, 2011.

[109]   S. J. Rodrigues, R. P. Chartoff, D. A. Klosterman, M. Agarwala, and N. Hecht, "Solid Freeform Fabrication of Functional Silicon Nitride Ceramics By Laminated Object Manufacturing," in *Proceedings of Solid Freeform Fabrication Symposium*, 2000, pp. 1–8.

[110]   Y. Zhang, X. He, S. Du, and J. Zhang, "Al2O3 ceramics preparation by LOM (laminated object manufacturing)," *Int. J. Adv. Manuf. Technol.*, vol. 17, no. 7, pp. 531–534, 2001.

[111]   H. Zhong *et al.*, "Preparation of SiC ceramics by laminated object manufacturing and pressureless sintering," *J. Ceram. Sci. Technol.*, vol. 6, no. 2, pp. 133–140, 2015.

[112]   G. Kalmanovich, L. Dodin, and S. Tu, "'Curved-Layer' Laminated Object Manufacturing," in *Proceedings of the 7th International Conference on Rapid Prototyping*, 1997, pp. 51–59.

[113]   D. Klosterman *et al.*, "Curved layer LOM of ceramics and composites," in *Solid Freeform Fabrication Symposium proceedings. University of Texas, Austin*, 1998, pp. 671–680.

[114]   J. D. Cawley, P. Wei, Z. E. Liu, W. S. Newman, and B. B. Mathewson, "Al2O3 Ceramics Made by CAM-LEM (Computer-Aided Manufacturing Engineering Materials) Technology," in *Proceedings of the Solid Freeform Fabrication Symposium*, 1995, pp. 9–16.

[115]   Y. Zheng, S. Choi, B. B. Mathewson, and W. S. Newman, "Progress in Computer-Aided Manufacturing of Laminated Engineering Materials Utilizing Thick, Tangent-Cut Layers," in *Proceedings of the 7th Solid Freeform Fabrication Symposium (SFF)*, 1996, pp. 355–362.

[116]   S. Liu, F. Ye, L. Liu, and Q. Liu, "Feasibility of preparing of silicon nitride ceramics components by aqueous tape casting in combination with laminated object manufacturing," *Mater. Des.*, vol. 66, pp. 331–335, 2015.

[117]   Z. E. Liu, T. C. Ko, J. Best, J. D. Cawley, and   a H. Heuer, "CAM-LEM processing: materials flexibility," in *Proceedings of Solid Freeform Fabrication Symposium*, 1997, pp. 379–386.

[118]   G. E. Hilmas, J. L. Lombardi, and R. A. Hoffman, "Advances in the Fabrication of Functionally Graded Materials Using Extrusion Freeform Fabrication," in *Functionally Graded Materials 1996*, I. Shiota and Y. Miyamoto, Eds. Amsterdam: Elsevier Science B.V., 1997, pp. 319–324.

[119]   T. a Baer, J. Cesarano III, P. Calvert, J. Cesarano, T. a Baer, and P. Calvert, "Recent Developments in Freeform Fabrication of Dense Ceramics From Slurry Deposition," in *Proceedings of Solid Freeform Fabrication Symposium*, 1997, pp. 25–32.

[120]   Q. Fu, E. Saiz, and A. P. Tomsia, "Direct Ink Writing of Highly Porous and Strong Glass Scaffolds for Load-bearing Bone Defects Repair and Regeneration," *Acta Biomater.*, vol. 7, no. 10, pp. 3547–3554, 2011.

[121]   M. Acosta, V. L. Wiesner, C. J. Martinez, R. W. Trice, and J. P. Youngblood, "Effect of polyvinylpyrrolidone additions on the rheology of aqueous, highly loaded alumina suspensions," *J. Am. Ceram. Soc.*, vol. 96, no. 5, pp. 1372–1382, 2013.

[122]   S. S. Nadkarni and J. E. Smay, "Concentrated barium titanate colloidal gels prepared by bridging flocculation for use in solid freeform fabrication," *J. Am. Ceram. Soc.*, vol. 89, no. 1, pp. 96–103, 2006.

[123]   E. Feilden, E. G. T. Blanca, F. Giuliani, E. Saiz, and L. Vandeperre, "Robocasting of structural ceramic parts with hydrogel inks," *J. Eur. Ceram. Soc.*, vol. 36, no. 10, pp. 2525–2533, 2016.

[124]   F. J. Martínez-Vázquez, A. Pajares, and P. Miranda, "A simple graphite-based support material for robocasting of ceramic parts," *J. Eur. Ceram. Soc.*, vol. 38, no. 4, pp. 2247–2250, 2018.

[125]   M. C. Leu *et al.*, "Freeze-Form Extrusion Fabrication of Composite Structures," in *Proceedings of Solid*

Freeform Fabrication Symposium, 2011, pp. 111–124.

[126]   L. Rueschhoff, W. Costakis, M. Michie, J. Youngblood, and R. Trice, "Additive Manufacturing of Dense Ceramic Parts via Direct Ink Writing of Aqueous Alumina Suspensions," *Int. J. Appl. Ceram. Technol.*, vol. 13, no. 5, pp. 821–830, 2016.

[127]   T. Schlordt, S. Schwanke, F. Keppner, T. Fey, N. Travitzky, and P. Greil, "Robocasting of alumina hollow filament lattice structures," *J. Eur. Ceram. Soc.*, vol. 33, no. 15–16, pp. 3243–3248, 2013.

[128]   W. J. Costakis, L. M. Rueschhoff, A. I. Diaz-Cano, J. P. Youngblood, and R. W. Trice, "Additive manufacturing of boron carbide via continuous filament direct ink writing of aqueous ceramic suspensions," *J. Eur. Ceram. Soc.*, vol. 36, no. 14, pp. 3249–3256, 2016.

[129]   M. K. Agarwala, R. Van Weeren, A. Bandyopadhyay, P. J. Whalen, A. Safari, and S. C. Danforth, "Fused Deposition of Ceramics and Metals: An Overview," in *Proceedings of Solid Freeform Fabrication Symposium*, 1996, pp. 385–392.

[130]   R. Vaidyanathan, J. Lombardi, and J. Walish, "Extrusion Freeform Fabrication of Functional Ceramic Prototypes," in *Proceedings of Solid Freeform Fabrication Symposium*, 1999, pp. 327–334.

[131]   M. Greul and R. Lenk, "Near-net-shape ceramic and composite parts by multiphase jet solidification (MJS)," *Ind. Ceram.*, vol. 20, no. 2, pp. 115–117, 2000.

[132]   U. Scheithauer, E. Schwarzer, H. J. Richter, and T. Moritz, "Thermoplastic 3D printing - An additive manufacturing method for producing dense ceramics," *Int. J. Appl. Ceram. Technol.*, vol. 12, no. 1, pp. 26–31, 2015.

[133]   M. Faes, J. Vleugels, F. Vogeler, and E. Ferraris, "Extrusion-based additive manufacturing of ZrO2 using photoinitiated polymerization," *CIRP J. Manuf. Sci. Technol.*, vol. 14, pp. 28–34, 2016.

[134]   M. S. Mason, T. Huang, R. G. Landers, M. C. Leu, and G. E. Hilmas, "Aqueous-based extrusion of high solids loading ceramic pastes: Process modeling and control," *J. Mater. Process. Technol.*, vol. 209, no. 6, pp. 2946–2957, 2009.

[135]   A. Ghazanfari, W. Li, M. C. Leu, J. L. Watts, and G. E. Hilmas, "Additive manufacturing and mechanical characterization of high density fully stabilized zirconia," *Ceram. Int.*, vol. 43, no. 8, pp. 6082–6088, 2017.

[136]   H. Shao, D. Zhao, T. Lin, J. He, and J. Wu, "3D gel-printing of zirconia ceramic parts," *Ceram. Int.*, vol. 43, no. 16, pp. 13938–13942, 2017.

[137]   M. K. Agarwala, A. Bandyopadhyay, and R. Van Weeren, "Fused Deposition of Ceramics (FDC) for Structural Silicon Nitride Components," in *Proceedings of Solid Freeform Fabrication Symposium*, 1996, pp. 336–344.

[138]   C. Dai *et al.*, "High quality, fully dense ceramic components manufactured using Fused Deposition of Ceramics (FDC)," in *Proceedings of Solid Freeform Fabrication Symposium*, 1997, pp. 411–420.

[139]   S. Rangarajan and G. Qi, "Powder processing, rheology, and mechanical properties of feedstock for fused deposition of Si3N4 ceramics," *J. Am. Ceram. Soc.*, vol. 69, pp. 1663–1669, 2000.

[140]   A. Bandyopadhyay *et al.*, "Processing of Piezocomposites by Fused Deposition Technique," in *Proceedings of the Tenth IEEE International Symposium on Applications of Ferroelectrics*, 1996, pp. 999–1002.

[141]   K. Stuffle, A. Mulligan, J. Lombardi, P. Calvert, and B. Fabes, "Solid Freebody Forming of Ceramics from Polymerizable Slurry," in *Proceedings of the Solid Freeform Fabrication Symposium*, 1993, pp. 60–63.

[142]   D. Kupp, H. Eifert, M. Greul, and M. Kunstner, "Rapid prototyping of functional metal and ceramic components by the multiphase jet solidification (MSJ) process," in *Proceedings of the Solid Freeform Fabrication Symposium*, 1997, pp. 1–9.

[143]   M. Greulich, M. Greul, and T. Pintat, "Fast, functional prototypes via multiphase jet solidification," *Rapid Prototyp. J.*, vol. 1, no. 1, pp. 20–25, 1995.

[144]   U. Scheithauer, T. Slawik, E. Schwarzer, H. J. Richter, T. Moritz, and A. Michaelis, "Additive manufacturing of

metal-ceramic-composites by thermoplastic 3D-printing (3DTP)," *J. Ceram. Sci. Technol.*, vol. 6, no. 2, pp. 125–132, 2015.

[145] U. Scheithauer, E. Schwarzer, C. Poitzsch, H.-J. Richter, T. Moritz, and M. Stelter, "Method for Producing Ceramic and/or Metal Components," WO 2015/177128 A1, 2015.

[146] U. Scheithauer *et al.*, "Droplet-based additive manufacturing of hard metal components by thermoplastic 3D Printing (T3DP)," *J. Ceram. Sci. Technol.*, vol. 8, no. 1, pp. 155–160, 2017.

[147] U. Scheithauer *et al.*, "Ceramic-Based 4D-Components: Additive Manufacturing (AM) of Ceramic-Based Functionally Graded Materials (FGM) by Thermoplastic 3D-Printing (T3DP)," *Materials (Basel).*, vol. 10, no. 1368, 2017.

[148] I. Ceserano, Joseph and P. D. Calvert, "Freeforming objects with low-binder slurry," US006027326A, 2000.

[149] B. A. Tuttle *et al.*, "Robocast Pb(Zr0.95Ti0.05)O3 Ceramic Monoliths and Composites," *J. Am. Ceram. Soc.*, vol. 74, pp. 872–874, 2001.

[150] J. E. Smay, J. Cesarano, and J. A. Lewis, "Colloidal inks for directed assembly of 3-D periodic structures," *Langmuir*, vol. 18, no. 14, pp. 5429–5437, 2002.

[151] J. A. Lewis, "Direct ink writing of 3D functional materials," *Adv. Funct. Mater.*, vol. 16, no. 17, pp. 2193–2204, 2006.

[152] J. C. Conrad, S. R. Ferreira, J. Yoshikawa, R. F. Shepherd, B. Y. Ahn, and J. A. Lewis, "Designing colloidal suspensions for directed materials assembly," *Curr. Opin. Colloid Interface Sci.*, vol. 16, no. 1, pp. 71–79, 2011.

[153] S. L. Morissette, J. a Lewis, J. Cesarano, D. B. Dimos, and T. Y. Baer, "Solid Freeform Fabrication of Aqueous Alumina-Poly(vinyl alcohol) Gelcasting Suspensions," *J. Am. Ceram. Soc.*, vol. 83, no. 10, pp. 2409–2416, 2000.

[154] T. Schlordt, F. Keppner, N. Travitzky, and P. Greil, "Robocasting of alumina lattice truss structures," *J. Ceram. Sci. Technol.*, vol. 3, no. 2, pp. 81–88, 2012.

[155] J. Azuaje *et al.*, "An efficient and recyclable 3D printed α-Al2O3 catalyst for the multicomponent assembly of bioactive heterocycles," *Appl. Catal. A Gen.*, vol. 530, pp. 203–210, 2017.

[156] J. Smay and J. Cesarano, "Directed Colloidal Assembly of Linear and Annular Lead Zirconate Titanate Arrays," *J. Am. ...*, vol. 95, pp. 290–308, 2008.

[157] J. N. Stuecker, J. Cesarano, and D. A. Hirschfeld, "Control of the viscous behavior of highly concentrated mullite suspensions for robocasting," *J. Mater. Process. Technol.*, vol. 142, no. 2, pp. 318–325, 2003.

[158] G. P. He, D. A. Hirschfeld, J. Cesarano III, and J. N. Stuecker, "Robocasting and Mechanical Testing of Aqueous Silicon Nitride Slurries," 2000.

[159] S. Zhao, W. Xiao, M. N. Rahaman, D. O'Brien, J. W. Seitz-Sampson, and B. Sonny Bal, "Robocasting of silicon nitride with controllable shape and architecture for biomedical applications," *Int. J. Appl. Ceram. Technol.*, vol. 14, no. 2, pp. 117–127, 2017.

[160] A. Kruisová *et al.*, "Ultrasonic bandgaps in 3D-printed periodic ceramic microlattices," *Ultrasonics*, vol. 82, pp. 91–100, 2018.

[161] S. Eqtesadi *et al.*, "Fabricating geometrically-complex B4C ceramic components by robocasting and pressureless spark plasma sintering," *Scr. Mater.*, vol. 145, pp. 14–18, 2018.

[162] P. Miranda, E. Saiz, K. Gryn, and A. P. Tomsia, "Sintering and robocasting of ß-tricalcium phosphate scaffolds for orthopaedic applications," *Acta Biomater.*, vol. 2, no. 4, pp. 457–466, 2006.

[163] C. Slots *et al.*, "Simple additive manufacturing of an osteoconductive ceramic using suspension melt extrusion," *Dent. Mater.*, vol. 33, no. 2, pp. 198–208, 2017.

[164] E. Saiz, L. Gremillard, G. Menendez, P. Miranda, K. Gryn, and A. P. Tomsia, "Preparation of porous hydroxyapatite scaffolds," *Mater. Sci. Eng. C*, vol. 27, no. 3, pp. 546–550, 2007.

[165] M. Houmard, Q. Fu, M. Genet, E. Saiz, and A. P. Tomsia, "On the structural, mechanical, and biodegradation properties of HA/β-TCP robocast scaffolds," *J. Biomed. Mater. Res. - Part B Appl. Biomater.*, vol. 101, no. 7, pp. 1233–1242, 2013.

[166] Y. Xie *et al.*, "Net shape fabrication of calcium phosphate scaffolds with multiple material domains," *Biofabrication*, vol. 8, p. 015005, 2016.

[167] C. Petit *et al.*, "Fracture behavior of robocast HA/β-TCP scaffolds studied by X-ray tomography and finite element modeling," *J. Eur. Ceram. Soc.*, vol. 37, no. 4, pp. 1735–1745, 2017.

[168] C. F. Marques *et al.*, "Biphasic calcium phosphate scaffolds fabricated by direct write assembly: Mechanical, anti-microbial and osteoblastic properties," *J. Eur. Ceram. Soc.*, vol. 37, no. 1, pp. 359–368, 2017.

[169] H. Shao *et al.*, "3D robocasting magnesium-doped wollastonite/TCP bioceramic scaffolds with improved bone regeneration capacity in critical sized calvarial defects," *J. Mater. Chem. B*, vol. 5, no. 16, pp. 2941–2951, 2017.

[170] Z. Fu *et al.*, "Robocasting of carbon-alumina core-shell composites using co-extrusion," *Rapid Prototyp. J.*, vol. 23, no. 2, pp. 423–433, 2017.

[171] X. Liu, M. N. Rahaman, G. E. Hilmas, and B. Sonny Bal, "Mechanical properties of bioactive glass (13-93) scaffolds fabricated by robotic deposition for structural bone repair," *Acta Biomater.*, vol. 9, no. 6, pp. 320–331, 2013.

[172] S. M. Olhero, H. R. Fernandes, C. F. Marques, B. C. G. Silva, and J. M. F. Ferreira, "Additive manufacturing of 3D porous alkali-free bioactive glass scaffolds for healthcare applications," *J. Mater. Sci.*, vol. 52, no. 20, pp. 12079–12088, 2017.

[173] S. Eqtesadi, A. Motealleh, R. Wendelbo, A. L. Ortiz, and P. Miranda, "Reinforcement with reduced graphene oxide of bioactive glass scaffolds fabricated by robocasting," *J. Eur. Ceram. Soc.*, vol. 37, no. 12, pp. 3695–3704, 2017.

[174] P. Biswas, S. Mamatha, S. Naskar, Y. S. Rao, R. Johnson, and G. Padmanabham, "3D extrusion printing of magnesium aluminate spinel ceramic parts using thermally induced gelation of methyl cellulose," *J. Alloys Compd.*, vol. 770, pp. 419–423, 2019.

[175] J. E. Smay and J. A. Lewis, "Solid Free-Form Fabrication of 3-D Ceramic Structures," in *Ceramics and Composites Processing Methods*, N. P. Bansal and A. R. Boccaccini, Eds. Hoboken, NJ, USA: John Wiley & Sons, Inc., 2012, pp. 459–484.

[176] G. Franchin, L. Wahl, and P. Colombo, "Direct ink writing of ceramic matrix composite structures," *J. Am. Ceram. Soc.*, vol. 100, pp. 4397–4401, 2017.

[177] E. Feilden, "Additive Manufacturing of Ceramics and Ceramic Composites via Robocasting," Imperial College London Submitted, 2017.

[178] H. Chen, X. Wang, F. Xue, Y. Huang, K. Zhou, and D. Zhang, "3D printing of SiC ceramic: Direct ink writing with a solution of preceramic polymers," *J. Eur. Ceram. Soc.*, vol. 38, no. 16, pp. 5294–5300, 2018.

[179] H. Xiong, H. Chen, L. Zhao, Y. Huang, K. Zhou, and D. Zhang, "SiC w /SiC p reinforced 3D-SiC ceramics using direct ink writing of polycarbosilane-based solution: Microstructure, composition and mechanical properties," *J. Eur. Ceram. Soc.*, vol. 39, no. 8, pp. 2648–2657, 2019.

[180] Y. Xia, Z. Lu, J. Cao, K. Miao, J. Li, and D. Li, "Microstructure and mechanical property of Cf/SiC core/shell composite fabricated by direct ink writing," *Scr. Mater.*, vol. 165, pp. 84–88, 2019.

[181] M. S. Mason, T. Huang, R. G. Landers, M. C. Leu, G. E. Hilmas, and M. W. Hayes, "Aqueous-based extrusion fabrication of ceramics on demand," in *Proceedings of Solid Freeform Fabrication Symposium*, 2007, pp. 124–134.

[182] T. Huang, G. E. Hilmas, W. G. Fahrenholtz, and M. C. Leu, "Dispersion of zirconium diboride in an aqueous, high-solids paste," *Int. J. Appl. Ceram. Technol.*, vol. 4, no. 5, pp. 470–479, 2007.

[183] A. S. Thornton, "Freeze-form extrusion fabrication of boron carbide," Missouri University of Science and Technology, 2015.

[184] T. S. Huang *et al.*, "Freeze extrusion fabrication of 13-93 bioactive glass scaffolds for repair and regeneration of load-bearing bones," *Ceram. Trans.*, vol. 228, pp. 45–55, 2011.

[185] A. Li *et al.*, "Freeze-form Extrusion Fabrication of Functionally Graded Material Composites Using Zirconium Carbide and Tungsten," in *Proceedings of Solid Freeform Fabrication Symposium*, 2012, pp. 467–479.

[186] H. Zomorodi and R. G. Landers, "Extrusion Based Additive Manufacturing Using Explicit Model Predictive Control," in *2016 American Control Conference (ACC)*, 2016, pp. 1747–1752.

[187] B. K. Deuser, L. Tang, R. G. Landers, M. C. Leu, and G. E. Hilmas, "Hybrid Extrusion Force-Velocity Control Using Freeze-Form Extrusion Fabrication for Functionally Graded Material Parts," *J. Manuf. Sci. Eng.*, vol. 135, no. 4, p. 041015, 2013.

[188] A. Ghazanfari, W. Li, M. C. Leu, and G. E. Hilmas, "A novel freeform extrusion fabrication process for producing solid ceramic components with uniform layered radiation drying," *Addit. Manuf.*, vol. 15, pp. 102–112, 2017.

[189] A. Ghazanfari, W. Li, M. C. Leu, Y. Zhuang, and J. Huang, "Advanced ceramic components with embedded sapphire optical fiber sensors for high temperature applications," *Mater. Des.*, vol. 112, pp. 197–206, 2016.

[190] A. Ghazanfari, W. Li, M. Leu, J. Watts, and G. Hilmas, "Mechanical characterization of parts produced by ceramic on-demand extrusion process," *Int. J. Appl. Ceram. Technol.*, vol. 14, no. 3, pp. 486–494, 2017.

[191] W. Li, A. Ghazanfari, D. McMillen, M. C. Leu, G. E. Hilmas, and J. Watts, "Fabricating ceramic components with water dissolvable support structures by the Ceramic On-Demand Extrusion process," *CIRP Ann. - Manuf. Technol.*, vol. 66, no. 1, pp. 225–228, 2017.

[192] W. Li, A. Ghazanfari, D. Mcmillen, M. C. Leu, G. E. Hilmas, and J. Watts, "Properties of Partially Stabilized Zirconia Components Fabricated by The Ceramic On-Demand Extrusion Process," *Proc. 27th Annu. Int. Solid Free. Fabr. Symp.*, pp. 916–928, 2016.

[193] W. Li, A. Ghazanfari, D. McMillen, M. C. Leu, G. E. Hilmas, and J. Watts, "Characterization of zirconia specimens fabricated by ceramic on-demand extrusion," *Ceram. Int.*, vol. 44, no. 11, pp. 12245–12252, 2018.

[194] G. D. Quinn and R. C. Bradt, "On the vickers indentation fracture toughness Test," *J. Am. Ceram. Soc.*, vol. 90, no. 3, pp. 673–680, 2007.

[195] W. Li *et al.*, "Fabricating Functionally Graded Materials by Ceramic On-Demand Extrusion with Dynamic Mixing," in *Proceedings of the 29th Annual International Solid Freeform Fabrication Symposium*, 2018, pp. 16–18.

[196] X. Ren, H. Shao, T. Lin, and H. Zheng, "3D gel-printing-An additive manufacturing method for producing complex shape parts," *Mater. Des.*, vol. 101, pp. 80–87, 2016.

[197] J. Hinton, M. Mirgkizoudi, A. Campos-Zatarain, D. Flynn, R. A. Harris, and R. W. Kay, "Digitally-Driven Hybrid Manufacture of Ceramic Thick-Film Substrates," in *7th Electronic System-Integration Technology Conference, ESTC 2018 - Proceedings*, 2018.

[198] J. Hinton, D. F. Flynn, R. A. Harris, and R. W. Kay, "A digitally-driven Hybrid Manufacturing process for the flexible production of engineering ceramic components," in *Proceedings of the 29th Annual International Solid Freeform Fabrication Symposium*, 2018, pp. 388–397.

[199] M. Vaezi, S. Chianrabutra, B. Mellor, and S. Yang, "Multiple material additive manufacturing – Part 1: a review," *Virtual Phys. Prototyp.*, vol. 8, no. 1, pp. 19–50, 2013.

[200] M. Vaezi, H. Seitz, and S. Yang, "A review on 3D micro-additive manufacturing technologies," *Int. J. Adv. Manuf. Technol.*, vol. 67, no. 5–8, pp. 1721–1754, 2013.

[201] B. J. De Gans and U. S. Schubert, "Inkjet printing of polymer micro-arrays and libraries: Instrumentation, requirements, and perspectives," *Macromol. Rapid Commun.*, vol. 24, no. 11, pp. 659–666, 2003.

[202] FUJIFILM Dimatix Inc., "Jettable Fluid Formulation Guidelines," 2013.

[203] B. W. Jo, A. Lee, K. H. Ahn, and S. J. Lee, "Evaluation of jet performance in drop-on-demand (DOD) inkjet printing," *Korean J. Chem. Eng.*, vol. 26, no. 2, pp. 339–348, 2009.

[204] N. Reis and B. Derby, "Ink Jet Deposition of Ceramic Suspensions: Modeling and Experiments of Droplet Formation," in *Material Research Society Symposium Proceedings*, 2000, vol. 625, pp. 117–122.

[205] D. Jang, D. Kim, and J. Moon, "Influence of Fluid Physical Properties on Ink-Jet Printability," *Langmuir*, vol. 25, no. 5, pp. 2629–2635, Mar. 2009.

[206] N. Reis, K. A. M. Seerden, B. Derby, J. Halloran, and J. R. G. Evans, "Direct Inkjet Deposition of Ceramic Green Bodies: II – Jet Behaviour and Deposit Formation," in *Material Research Society Symposium Proceedings*, 1999, vol. 542.

[207] K. A. M. Seerden, N. Reis, B. Derby, P. S. Grant, J. W. Halloran, and J. R. G. Evans, "Direct Ink-Jet Deposition of Ceramic Green Bodies: I - Formulation of Build Materials," in *Material Research Society Symposium Proceedings*, 1999, vol. 542, pp. 141–146.

[208] B. Derby, N. Reis, K. A. M. Seerden, P. S. Grant, and J. R. G. Evans, "Freeform Fabrication of Ceramics by Hot-Melt Ink-Jet Printing," in *Material Research Society Symposium Proceedings*, 2000, 2011/02/01., vol. 625, pp. 195–201.

[209] K. A. M. Seerden, N. Reis, J. R. G. Evans, P. S. Grant, J. W. Halloran, and B. Derby, "Ink-Jet Printing of Wax-Based Alumina Suspensions," *J. Am. Ceram. Soc.*, vol. 84, no. 11, pp. 2514–2520, 2001.

[210] M. Mott and J. R. G. Evans, "Solid freeforming of silicon carbide by ink-jet printing using a polymeric precursor," *J. Am. Ceram. Soc.*, vol. 84, no. 2, pp. 307–313, 2001.

[211] X. Zhao, J. R. G. Evans, M. J. Edirisinghe, and J. H. Song, "Ink-jet printing of ceramic pillar arrays," *J. Mater. Sci.*, vol. 37, no. 10, pp. 1987–1992, 2002.

[212] X. Zhao, J. R. G. Evans, M. J. Edirisinghe, and J. H. Song, "Direct ink-jet printing of vertical walls," *J. Am. Ceram. Soc.*, vol. 85, no. 8, pp. 2113–2115, 2002.

[213] B. Cappi, J. Ebert, and R. Telle, "Rheological Properties of Aqueous Si3N4 and MoSi2 Suspensions Tailor-Made for Direct Inkjet Printing," *J. Am. Ceram. Soc.*, vol. 94, no. 1, pp. 111–116, 2011.

[214] E. Özkol, J. Ebert, K. Uibel, A. M. Wätjen, and R. Telle, "Development of high solid content aqueous 3Y-TZP suspensions for direct inkjet printing using a thermal inkjet printer," *J. Eur. Ceram. Soc.*, vol. 29, no. 3, pp. 403–409, 2009.

[215] P. Gingter, A. M. Wätjen, M. Kramer, and R. Telle, "Functionally graded ceramic structures by direct thermal inkjet printing," *J. Ceram. Sci. Technol.*, vol. 6, no. 2, pp. 119–124, 2015.

[216] M. Lejeune, T. Chartier, C. Dossou-Yovo, and R. Noguera, "Ink-jet printing of ceramic micro-pillar arrays," *J. Eur. Ceram. Soc.*, vol. 29, no. 5, pp. 905–911, 2009.

[217] Z. Chen and N. Brandon, "Inkjet printing and nanoindentation of porous alumina multilayers," *Ceram. Int.*, vol. 42, no. 7, pp. 8316–8324, 2016.

[218] B. Cappi, E. Özkol, J. Ebert, and R. Telle, "Direct inkjet printing of Si3N4: Characterization of ink, green bodies and microstructure," *J. Eur. Ceram. Soc.*, vol. 28, no. 13, pp. 2625–2628, 2008.

[219] American Ceramic Society, "Additive Manufacturing," *American Ceramic Society Bulletin*, p. 52, 2014.

[220] P. Menchhofer and B. Becker, "Investigation of the Deposition and Densification Parameters on the Mechanical Properties of Pressurized Spray Deposited (PSD) 3-D Printed Ceramic Components," Oak Ridge, 2016.

[221] ASTM Standard C1684-18, "Standard Test Method for Flexural Strength of Advanced Ceramics at Ambient Temperature—Cylindrical Rod Strength." ASTM International, West Conshohocken, PA, USA, 2018.

[222] ASTM Standard C1326-13 (Reapproved 2018), "Standard Test Method for Knoop Indentation Hardness of Advanced Ceramics." ASTM International, West Conshohocken, PA, USA, 2013.

[223] T. L. Jones, J. J. Swab, C. S. Meredith, and B. Becker, "The First Static and Dynamic Analysis of 3-D Printed Sintered Ceramics for Body Armor Applications," 2016.

[224] M. DeVries *et al.*, "Quasi-static and dynamic response of 3D-printed alumina," *J. Eur. Ceram. Soc.*, vol. 38, no. 9, pp. 3305–3316, 2018.

[225] T. L. Jones, L. Vargas-Gonzalez, B. Scott, B. Goodman, and B. Becker, "An In-Depth Analysis of Competing 3-D Printed Methods for the Mobile Manufacturing of Body Armor at the Point of Need," Aberdeen, MD, USA, 2019.

[226] N. Reis, C. Ainsley, and B. Derby, "Ink-jet delivery of particle suspensions by piezoelectric droplet ejectors," *J. Appl. Phys.*, vol. 97, no. 9, 2005.

[227] M. Mott and J. R. . Evans, "Zirconia/alumina functionally graded material made by ceramic ink jet printing," *Mater. Sci. Eng. A*, vol. 271, no. 1–2, pp. 344–352, 1999.

[228] E. Özkol, W. Zhang, R. Telle, and J. Ebert, "Potentials of the 'Direct inkjet printing' method for manufacturing 3Y-TZP based dental restorations," *J. Eur. Ceram. Soc.*, vol. 32, no. 10, pp. 2193–2201, 2012.

[229] XJet, "XJet systems," 2017. [Online]. Available: http://xjet3d.com/systems/. [Accessed: 23-Nov-2017].

[230] XJet, "XJet 500Ceramic Specifications," Rehovot, Israel, 2017.

[231] E. M. Sachs, J. S. Haggerty, M. J. Cima, and P. A. Williams, "Three-dimensional printing techniques," US5204055, 1993.

[232] A. Butscher *et al.*, "Printability of calcium phosphate powders for three-dimensional printing of tissue engineering scaffolds," *Acta Biomater.*, vol. 8, no. 1, pp. 373–385, 2012.

[233] A. Farzadi, V. Waran, M. Solati-Hashjin, Z. A. A. Rahman, M. Asadi, and N. A. A. Osman, "Effect of layer printing delay on mechanical properties and dimensional accuracy of 3D printed porous prototypes in bone tissue engineering," *Ceram. Int.*, vol. 41, no. 7, pp. 8320–8330, 2015.

[234] M. Asadi-Eydivand, M. Solati-Hashjin, A. Farzad, and N. A. Abu Osman, "Effect of technical parameters on porous structure and strength of 3D printed calcium sulfate prototypes," *Robot. Comput. Integr. Manuf.*, vol. 37, pp. 57–67, 2016.

[235] A. Butscher, M. Bohner, S. Hofmann, L. Gauckler, and R. Müller, "Structural and material approaches to bone tissue engineering in powder-based three-dimensional printing," *Acta Biomater.*, vol. 7, no. 3, pp. 907–920, 2011.

[236] S. Yang, K.-F. Leong, Z. Du, and C.-K. Chua, "The design of scaffolds for use in tissue engineering. Part II. Rapid prototyping techniques.," *Tissue Eng.*, vol. 8, no. 1, pp. 1–11, Feb. 2002.

[237] S. M. Gaytan, M. Cadena, M. Aldaz, E. Herderick, F. Medina, and R. Wicker, "Analysis of ferroelectric ceramic fabricated by binder jetting technology," in *Proceedings of Solid Freeform Fabrication Symposium*, 2013, pp. 859–868.

[238] S. M. Gaytan *et al.*, "Fabrication of barium titanate by binder jetting additive manufacturing technology," *Ceram. Int.*, vol. 41, no. 5, pp. 6610–6619, Jun. 2015.

[239] B. Utela, R. L. Anderson, and H. Kuhn, "Advanced Ceramic Materials and Processes for Three-Dimensional Printing (3DP)," in *Proceedings of Solid Freeform Fabrication Symposium*, 2006, pp. 290–303.

[240] S. Zhang, H. Miyanaji, L. Yang, A. Ali, and J. J. S. Dilip, "An Experimental Study of Ceramic Dental Porcelain Materials Using A 3D Print (3DP) Process," *Proceeding Solid Free. Fabr. Symp.*, pp. 991–1011, 2014.

[241] J. A. Gonzalez, J. Mireles, Y. Lin, and R. B. Wicker, "Characterization of ceramic components fabricated using binder jetting additive manufacturing technology," *Ceram. Int.*, vol. 42, no. 9, pp. 10559–10564, 2016.

[242]   J. Yoo, M. J. Cima, S. Khanuja, and E. M. Sachs, "Structural ceramic components by 3D printing," in *Proceedings of Solid Freeform Fabrication Symposium*, 1993, pp. 40–50.

[243]   M. M. M. Carrijo *et al.*, "Fabrication of Ti3SiC2-based composites via three-dimensional printing: Influence of processing on the final properties," *Ceram. Int.*, vol. 42, no. 8, pp. 9557–9564, 2016.

[244]   W. Zhang, R. Melcher, N. Travitzky, R. K. Bordia, and P. Greil, "Three-Dimensional Printing of Complex-Shaped Alumina/ Glass Composites," *Adv. Eng. Mater.*, vol. 11, no. 12, pp. 1039–1043, 2009.

[245]   A. Zocca, C. M. Gomes, A. Staude, E. Bernardo, J. Günster, and P. Colombo, "SiOC ceramics with ordered porosity by 3D-printing of a preceramic polymer," *J. Mater. Res.*, vol. 28, no. 17, pp. 2243–2252, 2013.

[246]   A. Zocca *et al.*, "3D-printed silicate porous bioceramics using a non-sacrificial preceramic polymer binder," *Biofabrication*, vol. 7, no. 2, 2015.

[247]   Z. Fu, L. Schlier, N. Travitzky, and P. Greil, "Three-dimensional printing of SiSiC lattice truss structures," *Mater. Sci. Eng. A*, vol. 560, pp. 851–856, 2013.

[248]   J. E. Grau, "Fabrication of Engineered Ceramic Components by the Slurry-Based Three Dimensional Printing Process," Massachusetts Institute of Technology, 1998.

[249]   J. Moon, J. E. Grau, M. J. Cima, and E. M. Sachs, "Slurry chemistry control to produce easily redispersible ceramic powder compacts," *J. Am. Ceram. Soc.*, vol. 83, no. 10, pp. 2401–2403, 2000.

[250]   B. D. Kernan, E. M. Sachs, M. A. Oliveira, and M. J. Cima, "Three-dimensional printing of tungsten carbide-10 wt% cobalt using a cobalt oxide precursor," *Int. J. Refract. Met. Hard Mater.*, vol. 25, no. 1, pp. 82–94, 2007.

[251]   R. K. Holman, "Effects of the Polymeric Binder System in Slurry-Based Three Dimensional Printing of Ceramics," Massachusetts Institute of Technology, 2001.

[252]   J. Moon, J. E. Grau, V. Knezevic, M. J. Cima, and E. M. Sachs, "Ink-jet printing of binders for ceramic components," *J. Am. Ceram. Soc.*, vol. 85, no. 4, pp. 755–762, 2002.

[253]   M. Cima, M. Oliveira, and H. Wang, "Slurry-based 3DP and fine ceramic components," in *Proceedings of Solid Freeform Fabrication*, 2001, pp. 216–223.

[254]   Y. Jia, Y. Kanno, and Z. peng Xie, "New gel-casting process for alumina ceramics based on gelation of alginate," *J. Eur. Ceram. Soc.*, vol. 22, no. 12, pp. 1911–1916, 2002.

[255]   X. Wang, Z. P. Xie, Y. Huang, and Y. B. Cheng, "Gelcasting of silicon carbide based on gelation of sodium alginate," *Ceram. Int.*, vol. 28, no. 8, pp. 865–871, 2002.

[256]   H. Akhondi, E. Taheri-Nassaj, H. Sarpoolaky, and A. Taavoni-Gilan, "Gelcasting of alumina nanopowders based on gelation of sodium alginate," *Ceram. Int.*, vol. 35, no. 3, pp. 1033–1037, 2009.

[257]   S. Baskaran, G. D. Maupin, and G. L. Graff, "Freeform fabrication of ceramics," *American Ceramic Society Bulletin*, vol. 77, no. 7. pp. 53–58, 1998.

[258]   A. Mostafaei, A. M. Elliott, J. E. Barnes, C. L. Cramer, P. Nandwana, and M. Chmielus, "Binder jet 3D printing – process parameters, materials, properties, and challenges," *Prog. Mater. Sci.*, p. 100684, 2020.

[259]   M. Ziaee and N. B. Crane, "Binder jetting: A review of process, materials, and methods," *Addit. Manuf.*, vol. 28, pp. 781–801, 2019.

[260]   D. Snelling *et al.*, "The effects of 3D printed molds on metal castings," *24th Int. SFF Symp. - An Addit. Manuf. Conf. SFF 2013*, pp. 827–845, 2013.

[261]   C. Hinczewski, S. Corbel, and T. Chartier, "Ceramic suspensions suitable for stereolithography," *J. Eur. Ceram. Soc.*, vol. 18, no. 6, pp. 583–590, 1998.

[262]   W. Zhou, D. Li, and H. Wang, "A novel aqueous ceramic suspension for ceramic stereolithography," *Rapid Prototyp. J.*, vol. 16, no. 1, pp. 29–35, 2010.

[263]   T. A. Pham, D. P. Kim, T. W. Lim, S. H. Park, D. Y. Yang, and K. S. Lee, "Three-dimensional SiCN ceramic

microstructures via nano-stereolithography of inorganic polymer photoresists," *Adv. Funct. Mater.*, vol. 16, no. 9, pp. 1235–1241, 2006.

[264] T. Chartier, M. Ferrato, J. F. Baumard, and G. Coudamy, "Debinding of ceramics: a review," *Acta Ceram.*, vol. 6, no. 6, p. 17, 1994.

[265] W. Zimbeck, M. Pope, and R. W. Rice, "Microstructures and Strengths of Metals and Ceramics made by Photopolymer-based Rapid Prototyping," in *Solid Freeform Fabrication Proceedings*, 1996, pp. 411–418.

[266] W. M. Sigmund, N. S. Bell, and L. Bergstrom, "Novel powder-processing methods for advanced ceramics," *J. Am. Ceram. Soc.*, vol. 83, no. 7, pp. 1557–1574, 2000.

[267] H. Liao, "Stereolithography Using Compositions Containing Ceramic Powders," University of Toronto, 1997.

[268] K. C. Wu and J. W. Halloran, "Photopolymerization monitoring of ceramic stereolithography resins by FTIR methods," *J. Mater. Sci.*, vol. 40, no. 1, pp. 71–76, 2005.

[269] A. Badev *et al.*, "Photopolymerization kinetics of a polyether acrylate in the presence of ceramic fillers used in stereolithography," *J. Photochem. Photobiol. A Chem.*, vol. 222, no. 1, pp. 117–122, 2011.

[270] G. a Brady, T. M. Chu, and J. W. Halloran, "Curing Behavior of Ceramic Resin for Stereolithography," *Solid Free. Fabr. Symp.*, no. 1, pp. 403–410, 1996.

[271] M. L. Griffith and J. Halloran, "Ultraviolet Curing of Highly Loaded Ceramic Suspensions for Stereolithography of Ceramics," in *Solid Freeform Fabrication Symposium*, 1994, pp. 396–403.

[272] C. Sun and X. Zhang, "The influences of the material properties on ceramic micro-stereolithography," *Sensors Actuators, A Phys.*, vol. 101, no. 3, pp. 364–370, 2002.

[273] M. Wozniak, Y. de Hazan, T. Graule, and D. Kata, "Rheology of UV curable colloidal silica dispersions for rapid prototyping applications," *J. Eur. Ceram. Soc.*, vol. 31, no. 13, pp. 2221–2229, 2011.

[274] P. F. Jacobs, "Fundamentals of stereolithography," in *Proceedings of the 1st European Conference on Rapid Prototyping*, 1992.

[275] H. Wu *et al.*, "Fabrication of dense zirconia-toughened alumina ceramics through a stereolithography-based additive manufacturing," *Ceram. Int.*, vol. 43, pp. 968–972, 2017.

[276] X. Tian, W. Zhang, D. Li, and J. G. Heinrich, "Reaction-bonded SiC derived from resin precursors by Stereolithography," *Ceram. Int.*, vol. 38, no. 1, pp. 589–597, 2012.

[277] S. C. Ventura, S. C. Narang, S. Sharma, and J. Stotts, "A new sff process for functional ceramic components," *Solid Free. Fabr. Symp. Proc.*, pp. 327–334, 1996.

[278] J. W. Halloran *et al.*, "Photopolymerization of powder suspensions for shaping ceramics," *J. Eur. Ceram. Soc.*, vol. 31, no. 14, pp. 2613–2619, 2011.

[279] X. Song, Y. Chen, T. W. Lee, S. Wu, and L. Cheng, "Ceramic fabrication using Mask-Image-Projection-based Stereolithography integrated with tape-casting," *J. Manuf. Process.*, vol. 20, pp. 456–464, 2015.

[280] M. Schwentenwein and J. Homa, "Additive manufacturing of dense alumina ceramics," *Int. J. Appl. Ceram. Technol.*, vol. 12, no. 1, pp. 1–7, 2015.

[281] W. Harrer, M. Schwentenwein, T. Lube, and R. Danzer, "Fractography of zirconia-specimens made using additive manufacturing (LCM) technology," *J. Eur. Ceram. Soc.*, vol. 37, no. 14, pp. 4331–4338, 2017.

[282] R. He *et al.*, "Fabrication of complex-shaped zirconia ceramic parts via a DLP-stereolithography-based 3D printing method," *Ceram. Int.*, vol. 44, pp. 3412–3416, 2018.

[283] Y. de Hazan and D. Penner, "SiC and SiOC ceramic articles produced by stereolithography of acrylate modified polycarbosilane systems," *J. Eur. Ceram. Soc.*, vol. 37, no. 16, pp. 5205–5212, 2017.

[284] J. M. Hundley *et al.*, "Geometric characterization of additively manufactured polymer derived ceramics," *Addit. Manuf.*, vol. 18, pp. 95–102, 2017.

[285]   J. Schmidt and P. Colombo, "Digital light processing of ceramic components from polysiloxanes," *J. Eur. Ceram. Soc.*, vol. 38, no. 1, pp. 57–66, 2018.

[286]   T. A. Schaedler *et al.*, "Ultralight metallic microlattices.," *Science*, vol. 334, no. 6058, pp. 962–5, 2011.

[287]   "Lithoz." [Online]. Available: http://www.lithoz.com/en/. [Accessed: 13-Mar-2016].

[288]   "Prodways." [Online]. Available: http://www.prodways.com/en/printer/promaker-v6000/. [Accessed: 13-Mar-2016].

[289]   M. D. Bruijcker, *Press release of Admatec Europe BV: Four new printers installed for series production of functional ceramic components; printing ceramics proves to be a production solution*. 2014.

[290]   DDM Systems, "Technologies," 2014. [Online]. Available: http://www.ddmsys.com/technologies/. [Accessed: 11-Feb-2018].

[291]   Prodways, "Prodways Movinglight® Technology." [Online]. Available: https://www.prodways.com/en/the-prodways-movinglight-technology/. [Accessed: 12-Feb-2018].

[292]   A. Licciulli, C. Esposito Corcione, A. Greco, V. Amicarelli, and A. Maffezzoli, "Laser stereolithography of ZrO2 toughened Al2O3," *J. Eur. Ceram. Soc.*, vol. 25, no. 9, pp. 1581–1589, 2005.

[293]   H. Xing, B. Zou, S. Li, and X. Fu, "Study on surface quality, precision and mechanical properties of 3D printed ZrO2 ceramic components by laser scanning stereolithography," *Ceram. Int.*, vol. 43, no. 18, pp. 16340–16347, 2017.

[294]   R. J. Huang *et al.*, "Fabrication of complex shaped ceramic parts with surface-oxidized Si 3 N 4 powder via digital light processing based stereolithography method," *Ceram. Int.*, vol. 45, no. 4, pp. 5158–5162, 2019.

[295]   R. He, G. Ding, K. Zhang, Y. Li, and D. Fang, "Fabrication of SiC ceramic architectures using stereolithography combined with precursor infiltration and pyrolysis," *Ceram. Int.*, vol. 45, no. 11, pp. 14006–14014, 2019.

[296]   G. Ding *et al.*, "Stereolithography-based additive manufacturing of gray-colored SiC ceramic green body," *J. Am. Ceram. Soc.*, no. 102, pp. 7198–7209, 2019.

[297]   A. Zocca, "Additive Manufacturing of porous ceramic structures," Clausthal University of Technology, 2015.

[298]   C. Y. Yap *et al.*, "Review of selective laser melting: Materials and applications," *Appl. Phys. Rev.*, vol. 2, no. 4, 2015.

[299]   J.-P. Kruth, G. Levy, F. Klocke, and T. H. C. Childs, "Consolidation phenomena in laser and powder-bed based layered manufacturing," *CIRP Ann. - Manuf. Technol.*, vol. 56, no. 2, pp. 730–759, 2007.

[300]   F. Niu, D. Wu, S. Zhou, and G. Ma, "Power prediction for laser engineered net shaping of Al2O3 ceramic parts," *J. Eur. Ceram. Soc.*, vol. 34, no. 15, pp. 3811–3817, 2014.

[301]   S. Meyers, J.-P. Kruth, and J. Vleugels, "Direct Selective Laser Sintering of Reaction Bonded Silicon Carbide," in *Proceedings of Solid Freeform Fabrication Symposium*, 2015, pp. 1750–1758.

[302]   J. G. Heinrich *et al.*, "Microstructural evolution during direct laser sintering in the Al2O3–SiO2 system," *J. Mater. Sci.*, vol. 42, no. 14, pp. 5307–5311, 2007.

[303]   I. Shishkovsky, I. Yadroitsev, P. Bertrand, and I. Smurov, "Alumina-zirconium ceramics synthesis by selective laser sintering/melting," *Appl. Surf. Sci.*, vol. 254, no. 4, pp. 966–970, 2007.

[304]   J. Wilkes, Y. Hagedorn, W. Meiners, and K. Wissenbach, "Additive manufacturing of ZrO2-Al2O3 ceramic components by selective laser melting," *Rapid Prototyp. J.*, vol. 19, no. 1, pp. 51–57, Jan. 2013.

[305]   F. H. Liu, "Synthesis of bioceramic scaffolds for bone tissue engineering by rapid prototyping technique," *J. Sol-Gel Sci. Technol.*, vol. 64, no. 3, pp. 704–710, 2012.

[306]   A. Zocca, P. Colombo, J. Günster, T. Mühler, and J. G. Heinrich, "Selective laser densification of lithium aluminosilicate glass ceramic tapes," *Appl. Surf. Sci.*, vol. 265, pp. 610–614, 2013.

[307] F. Klocke and C. Ader, "Direct Laser Sintering of Ceramics," in *Proceedings of Solid Freeform Fabrication Symposium*, 2003, p. 9.

[308] Y. Tang, J. Y. H. Fuh, H. T. Loh, Y. S. Wong, and L. Lu, "Direct laser sintering of a silica sand," *Mater. Des.*, vol. 24, pp. 623–629, 2003.

[309] P. Bertrand, F. Bayle, C. Combe, P. Goeuriot, and I. Smurov, "Ceramic components manufacturing by selective laser sintering," *Appl. Surf. Sci.*, vol. 254, no. 4, pp. 989–992, 2007.

[310] J. Wilkes, Y.-C. Hagedorn, S. Ocylok, W. Meiners, and K. Wissenbach, "Rapid Manufacturing of Ceramic Parts by Selective Laser Melting," in *Advanced Processing and Manufacturing Technologies for Structural and Multifunctional Materials IV*, John Wiley & Sons, Inc., 2010, pp. 137–148.

[311] Y.-C. Hagedorn, J. Wilkes, W. Meiners, K. Wissenbach, and R. Poprawe, "Net shaped high performance oxide ceramic parts by Selective Laser Melting," *Phys. Procedia*, vol. 5, no. 2, pp. 587–594, 2010.

[312] Y.-C. Hagedorn, N. Balachandran, W. Meiners, K. Wissenbach, and R. Poprawe, "SLM of Net-Shaped High Strength Ceramics: New Opportunities for Producing Dental Restorations," in *Proceedings of Solid Freeform Fabrication Symposium*, 2011, pp. 536–546.

[313] W. E. Frazier, "Metal additive manufacturing: A review," *J. Mater. Eng. Perform.*, vol. 23, no. 6, pp. 1917–1928, 2014.

[314] T. Muehler, C. M. Gomes, J. Heinrich, and J. Guenster, "Slurry-Based Additive Manufacturing of Ceramics," *Int. J. Appl. Ceram. Technol.*, vol. 12, no. 1, pp. 18–25, 2015.

[315] A. Gahler, J. G. Heinrich, and J. Günster, "Direct laser sintering of Al2O3-SiO2 dental ceramic components by layer-wise slurry deposition," *J. Am. Ceram. Soc.*, vol. 89, no. 10, pp. 3076–3080, 2006.

[316] X. Tian, D. Li, and J. G. Heinrich, "Net-Shaping of Ceramic Components by Using Rapid Prototyping Technologies," in *Advances in Ceramics - Synthesis and Characterization, Processing and Specific Applications*, Prof. Costas Sikalidis, Ed. InTech, 2011, pp. 291–310.

[317] F. El-Diasty, F. A. Abdel Wahab, and M. Abdel-Baki, "Optical band gap studies on lithium aluminum silicate glasses doped with Cr3+ ions," *J. Appl. Phys.*, vol. 100, no. 9, 2006.

[318] T. Mühler, C. Gomes, M. E. Ascheri, D. Nicolaides, J. G. Heinrich, and J. Günster, "Slurry-based powder beds for the selective laser sintering of silicate ceramics," *J. Ceram. Sci. Technol.*, vol. 6, no. 2, pp. 113–118, 2015.

[319] X. Tian, D. Li, and J. G. Heinrich, "Rapid prototyping of porcelain products by layer-wise slurry deposition (LSD) and direct laser sintering," *Rapid Prototyp. J.*, vol. 18, no. 5, pp. 362–373, 2012.

[320] F. Wang, J. Mei, H. Jiang, and X. Wu, "Laser fabrication of Ti6Al4V/TiC composites using simultaneous powder and wire feed," *Mater. Sci. Eng. A*, vol. 445–446, pp. 461–466, 2007.

[321] F. Y. Niu, D. J. Wu, S. Yan, G. Y. Ma, and B. Zhang, "Process Optimization for Suppressing Cracks in Laser Engineered Net Shaping of Al2O3 Ceramics," *JOM*, vol. 69, no. 3, pp. 557–562, 2017.

[322] F. Niu, D. Wu, G. Ma, S. Zhou, and B. Zhang, "Effect of second-phase doping on laser deposited Al2O3 ceramics," *Rapid Prototyp. J.*, vol. 21, no. 2, pp. 201–206, 2015.

[323] F. Niu, D. Wu, G. Ma, J. Wang, M. Guo, and B. Zhang, "Nanosized microstructure of Al2O3-ZrO2 (Y2O3) eutectics fabricated by laser engineered net shaping," *Scr. Mater.*, vol. 95, no. 1, pp. 39–41, 2015.

[324] F. Niu, D. Wu, G. Ma, J. Wang, J. Zhuang, and Z. Jin, "Rapid Fabrication of Eutectic Ceramic Structures by Laser Engineered Net Shaping," *Procedia CIRP*, vol. 42, no. Isem Xviii, pp. 91–95, 2016.

[325] A. Larrea, V. M. Orera, R. I. Merino, and J. I. Peña, "Microstructure and mechanical properties of Al2O3-YSZ and Al2O3-YAG directionally solidified eutectic plates," *J. Eur. Ceram. Soc.*, vol. 25, pp. 1419–1429, 2005.

[326] M. Dehurtevent, L. Robberecht, J. C. Hornez, A. Thuault, E. Deveaux, and P. B??hin, "Stereolithography: A new method for processing dental ceramics by additive computer-aided manufacturing," *Dent. Mater.*, vol. 33, no. 5, pp. 477–485, 2017.

[327] M. Yu *et al.*, "Optimization of the tape casting process for development of high performance alumina ceramics," *Ceram. Int.*, vol. 41, no. 10, pp. 14845–14853, 2015.

[328] A. M'Barki, L. Bocquet, and A. Stevenson, "Linking Rheology and Printability for Dense and Strong Ceramics by Direct Ink Writing," *Sci. Rep.*, vol. 7, no. 1, pp. 1–10, 2017.

[329] S. Mamatha, P. Biswas, P. Ramavath, D. Das, and R. Johnson, "3D printing of complex shaped alumina parts," *Ceram. Int.*, vol. 44, no. 16, pp. 19278–19281, 2018.

[330] M. Zhou *et al.*, "Preparation of a defect-free alumina cutting tool via additive manufacturing based on stereolithography – Optimization of the drying and debinding processes," *Ceram. Int.*, vol. 42, no. 10, pp. 11598–11602, 2016.

[331] T. Hotta, H. Abe, M. Naito, M. Takahashi, K. Uematsu, and Z. Kato, "Effect of coarse particles on the strength of alumina made by slip casting," *Powder Technol.*, vol. 149, no. 2–3, pp. 106–111, 2005.

[332] C. Li, S. Li, D. An, and Z. Xie, "Microstructure and mechanical properties of spark plasma sintered SiC ceramics aided by B4C," *Ceram. Int.*, vol. 46, no. 8, pp. 10142–10146, 2020.

[333] S. Kultayeva and Y. Kim, "Mechanical , thermal , and electrical properties of pressureless sintered SiC – AlN ceramics," *Ceram. Int.*, no. April, pp. 1–10, 2020.

[334] H. Rashid, "The effect of surface roughness on ceramics used in dentistry: A review of literature," *Eur. J. Dent.*, vol. 8, no. 4, pp. 571–579, Oct. 2014.

[335] R. Janssen, S. Scheppokat, and N. Claussen, "Tailor-made ceramic-based components-Advantages by reactive processing and advanced shaping techniques," *J. Eur. Ceram. Soc.*, vol. 28, no. 7, pp. 1369–1379, 2008.

[336] K. Liu, T. Wu, D. L. Bourell, Y. Tan, J. Wang, and M. He, "Laser additive manufacturing and homogeneous densification of complicated shape SiC ceramic parts," *Ceram. Int.*, vol. 44, no. 17, pp. 21067–21075, 2018.

[337] G. Standke, T. Müller, A. Neubrand, J. Weise, and M. Göpfert, "Cost-efficient metal-ceramic composites - novel foam-preforms, casting processes and characterisation," *Adv. Eng. Mater.*, vol. 12, no. 3, pp. 189–196, 2010.

[338] J. Liu, "Processing and properties of interpenetrating composites," Loughborough University, 2012.

[339] P. Chabera, A. Boczkowska, A. Witek, and A. Oziębło, "Fabrication and characterization of composite materials based on porous ceramic preform infiltrated by elastomer," *Bull. Polish Acad. Sci. Tech. Sci.*, vol. 63, no. 1, pp. 193–199, 2015.

[340] Y. J. Seol, D. Y. Park, J. Y. Park, S. W. Kim, S. J. Park, and D. W. Cho, "A new method of fabricating robust freeform 3D ceramic scaffolds for bone tissue regeneration," *Biotechnol. Bioeng.*, vol. 110, no. 5, pp. 1444–1455, 2013.

Vitae

Yazid Lakhdar holds a Master's Degree in Materials Science from Polytech Lille (France), which included several academic and industrial placements on the themes of polymer composites and fibre reinforcements. In 2015, he joined the EPSRC Centre for Doctoral Training in Additive Manufacturing at the University of Nottingham to research a PhD on 3D printing of boron carbide. Yazid joined Emma Kendrick's Energy Materials Group at the University of Birmingham as a Research Fellow in November 2019 to investigate novel electrode materials and conditioning procedures for ultra-power lithium-ion batteries.

Ruth Goodridge is Professor of Additive Manufacturing at the University of Nottingham, UK. She has a BMedSc (Hons) degree in Biomaterials from the University of Birmingham, UK and a PhD investigating laser sintering of bioceramics from the University of Leeds, UK. Upon completion of her PhD in 2004, she was awarded a 2 year JSPS Fellowship to investigate new glass-ceramic materials for laser sintering at NAIST, Japan. She has worked in the field of Additive Manufacturing for 20 years; her current research focuses on powder-bed fusion of polymers, ceramics and glass, as well as Healthcare applications of Additive Manufacturing.

Anna Terry is a research engineer in Additive Manufacturing at AWE and graduate in Materials Science from the University of Birmingham. Her work focuses on the development of new materials and bespoke AM techniques and their implementation.

Chris Tuck is Professor of Materials Engineering and Associate Pro-Vice Chancellor for Research and Knowledge Exchange in the Faculty of Engineering at The University of Nottingham. He has worked in the Additive Manufacturing area since 2003, with a focus on materials and process relationships. Chris is Director of the EPSRC Centre for Doctoral Training in Additive Manufacturing and 3D Printing, a training and research programme for 66 PhD students co-sponsored by industry. He has been an Executive Member of the ASTM F42 AM standards committee and a participant in the BSi initiative of AM standards development. Chris is a regular presenter at international conferences, a panel member for EPSRC and a reviewer for European and US funding agencies including NASA. He is also a reviewer for numerous international journals in the fields of Additive Manufacturing and 3D printing materials, business and socio-economic aspects as well as optical sensor systems and methods.

Jon Binner is Professor of Ceramic Science & Engineering in the School of Metallurgy and Materials and
Jon Binner is Professor of Ceramic Science & Engineering in the School of Metallurgy and Materials and
Jon Binner is Professor of Ceramic Science & Engineering in the School of Metallurgy and Materials and
Jon Binner is Professor of Ceramic Science & Engineering in the School of Metallurgy and Materials and
Jon Binner is Professor of Ceramic Science & Engineering in the School of Metallurgy and Materials and
Jon Binner is Professor of Ceramic Science & Engineering in the School of Metallurgy and Materials and
Jon Binner is Professor of Ceramic Science & Engineering in the School of Metallurgy and Materials and
Jon Binner is Professor of Ceramic Science & Engineering in the School of Metallurgy and Materials and
Jon Binner is Professor of Ceramic Science & Engineering in the School of Metallurgy and Materials and
Jon Binner is Professor of Ceramic Science & Engineering in the School of Metallurgy and Materials and
Jon Binner is Professor of Ceramic Science & Engineering in the School of Metallurgy and Materials and
Jon Binner is Professor of Ceramic Science & Engineering in the School of Metallurgy and Materials and
Jon Binner is Professor of Ceramic Science & Engineering in the School of Metallurgy and Materials and
Jon Binner is Professor of Ceramic Science & Engineering in the School of Metallurgy and Materials and
Jon Binner is Professor of Ceramic Science & Engineering in the School of Metallurgy and Materials and
Jon Binner is Professor of Ceramic Science & Engineering in the School of Metallurgy and Materials and

Jon Binner is Professor of Ceramic Science & Engineering in the School of Metallurgy and Materials and
Jon Binner is Professor of Ceramic Science & Engineering in the School of Metallurgy and Materials and
Jon Binner is Professor of Ceramic Science & Engineering in the School of Metallurgy and Materials and
Jon Binner is Professor of Ceramic Science & Engineering in the School of Metallurgy and Materials and
Jon Binner is Professor of Ceramic Science & Engineering in the School of Metallurgy and Materials and
Jon Binner is Professor of Ceramic Science & Engineering in the School of Metallurgy and Materials and